Implications of serotonin transporter distribution in the healthy and diseased human brain, investigated by positron emission tomography

Doctoral thesis at the Medical University of Vienna
in the program Clinical Neurosciences
for obtaining the academic degree

Doctor of Medical Science

submitted by
Mag. rer. nat. Georg S. Kranz

supervised by
Assoc.-Prof. PD Dr. Rupert Lanzenberger

Functional, Molecular and Translational Neuroimaging Lab – PET & MRI
Department of Psychiatry and Psychotherapy
Medical University of Vienna
Waehringer Guertel 18-20, 1090 Vienna, Austria
http://www.meduniwien.ac.at/neuroimaging/

Vienna, 05/2013

MEDICAL UNIVERSITY OF VIENNA
CLINICAL DIVISION OF BIOLOGICAL PSYCHIATRY

Declaration

This work was carried out at the Functional, Molecular & Translational Neuroimaging Lab (http://www.meduniwien.ac.at/neuroimaging/, head: Assoc.-Prof. PD Dr. med. Rupert Lanzenberger) at the Department of Psychiatry and Psychotherapy (head: O.Univ.-Prof. Dr. h.c.mult. Dr. med. Siegfried Kasper), Medical University of Vienna.

PET measurements were performed at the Department of Nuclear Medicine, radiotracer synthesis was done at the Radiopharmaceutical Sciences (http://www.radiopharmaceutical-sciences.net/joomla/, heads: Assoc.-Prof. PD. Dr. Wolfgang Wadsak [Production Manager PET], PD. Dr. Markus Mitterhauser [Radiopharmacy]), Medical University of Vienna.

Table of Contents

Abstract

The serotonin transporter (SERT), an integral part of the serotonergic system, has developed into a subject of great interest in the field of biological psychiatry. Sustained SERT blockage was shown to have strong antidepressant and anxiolytic effects, which led to the development of today's most widely prescribed antidepressants, the selective serotonin reuptake inhibitors (SSRIs). The regional distribution of the SERT in the human brain and its blockage by SSRIs can be effectively studied with positron emission tomography (PET) and suitable radioligands *in vivo.* Although several imaging studies on the SERT have been performed in the last decades, basic knowledge of SERT distribution and its implications for lateralized brain functions, gender identity, drug occupancy and for antidepressant treatment response has yet to be obtained.

In order to directly address these knowledge gaps, we performed three PET studies using the radioligand [^{11}C]DASB in healthy subjects, transsexuals and patients with major depression. In our first study, we find robust asymmetry of SERT binding over the entire study population, which echoes previous findings of serotonergic asymmetry and thereby solidifies the concept of an asymmetric serotonergic system. Moreover, we show strong SERT asymmetry in the midcingulate cortex in males, but not in male-to female transsexuals or in females, which implies that asymmetry in this region reflects gender identity. In our second study, we reveal that regional SERT pretreatment binding and antidepressant drug plasma levels predict SERT occupancy. We further show that SERT occupancy exhibits regional variability. Together, these findings suggest a region-specific distribution of SERT blockage by SSRIs as well as their dependence on pretreatment SERT binding. In our third study, we find that antidepressant treatment response is predicted by pre-treatment SERT binding, but only when normalizing SERT binding in terminal regions to that in the midbrain raphe region.

The publications arising from this thesis expand our understanding of the SERT both on a fundamental and neuroscientific, as well as on a clinically applicable level. This clinical relevance is established by way of an increased understanding of antidepressant drug action and the discovery of a potential biological marker for antidepressant treatment response.

Kurzfassung

Einem zentralen Bestandteil des Serotoninsystems, dem Serotonintransporter (SERT), ist in den letzten Jahrzehnten viel Aufmerksamkeit in der Psychiatrie zuteil geworden. Der Befund, dass anhaltende SERT-Blockade sich als stark antidepressiv und anxiolytisch erweist, hatte zur Entwicklung der Selektiven Serotonin Wiederaufnahme Hemmer (SSRI), der heute am häufigsten verschriebenen Antidepressiva, geführt. Die regionale Verteilung des SERT im menschlichen Gehirn und seine Blockade durch SSRIs kann heute mithilfe der Positronen-Emissionstomographie (PET) und geeigneten Radioliganden *in vivo* untersucht werden. Trotz reger Beforschung des SERT mit PET in der Vergangenheit, sind grundlegende Fragen seiner Verteilung, etwa im Zusammenhang mit der zerebralen Lateralisierung, mit der Geschlechtsidentität, mit seiner Okkupanz durch Medikamente oder mit dem antidepressiven Wirkmechanismus noch ungeklärt.

Die vorliegende Arbeit beinhaltet drei PET Studien mit dem Radioliganden [^{11}C]DASB, die sich der Beantwortung dieser Fragen anhand eines gesunden und zwei psychiatrischen Kollektiven (transsexuellen und depressiven PatientInnen) widmen. Die erste Studie zeigt, dass der SERT stark asymmetrisch im menschlichen Gehirn verteilt ist, ein Befund, der zusammen mit bereits beschriebenen serotonergen Asymmetrien auf eine Lateralisierung der Serotoninsystems schließen lässt. Ferner zeigt sich eine SERT Asymmetrie im mittleren cingulären Kortex nur in Männern, aber nicht in Mann-zu-Frau Transsexuellen und Frauen; die SERT Asymmetrie scheint daher in dieser Hirnregion die Geschlechtsidentität widerzuspiegeln. Die zweite Studie zeigt, dass sich sowohl durch die regionale SERT Verteilung vor Behandlung, als auch durch die Plasmakonzentration antidepressiver Medikamente die SERT Okkupanz vorhersagen lässt. Des Weiteren findet sich eine regionale Variabilität der SERT Okkupanzstärke. Die zweite Studie lässt damit den Schluss auf eine regionen-spezifische Verteilung der SERT Blockade durch SSRIs und ihre Abhängigkeit von der SERT Verteilung vor Behandlung zu. Die dritte Studie zeigt, dass die antidepressive Wirkung von SSRIs durch das Verhältnis der SERT Verteilung in Projektionsgebieten zur SERT Verteilung in den Raphekernen vor Behandlung vorhergesagt werden kann.

Die drei Publikationen der vorliegenden Doktorarbeit bereichern nicht nur unser Grundlagenwissen über den SERT, sondern haben auch potentiell klinische Relevanz, indem sie unser Verständnis der antidepressiven Medikamentenwirkung erweitern und zur Entdeckung eines potentiellen biologischen Markers für den antidepressiven Behandlungserfolg beitragen.

Publications arising from this thesis

Publications

Kranz G.S., Hahn A., Baldinger P., Haeusler D., Philippe C., Kaufmann U., Wadsak W., Savli M., Hoeflich A., Kraus C., Vanicek T., Mitterhauser M., Kasper S., Lanzenberger R. (2012). Cerebral Serotonin Transporter Asymmetry in Females, Males and Male-to-Female Transsexuals measured by PET in vivo. *Brain Structure and Function*, in press. [2011, IF: 5.628].

Baldinger P,* **Kranz G.S.,*** Haeusler D, Savli M, Spies M, Philippe C, Hahn A, Hoeflich A, Wadsak W, Mitterhauser M, Lanzenberger R, Kasper, S. (2013). Regional differences in SERT occupancy after acute and prolonged SSRI intake investigated by brain PET. *NeuroImage.* [2011, IF: 5.895], submitted, *contributed equally*.

Lanzenberger R, **Kranz G.S.**, Häusler D, Akimova E, Savli M, Hahn A, Wadsak W, Spindelegger C, Philippe C, Fink M, Mitterhauser M, Kasper S. (2012). Prediction of SSRI treatment response in major depression based on serotonin transporter interplay between median raphe nucleus and projection areas. *NeuroImage* 63(2):874-881. [2011, IF: 5.895].

Related publications

Kranz G.S., Hahn A., Savli M., & Lanzenberger R. (2012). Challenges in the differentiation of midbrain raphe nuclei in neuroimaging research. *Proceedings of the National Academy of Sciences of the United States of America (PNAS), 109(29),* doi:10.1073/pnas.1206247109. [2011, IF: 9.681].

Kranz G.S., Kasper S., Lanzenberger R. (2010). Reward and the Serotonergic System. *Neuroscience* 166 (4), 1023-1035. [2011, IF: 3.380].

Lanzenberger R., Mitterhauser M., **Kranz G.S.,** Spindelegger, Ch., Wadsak, W., Stein, P., Moser, U., Savli, M., Kletter, K. & Kasper, S. (2011). Progesterone level predicts serotonin-1A receptor binding in the male human brain. *Neuroendocrinology,* 94(1):84-8. [2011, IF: 2.376].

Acknowledgments and project funding

I would like to express my gratitude to all those who supported me in completing this thesis. First of all, I like to thank my supervisor Assoc.-Prof. PD Dr.med. Rupert Lanzenberger for his scientific and personal support over the last years. Special thanks also to O.Prof. Dr.h.c.mult. Dr.med. Siegfried Kasper for the opportunity to carry out the research at the Department of Psychiatry and Psychotherapy. I would also like to thank the two members of my thesis committee, Ao. Prof. DDr. Susanne Asenbaum-Nan, MSc. MBA and Prof. Dr. med. Clemens Tempfer, MBA, and the coordinator of the PhD program *Clinical Neurosciences* Prof. Dr.med. Johannes Hainfellner for their supervision and encouragement throughout my doctoral studies.

Furthermore, great thanks go to the research team of the Functional, Molecular & Translational Neuroimaging Lab, especially to Marie Spies for linguistic support and to Dr. Markus Savli and Dr. Andreas Hahn for the helpful discussions and comments on the thesis.

My special thanks are extended to the staff of our cooperation partners at the PET centre and Radiopharmaceutical Sciences, especially to Assoc.-Prof. PD Dr. Wolfgang Wadsak and PD Dr. Markus Mitterhauser, for radiotracer synthesis and for technical support, and at the Department of Obstetrics and Gynecology, Dr.med. Ulrike Kaufmann, for recruitment of transsexual subjects. Finally, I am grateful to all patients and healthy controls for participating in our studies.

This work was funded by Grants from the Austrian National Bank (P 13214 to R. Lanzenberger; P 13675 to M. Mitterhauser) and the Austrian Science Fund (FWF, P 23021 to R. Lanzenberger) and by an investigator-initiated and unrestricted research grant from H. Lundbeck A/S, Denmark to S. Kasper.

I. BACKGROUND

1.1. General introduction

The brain's serotonergic system constitutes one of the major modulatory neurotransmitter systems in the human brain. Its neurons project from the raphe nuclei in the midbrain and brainstem, where the neuron's cell bodies are found, to virtually all cortical regions and many subcortical structures. It is therefore plausible why this system has been associated with many physiological functions, as well as a multitude of cognitive and emotional processes (Muller & Jacobs, 2010). The term "serotonergic system", is typically used to describe the biogenic amine serotonin (5-hydroxytryptamine, 5-HT) and the neurons producing it, including their cell bodies and dendrites within the raphe nuclei, their projections, as well as the at least 14 different 5-HT receptors located at pre-and postsynaptic sites and the serotonin transporter (SERT). The SERT plays a key role in the serotonergic system because it reuptakes the released serotonin back into the presynaptic neuron. It is thus important for the regulation of serotonin transmission, together with the vesicular monoamine transporter 2 (VMAT2) (Muller & Jacobs, 2010).

The SERT also plays an important role in psychiatry, as one of the most potent antidepressant treatments, the selective serotonin reuptake inhibitors (SSRIs), specifically target the SERT. The rise of the first data linking depression to a deficit of serotonin in the early 1970's (e.g., Coppen et al, 1972) lead to the formulation of the serotonin hypothesis of depression. Subsequently all effort in psychotropic drug development was investigated in the design of a class of psychopharmacologic medications that specifically block SERT function (Wong et al, 1995). From this time on, research on the SERT expanded and involved many different disciplines such as pharmacology, chemistry, genetics, electrophysiology, and imaging. This led to an extensive gain of knowledge on SERT structure, function and distribution. This gain in knowledge is fundamental to our present understanding of how the SERT is related to psychiatric symptoms.

Therefore, it is surprising, that some rather basic questions concerning the SERT are yet to be answered. For example, it is not clear whether serotonin reuptake leads to an increase or a reduction in SERT cell surface expression (see e.g., Steiner et al, 2008 vs. Kittler et al, 2010) Furthermore, it is uncertain how SERT blockage and antidepressant treatment outcome relate to each other, i.e., whether we can predict treatment outcome by the amount of SERT blockage by SSRIs. The corresponding literature is quite inconclusive on that matter. Even more basically, the question whether SERT blockage / occupancy relate to SERT expression is yet to be answered. Other issues concern a potential difference in SERT expression between women and men, or a potential difference in SERT expression between the right and left hemisphere. As is often the case, research on these issues may provide no strait Yes- or No -answers but rather give a differentiated picture of the matter. New findings may thus lead to a reformulation of existing questions as well as raise new questions that were not considered previously. It is the aim of the present thesis to contribute to this endeavor.

1.2. The serotonin transporter (SERT) and its role in psychiatry and psychopharmacological treatment

1.2.1. SERT structure and function

The SERT is an integral membrane protein belonging to the solute carrier 6 (*SLC6*) gene family. In addition to the SERT, plasma membrane transporters that belong to this family include those responsible for the uptake of monoamines norepinephrine (NE) and dopamine (DA) and the amino acids glycine and GABA. Only one transporter exists for each monoamine (the SERT, NET and DAT, respectively), whereas four transporters exist for GABA and two exist for glycine (Kristensen et al, 2011). The SLC6 transporters use the co-transport of extracellular Na^+ as energy source for neurotransmitter translocation while the SERT (encoded by *SLC6A4*) additionally requires the counter-transport of K^+ (Chen 2004). Cl^- is also co-transported into the cell. The transport activity follows Michaelis-Menten kinetics with K_M values in 0.2-1.0 mM range and a turnover rate ranging from one to three 5-HT molecules per second (Kristensen et al, 2011).

The SERT consists of 630 amino acids and is proposed to have 12 transmembrane (TM) helices with N- and C-termini located intracellularly (Ramamoorthy et al, 1993) (see Fig 1). Although the tertiary structure of the SERT is still unknown, three-dimensional models have been proposed based on the x-ray crystal structure of a bacterial homologue, the *Aquifex aeolicus's* Leucine Transporter (LeuT) (Celik et al, 2008; Jorgensen et al, 2007; Ravna, 2006; Yamashita et al, 2005). Modeling the SERT in that manner led to substantial knowledge gain about the specific residues that contribute to the binding of 5-HT and SERT inhibitors, to SERT translocation, post-translational modifications and interactions with intracellular proteins (Kristensen et al, 2011). Thus, it is now proposed that the 5-HT specific binding site (S1) lies deep within the transporter, surrounded by residues from TM1, TM3, TM6 and TM8 (LeuT numbering) (Celik et al, 2008). Biochemical research in combination with molecular dynamics simulations suggested also a secondary binding site (S2), in addition to the high-affinity substrate-specific (orthosteric) binding site (Shi et al, 2008). This low-affinity allosteric binding site was proposed to lie in the extracellular pathway of LeuT, which forms the path from the extracellular medium toward the primary binding site.

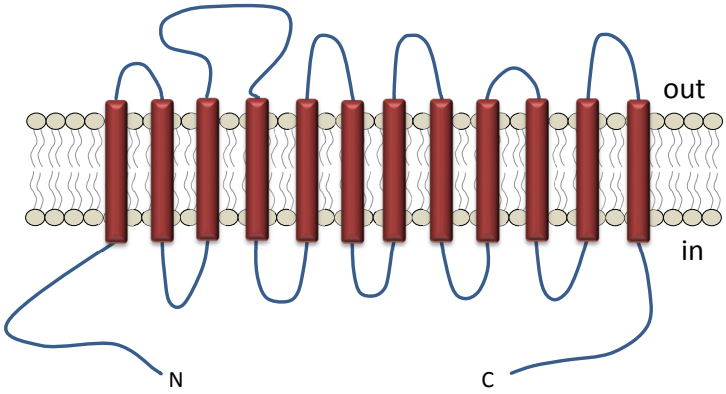

Fig 1. *The twelve transmembrane model of a single SERT subunit. The 12 TM α-helices are represented by red bars and are connected by intra- and extracellular loops (blue) with an N and C terminal located intracellularly (in).*

Our current understanding of 5-HT transport follows the so called "alternating access" model for secondary active transporters (Jardetzky, 1966). Based on this fundamental concept, at least three conformational states during the transport cycle are proposed: an outward-facing open

conformation, an outward-facing occluded conformation, and an inward-facing open conformation. Simultaneous binding of sodium and 5-HT to the specific binding site triggers a conformational change in the central translocation pathway from the outward-facing open state to the outward-facing occluded state und subsequent inward-facing conformation (Krishnamurthy et al, 2009). After releasing the 5-HT molecule and the ions, the transporter recycles back into the outward-facing state through a potassium-bound intermediate conformation (see Fig 2). Furthermore, Shi et al. demonstrated that both binding sites – S1 and S2, can be occupied simultaneously, where the allosteric binding may facilitate substrate transport by triggering intracellular release of sodium and substrate from the orthosteric binding site (Shi et al, 2008).

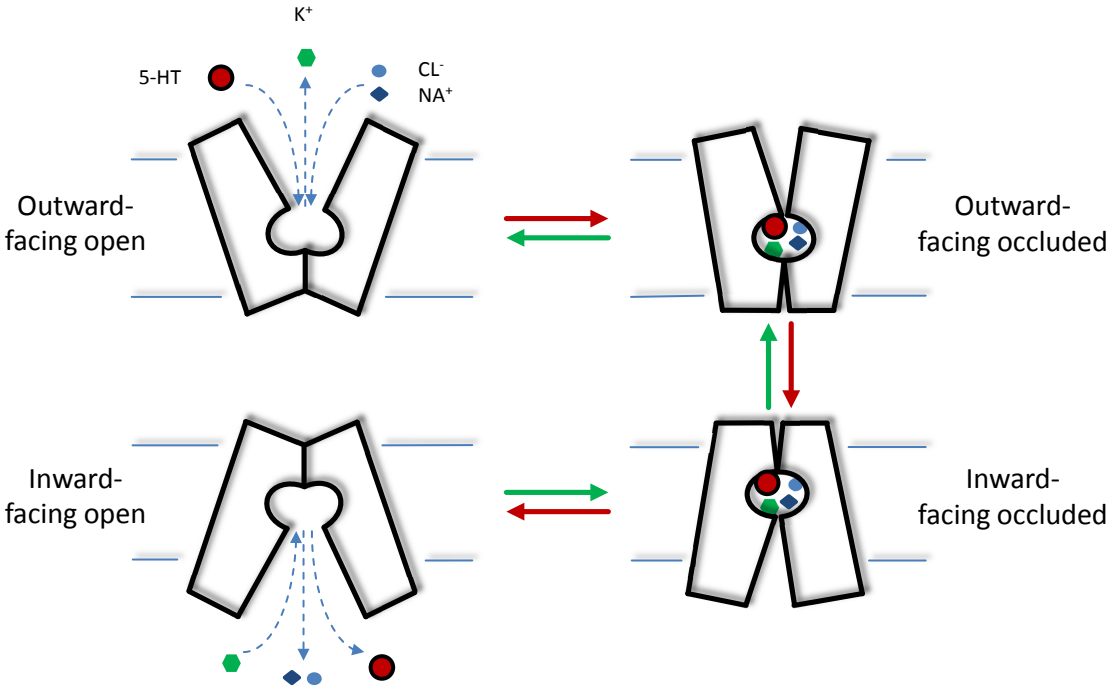

Fig 2. *Alternating access model of the SERT. Schematic representation of the conformational states during the transport cycle from an outward-facing open to an inward-facing open state (red arrows). After releasing the 5-HT molecule and the NA^+ into the cytosol, the transporter cycles back through a potassium bound state (green arrows) (based on Kristensen et al, 2011).*

1.2.2. SERT regulation

Knowledge of LeuT structure also spanked interest in SERT structure and function from a molecular pharmacology point of view (Kristensen et al, 2011). As the SERT is an important drug target, research focused on the location and structure of drug binding sites and revealed important principles regarding drug inhibition. Earlier studies already indicated that residues located in the transmembrane domains and loop regions of the extracellular pathway as well as binding sites are critical for recognition of SSRIs (Mortensen et al, 2001). It is now believed that a competitive inhibitor, which competes with 5-HT for binding in the primary binding site S1, traps the SERT in an outward-open or outward-occluded conformational state (Andersen et al, 2010; Sinning et al, 2010). This has been suggested for most Tricyclic antidepressants (TCAs) and SSRIs, although some have argued for a noncompetitive inhibition of these compounds via binding to sites that are dissimilar to S1 (Zhou et al, 2007; Zhou et al, 2009). However, several studies have found that most SSRIs and TCAs bind both to the primary and secondary binding site and it is proposed that binding to the allosteric site S2 increases the inhibitory effect of the drug by an increase of affinity to S1 (Chen et al, 2005a; Chen et al, 2005b; Shi et al, 2008).

Drugs that block SERT function such as SSRIs may also affect post-translational modifications of the SERT including phosphorylation and glycosylation. Substrate- and inhibitor-mediated trafficking has been proposed since the late 1990s (Ramamoorthy & Blakely, 1999; Ramamoorthy et al, 1998). For example, protein kinase C (PKC) mediated phosphorylation was shown to decrease serotonin transport as a result of SERT internalization. This was evident as PKC activators increased phosphorylation levels of SERT, leading to redistribution from the cell surface to an intracellular compartment. Serotonin and other ligands that permeate the transporter were shown to reduce PKC activator mediated SERT internalization. Antidepressants such as TCAs and SSRIs blocked the ability of 5-HT to limit SERT internalization (Ramamoorthy & Blakely, 1999; Ramamoorthy et al, 1998). In the same vein, studies showed that prolonged exposure to 5-HT led to an increase of SERT cell surface expression (Whitworth et al, 2002), whereas chronic exposure to SSRIs led to a marked down-regulation of SERTs on the cell surface (Benmansour et al, 2002). The research team led by Ramamoorthy therefore proposed a “use it or lose it” model for SERT regulation, which holds that transport activity stabilizes and even

enhances SERT cell surface expression, whereas transporter blockage leads to SERT internalization (Steiner et al, 2008). This is in contrast to studies investigating DAT surface expression, which show that the inhibitors cocaine and methylphenidate increase DAT (Daws et al, 2002). On the other hand, dopamine and amphetamine lead to DAT internalization (Chi & Reith, 2003; Kahlig et al, 2004). This illustrates that findings characteristic for one transporter cannot necessarily be extrapolated to other members of the *SLC6* gene family. Yet, a recent study investigating drug induced SERT internalization revealed that 5-HT itself led to a dose dependent reduction of cell surface-expressed SERT molecules (Kittler et al, 2010). A study by Brenner et al. may provide further inconsistency on this issue. Investigating the platelet SERT, they observed a biphasic effect of exogenous 5-HT on the density of transporter molecules expressed on the plasma membrane. Whereas low 5-HT concentrations led to enhanced SERT expression, higher concentrations had the opposite effect, leading to reduced surface expression (Brenner et al, 2007).

In addition to PKC, several other SERT-associated proteins have been suggested to promote SERT endocytosis, such as the serine/threonine phosphatase PP2A, the plasma membrane SNARE protein syntaxin 1A, the secretory carrier membrane protein 2 (SCAMP2), an carboxy-terminal association of SERT with neuronal nitric oxide synthase (nNOS or NOS1), and the α2 adrenergic receptor (see Steiner et al, 2008 for review). Conversely, several SERT-associated proteins that increase transporter surface expression, including A3 adenosine receptor (A3AR)-dependent elevations of SERT have been identified (Steiner et al, 2008). Interestingly, protein kinase G (PKG) mediated phosphorylation of the SERT was shown to up-regulate SERT without increasing SERT cell surface expression (Ramamoorthy et al, 2007), which suggests trafficking-dependent, as well as trafficking-independent modulation of SERT activity (Steiner et al, 2008). However, others have suggested that PKG-mediated SERT up-regulation also includes trafficking of the transporter (Zhu et al, 2004), indicating that PKC enhances both SERT cell surface expression as well as trafficking-independent SERT function via increased 5-HT affinity (Steiner et al, 2008). Even PKC dependent SERT down-regulation was shown to be partly independent of endocytosis, depending on the phosphorylation site on SERT (Jayanthi et al, 2005). Thus,

changes in SERT utilization via a change in 5-HT availability or by SERT inhibitors may not only affect SERT distribution but also its affinity state.

1.2.3. SERT blockage in relation to antidepressant treatment

As the SERT sustains neuronal 5-HT storage in the cell and regulates extracellular 5-HT levels, it is essential for brain 5-HT homeostasis. This becomes evident in SERT KO mice that show a 60-80% reduction in 5-HT concentrations in several brain regions (Bengel et al, 1998). From a psychiatric perspective it is therefore of major interest, how drugs that inhibit SERT function affect SERT trafficking and how these modifications may relate to antidepressant treatment effects. It is well known, that the onset of antidepressant effects greatly lags behind treatment start, with a delay of about two to three weeks (Gelenberg & Chesen, 2000). Acute blockage of the SERT *per se* was therefore soon acknowledged to be insufficient in explaining the antidepressant effect. Thus, studies started to search for molecular changes and down-stream modifications triggered by SSRI blockage that temporally coincide with the delayed treatment effect (see Pineyro & Blier, 1999 for review). Benmansour et al. was one of the first to propose SERT trafficking itself as a candidate, by investigating the time course for SERT down-regulation after chronic SSRI treatment *in vivo* (Benmansour et al, 2002). Rats were treated 4, 10, 15 or 21 days subcutaneously with sertraline and SERT binding was measured after varying washout periods using [^{3}H]-cyanoimipramine as a ligand. The authors showed that after 4 or 10 days of treatment, SERT binding decreased only by 15 to 30%. However, after 15 days of treatment, they detected strong SERT down-regulation of about 80% which persisted up to 21 days. Furthermore, *in vivo* chronoamperometry in the dorsal hippocampus showed that 5-HT uptake after 4 or 10 days of treatment was comparable to a control group receiving vehicle, whereas, after 15 days of treatment, 5-HT clearance was markedly decreased. These results led Benmansour et al. to propose that SERT down-regulation may be the crucial mechanism underlying the antidepressant treatment effect. Subsequent *in vivo* studies similarly observed substantial SERT down-regulation after chronic treatment with various SSRIs (Gould et al, 2003; Mirza et al, 2007). Cell culture studies provided further evidence of SERT down-regulation, although this was already observed after a few hours of treatment (Gould et al, 2003; Horschitz

et al, 2001; Lau et al, 2008). This suggests that SERT trafficking takes longer *in vivo* than *in situ,* a finding that is also observed for 5-HT_{2A} receptor internalization by clozapine treatment (Willins et al, 1998). Taken together, studies provide fairly consistent evidence of SERT trafficking to intracellular compartments upon transporter blockage, leading recent mathematical models of antidepressant treatment effects to base their assumptions on SERT down-regulation (Best et al, 2011).

However, as all players within the serotonergic system are interrelated, it is evident that sustained SERT blockage also affects the expression and the sensitivity of the various 5-HT receptors. Indeed, this has been demonstrated for subtypes of the 5-HT1 receptor family (Le Poul et al, 1995; Le Poul et al, 1997; Newman et al, 2004), the 5-HT2 receptors (Kong et al, 2002; Massou et al, 1997), 5-HT3 receptors (Fan, 1994), 5-HT4 receptors (Licht et al, 2009; Vidal et al, 2009), and 5-HT7 receptors (Mullins et al, 1999). Some of these receptors are autoreceptors (5-HT_{1A} and 5-HT_{1B}) located at soma, dendrites and presynaptic sites of serotonergic neurons, whereas others are heteroreceptors located downstreatm at postsynaptic sites on neurons of other neurotransmitters. Considering the close connections between modulatory neurotransmitter systems (Alex & Pehek, 2007; El Mansari et al, 2010), it is thus quite evident that antidepressant induced SERT blockage, and subsequent elevations in 5-HT affect other modulatory neurotransmitter systems besides glutamate and GABA. Serotonergic modulation has been described for the dopaminergic (Alex & Pehek, 2007) as well as the norepinephrinergic system (Mateo et al, 2000) and vice versa. Moreover, antidepressants were shown to affect intracellular signaling pathways leading to a modulation of adult cell proliferation and neurogenesis in the hippocampus (Malberg et al, 2000; Manev et al, 2001). This was observed only after prolonged treatment, which might suggest neurogenesis as the final common mechanism underlying the therapeutic effect of antidepressants.

From a phenomenological perspective, major depressive disorder (MDD) comprises a variety of symptoms within virtually all psychological dimensions, ranging from emotion and motivation to cognition, attention and memory. Antidepressant treatment has been shown to alleviate these symptoms to different degrees, a fact that has been associated with the specific

pharmacological profile of the different antidepressants (e.g., Nutt et al, 2007). Still, with respect to the diverse biological mechanisms related to SERT blockage mentioned above, one may ask whether these specific mechanisms can be related to the alleviation of specific symptoms. Moreover, the SERT is not equally distributed within the serotonergic projection sites but has a distinct pattern within cortical and subcortical regions (see section 1.4.1.). Thus, it is likely that the distribution within regions with different functions results in varying serotonergic roles within these functions (e.g., Reimold et al, 2008; Takano et al, 2007). To answer these questions, research that is focused on the quantification of the SERT in the living human brain is necessary, which will be the subject of the next two sections.

1.3. Quantification of the brain SERT with PET and [^{11}C]DASB

1.3.1. PET and SPECT to study the SERT

In vivo imaging of the brain SERT makes use of two diagnostic methods from nuclear medicine, single-photon emission computed tomography (SPECT) and positron emission tomography (PET) (Huang et al, 2010). Unlike conventional computed tomography (CT), where the source of radiation is outside the body, PET and SPECT require a short-lived radionuclide that is applied via the bloodstream to a living subject. While SPECT uses gamma-emitting radionuclides, PET tracers emit positrons, also known as positive beta decay. After traveling a short distance of few millimeters in tissue, the emitted positron interacts with an electron leading to annihilation and emission of two gamma photons in approximately opposite directions (Cherry et al, 2003). Detectors arranged in rings and consisting of a scintillator and a photomultiplier are used to detect these pairs of coincident photons. That is, only photons that arrive simultaneously are detected, whereas those, whose detection does not coincide, are ignored. Coincidence detection using PET thus provides better radiation event localization compared to SPECT, where only one single photon is emitted and detected via gamma cameras that are rotated around the body (Cherry et al, 2003). Consequently, PET provides images with much higher resolution and better signal-to-noise ratio. These advantages over SPECT, however, come at increased financial cost, partly because PET radionuclides are less easily-obtained and shorter-lived, often making

an on-site cyclotron necessary. Whereas ^{18}Fluor, for example, has a half-life of 110 min and can be easily purchased and transported, the half-life for ^{11}Carbon is only 20 min, for ^{13}Nitrogen only 10 min, and for ^{15}Oxygen only 2 min (Wadsak & Mitterhauser, 2010).

In order to visualize the distribution of certain proteins, such as the SERT, with PET and SPECT, it is necessary that radionuclides are attached to a biologically active ligand (Wadsak & Mitterhauser, 2010). Together, both parts form the so called "radioligand", "radiopharmaceutical" or simply "tracer". A high degree of selectivity and specificity towards the target site (such as the SERT) is necessary for a suitable ligand and proper radionuclides should have a half-life long enough for effective radiolabelling (Wadsak & Mitterhauser, 2010). Thus, to qualify as an effective radioligand, several requirements must be fulfilled (illustrated in detail by Huang et al, 2010): First of all, a tracer must have an appropriate lipophilicity in order to cross the blood-brain barrier (BBB). That is, too low as well as too strong lipophilic tracers are detrimental, as strong lipophilicity is often associated with increased binding to non-targets (non-specific binding). Tracer affinity to the target also affects the ratio of specific to non-specific binding, with K_D's (equilibrium dissociation constant, i.e. inverse of binding affinity) in the range of 0.01 nM to 10 nM being preferred. Furthermore, tracer affinity determines the duration of the scan. This becomes clear when considering the quantification of PET data. As opposed to irreversible tracers, which are permanently bound to their targets, tracers that bind to receptors or transporters must be reversible in nature for human suitability. In order to quantify the binding potential which is indicative of target density (see section 1.3.3), a tracer has to reach equilibrium between association to and dissociation from the target. As increased affinity leads to a slower dissociation, a longer measurement time is required to reach equilibrium (Huang et al, 2010). As already mentioned above, binding selectivity is another prerequisite for a suitable radioligand. That is, a tracer should have appropriate affinity to only one receptor (-subtype) or transporter. The desired selectivity ratio is greater or equals 100 for targets over non-targets. Finally, requirements also address the metabolic profile of a tracer, i.e., radiolabeled metabolites should not be capable of entering the brain, as this would profoundly decrease the signal-to-noise ratio due to an increase of non-specific binding.

1.3.2. PET and SPECT radiopharmaceuticals for the SERT

Great efforts have been devoted to the development of suitable PET and SPECT SERT tracers within the last two decades (Huang et al, 2010). In the light of the high selectivity and affinity of SSRIs for the SERT, tracer development was initially focused on the radiolabeling of SSRIs. However, although these compounds showed high selectivity and affinity *in vitro*, they were not suitable for *in vivo* imaging of the SERT, illustrating that *in vitro* measures cannot readily be translated into *in vivo* performance (Huang et al, 2010). A great number of radiotracers suffered the same fate, leaving only a handful of tracers that were considered suitable for measuring the SERT in humans *in vivo*. One of the first SPECT tracers used for imaging the SERT in humans was the phenyltropane compound [^{123}I]β-CIT. However, this tracer also showed considerable affinity for the DAT. The lack of selectivity restricted its usability for SERT imaging to the midbrain, where DAT expression is lower, as compared to thalamus and striatum. Still, [^{123}I]β-CIT was used in a number of clinical studies following its validation for imaging the SERT in humans (e.g., Kugaya et al, 2004). One of the first PET ligands validated for quantification of the human SERT was an ^{11}Carbon labeled selective serotonin reuptake inhibitor from the McNeil Laboratories, [^{11}C](+)-McN5652. Although this tracer has until recently been used in clinical studies (e.g., Bailer et al, 2007), it has several disadvantages including high non-specific binding and slow clearance from the brain, among others. As a result, relatively long scanning time (up to 120 min) was necessary, and [^{11}C](+)-McN5652 was soon replaced by better tracers for imaging the human SERT (Huang et al, 2010). These tracers, a substituted diarylsulfide class of compounds, include the SPECT ligand [^{123}I]ADAM and the PET ligands [^{11}C]MADAM, [^{11}C]HOMADAM, [^{11}C]DASB and [^{11}C]AFM for human use (Huang et al, 2010). Although [^{11}C]AFM was shown to provide higher specific SERT binding signals than [^{11}C]DASB (Huang et al, 2010), the latter has been the most widely used PET tracer, which is reflected in the number of PubMed entries, ranging from 8 for [^{11}C]MADAM and [^{11}C]HOMADAM, to 10 for [^{11}C]AFM and 85 for [^{11}C]DASB (reporting date of April 18th 2013, http://www.ncbi.nlm.nih.gov/pubmed/). Following initial human studies at the beginning of the millennium (Houle et al, 2000), [^{11}C]DASB has been used to study the human SERT in a variety of psychiatric diseases, as well as in treatment studies and basic neuroscientific approaches including multimodal imaging with PET and fMRI, imaging genetics and brain network analyses.

1.3.3. Quantitative data analysis

Estimating the extent of regional SERT expression in the human brain is achieved by quantitative analysis of the PET data by means of calculation of the so-called binding potential (BP) (Innis et al, 2007). Since introduction of the binding potential in 1984, it has constituted the main outcome measure in neuroreceptor/transporter quantification (Mintun et al, 1984). The binding potential originates from *in vitro* binding assays and is defined as the ratio of target density B_{max} to dissociation constant K_D at equilibrium:

$$BP = \frac{B_{max}}{K_D} = B_{max} * affinity$$

Whereas target density and tracer affinity can be quantified separately using saturation binding assays *in vitro*, this is not appropriate for human PET studies *in vivo*. Tracer doses and occupation of the target must be negligible (<1% to 10%) in order ensure accurate modeling and to avoid physiological effects (Innis et al, 2007). However, assuming that the affinity (inverse of K_D) of a given radioligand is constant across subjects and brain regions, the binding potential directly reflects target density, i.e. SERT density (Innis et al, 2007). Calculating the binding potential needs to take several factors regarding ligand binding in the brain into account. That is, as the radiotracer crosses the blood-brain barrier (BBB) it will be present as specifically bound to the target, as nonspecifically bound (other receptors or transporters, cell membranes, etc.) and as free and unbound tracer. Thus, the recorded activity will stem from tracer in different binding conditions, or so called compartments. Movement from one to another compartment is defined by so called rate constants (K). Radioligand binding reaches equilibrium concentrations over time when no net transfer occurs between two adjacent compartments. The conceptual framework and the calculation of the binding potential are therefore only useful for ligands that are reversible in nature (see section 1.3.1 above, or Innis et al, 2007). A model that differentiates between four of such compartments (with three compartments within the brain, i.e., three tissue compartment-model) is depicted in Figure 4:

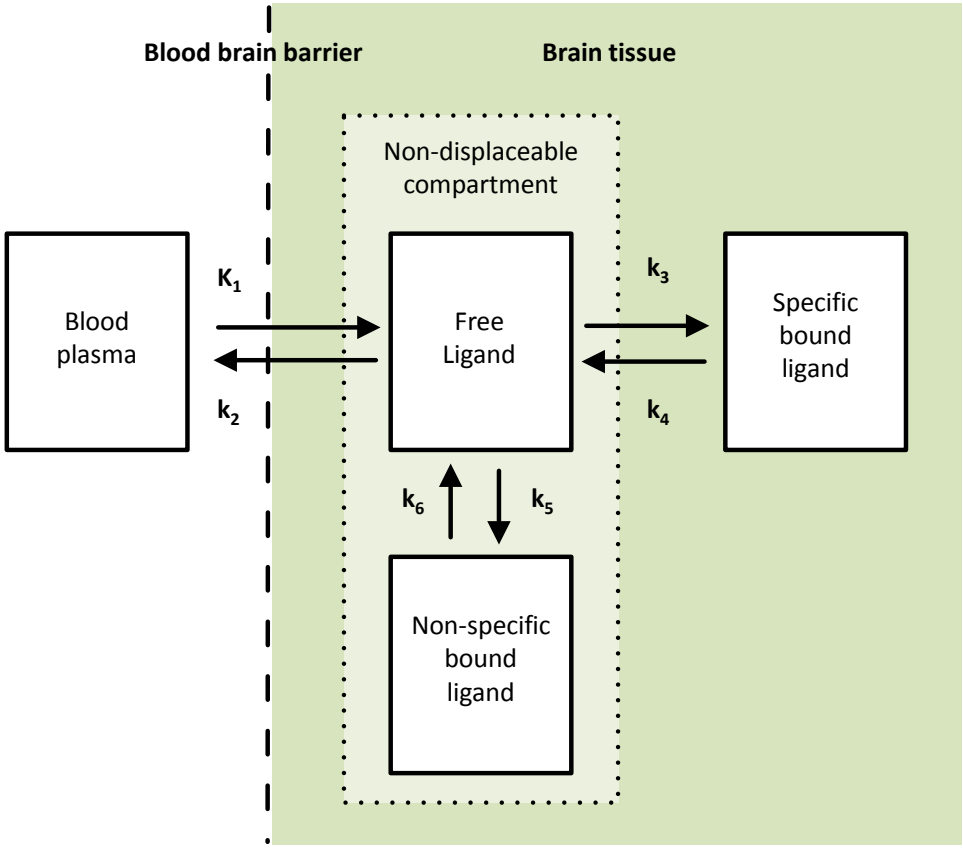

Fig 3. *Tree tissue compartment model (based on Slifstein & Laruelle, 2001).*

In this model, after application of the radiotracer in the plasma compartment, the tracer will cross the BBB and distribute to an intracerebral unbound compartment, a nonspecifically bound and a specifically bound compartment. Arrows in Fig 3 represent the kinetic rate constants. K_1 and k_2 characterize the rate of influx and efflux across the BBB, whereas k_3 and k_4 represent the association and dissociation rate constants from free ligand to the specifically bound tracer, respectively. Rate constants between free and non-specific bound ligand are represented by k_5 and k_6. The model outlined above can be converted into a two tissue compartment model (i.e., two compartments within the brain). This is based on the assumption that the exchange from radiotracer between the free and nonspecifically bound compartments is much faster than the exchange of tracer between a free and specifically bound state (Slifstein & Laruelle, 2001). The free and nonspecific bound compartment can therefore be merged to a non-displaceable compartment because a change in the fee compartment is instantaneously counterbalanced by a change in the nonspecific compartment so that the equilibrium ratio between the two

compartments is immediately restored (Slifstein & Laruelle, 2001). Brain regions that are almost devoid of targets can be described by a one tissue compartment model, because the specific bound compartment is omitted (Ichise et al, 2001). For the SERT, this is the case in the cerebellar cortex (see later).

Calculating the binding potential can be achieved via different quantification methods. For each method, different assumptions must be made where some radiotracers will meet assumptions better than others. Within the tracer kinetic modeling, the binding potential is calculated via estimation of the rate constants $K_{1\text{-}4}$ at equilibrium (Slifstein & Laruelle, 2001). The binding potential as defined above is based on the bimolecular reaction described by Michaelis-Menten (1913):

$$[L] + [R] \underset{k_{off}}{\overset{k_{on}}{\rightleftharpoons}} [LR]$$

Free ligand [L] and unbound receptor [R] (or transporter) associate to a bound receptor ligand complex [LR], with k_{on} and k_{off} being the association and dissociation kinetic rate constants, respectively. The reaction is based on a simple two tissue compartment model from *in vitro* binding assays. Over time, no net transfer of ligands occurs between the two compartments and the ligand reaches equilibrium concentration in each compartment (Ichise et al, 2001). The reaction and its relationship to BP can now be described using the equation

$$k_{on}[L][R] = k_{off}[LR]$$

and rearrangement leads to

$$\frac{[L][R]}{[LR]} = \frac{k_{off}}{k_{on}} = KD$$

with B_{max} evidently defined as [R]+[RL] (Ichise et al, 2001). Moving to the two tissue compartment as described above, we can define k_3 as the product of k_{on} and the concentration of available receptors (R-RL). At tracer dose, the bound receptor ligand complex [RL] will be very small compared to unbound receptors [R]. The available receptor [R] will thus be approximately B_{max} and hence k_3 the product of k_{on} and B_{max} (Ginovart et al, 2001). Furthermore, k_4 is equal to k_{off}. At equilibrium, the binding potential can thus be defined as k_3/k_4. That is, the binding

potential is equal to the ratio of specifically bound to free concentration of radioligand at equilibrium (Ichise et al, 2001):

$$\mathrm{BP} = \frac{\mathrm{B_{max}}}{\mathrm{K_D}} = \frac{[\mathrm{LR}]}{[\mathrm{L}]}$$

Estimation of the reference concentration [L] is achieved in several ways, leading to varying validity in calculations of the binding potential. Calculating the binding potential as the ratio of specifically bound radioligand in tissue to that of free radioligand concentration in plasma at equilibrium is denoted by BP_F (Innis et al, 2007). The ratio at equilibrium of specifically bound to total radioligand in plasma is referred to as BP_P. Both measurements are based on the assumption that the radioligand will permeate through the BBB by passive diffusion with concentrations of free ligand in tissue [L] being equal to the free concentration in plasma. Although these two estimations of the "true" *in vitro* binding potential may be most accurate, they require the measurement of radioligand in plasma by means of arterial blood sampling. A less invasive way of estimating the binding potential is achieved by calculating the ratio of specifically bound radioligand to that of nondisplaceable tracer in tissue, denoted by BP_{ND} (Innis et al, 2007). This strategy is used in reference tissue methods, where the radioligand concentration in target-rich regions is compared to that of target-free regions. However, when using BP_{ND}, it is assumed that nondisplaceable radioligand uptake is independent of treatment effects or subject groups (Innis et al, 2007), an assumption which cannot be taken for granted in many clinical settings.

As stated above, different quantification methods have been proposed for different radioligands. Estimating the binding potential via BP_{ND} for the SERT using [^{11}C]DASB was shown to be most appropriate using a linearized reference tissue parametric imaging method proposed by Ichise et al. (2003). This method was also used for estimating the binding potential in the publications arising from this thesis.

1.4. Imaging the SERT in the healthy and diseased human brain

Within the last two decades, a considerable number of PET and SPECT studies have been conducted to investigate the human SERT *in vivo*. Encouraged by the rise of SSRIs as potent antidepressant and antianxiety drugs, post mortem research and studies on the platelet SERT were followed by a collection of investigations focused on imaging the brain SERT in psychiatric conditions and under antidepressant treatment. Early on, these studies were accompanied by research dedicated to more basic neuroscientific questions such as those regarding SERT distribution in the healthy human brain (e.g., Backstrom et al, 1989).

1.4.1. SERT distribution in the human brain

Autoradiographic studies in the 1980s were the first to demonstrate a heterogeneous distribution of 5-HT uptake sites in the rodent brain (D'Amato et al, 1987; Savaki et al, 1985). The discovery of high SERT density within the brainstem and midbrain structures matched the distribution of serotonergic cells and ascending projections described a few years earlier (Azmitia & Segal, 1978; Dahlstrom & Fuxe, 1964). That is, dense SERT labeling was found in the raphe nuclei and the periaqueductal gray, the locus ceruleus, substantia nigra, superior colliculus and the ventral caudate (D'Amato et al, 1987; Savaki et al, 1985). These findings were soon complemented by post mortem human studies in the late 1980s. Highest SERT densities were found in the midbrain and diencephalon followed by intermediate densities in the basal ganglia and lowest values in cortical structures, whereas almost no SERTs have been found in the cerebellum (Backstrom et al, 1989; Cortes et al, 1988). Finally, following studies in living nonhuman primates (e.g., Laruelle et al, 1993), initial *in vivo* SERT imaging in humans was performed in the mid-1990s (Kuikka et al, 1995; Szabo et al, 1995).

The development of superior radiotracers (see section 1.3.2.) made imaging the differential SERT distribution in cortical regions exhibiting lower signal-to-noise ratio possible (see Fig 4). In addition to dense SERT binding in the brainstem and midbrain structures and intermediate binding levels in diencephalic structures and the basal ganglia, it is now known that limbic

regions such as the subgenual anterior cingulate and insular cortex, as well as parts of the temporal cortex exhibit considerably high SERT binding (Kranz et al, 2010; Saulin et al, 2012; Savli et al, 2012). These imaging findings *in vivo* are substantiated by recent post mortem data (Varnas et al, 2004).

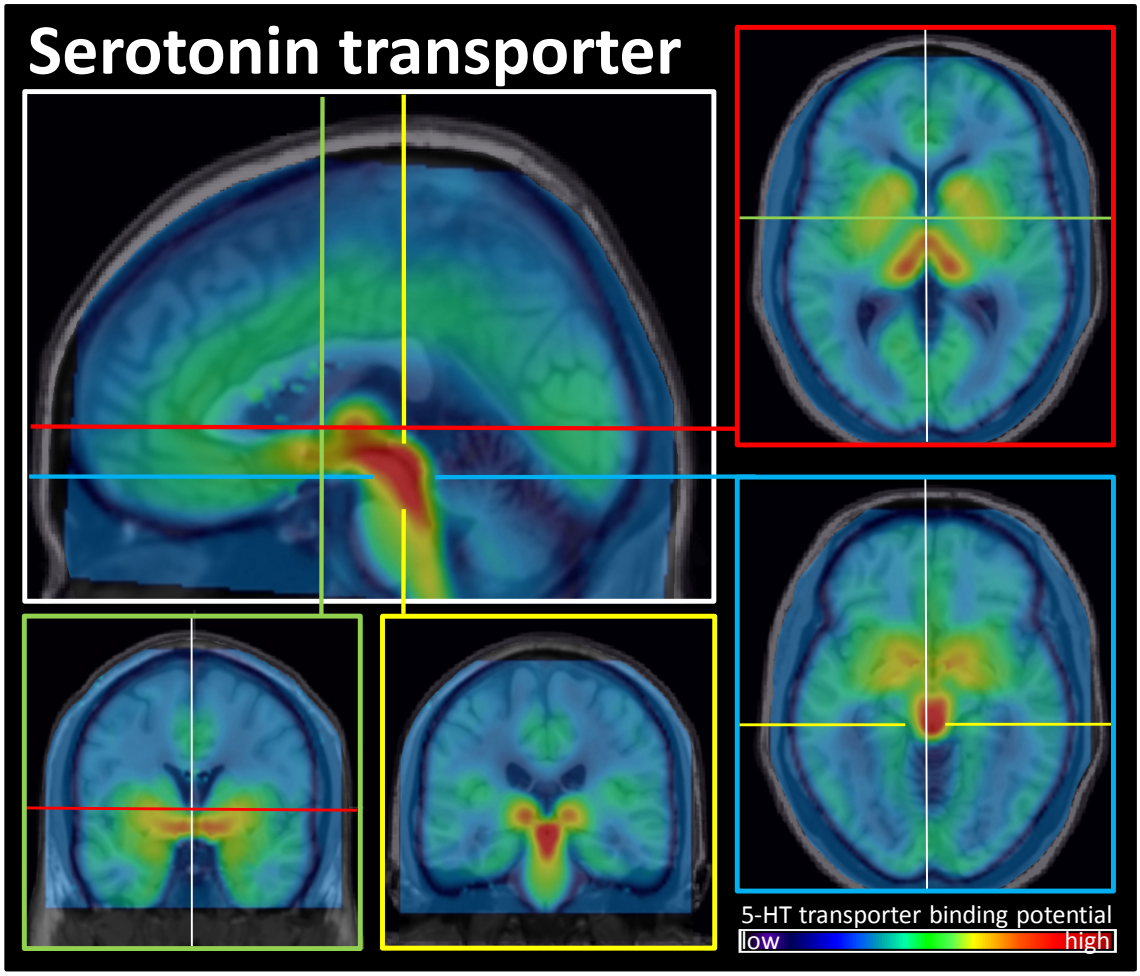

Fig 4. *Heterogeneous distribution of the SERT in the human brain. The figure shows triplanar structural images and superimposed distribution maps of SERT binding using [^{11}C]DASB. The color of a frame indicates the corresponding section within the other images (based on Kranz et al, 2010).*

Several studies have also laid their research focus on SERT distribution related to aging and gender in the healthy human brain. Based on Kakiuchi et al. (2001) who observed an age related decline in SERT binding in living monkeys, several studies substantiated this potential

relationship also in humans (e.g., Kuikka et al, 2001a; Pirker et al, 2000; van Dyck et al, 2000; Yamamoto et al, 2002, although see Buchert et al, 2006). Staley et al. were among the first to demonstrate increased SERT binding in healthy females versus males using SPECT (Staley et al, 2001). This observation was in accord with animal research, which demonstrated an increase in SERT binding upon estrogen administration in ovariectomized female and intact male rats (McQueen et al, 1997; McQueen et al, 1999). However, a short time thereafter, the same author reported SERT binding to be reduced in depressed females compared to depressed males (Staley et al, 2006). Similar observations in healthy subjects were reported by Jovanovic et al., who found reduced SERT binding potentials in several cortical and subcortical regions in females compared to males using PET and [^{11}C]MADAM (Jovanovic et al, 2008). Although, one year later, Jovanovic et al. (2009) were not able to demonstrate an effect of menstrual cycle phase on SERT or 5-HT_{1A} availability, a potential influence of ovarian steroids on the serotonergic system is most probable and may contribute to the known sex differences in the prevalence of psychiatric disorders (Bethea et al, 2002).

1.4.2. Imaging the SERT in psychiatric disorders

Proceeding from the documented efficacy of SSRIs not only in depression, but also in anxiety disorders including social phobia, panic and obsessive-compulsive disorder, in eating disorders, and premenstrual syndrome (for reviews, see Flament et al, 2012; Koen & Stein, 2011; Pearlstein, 2012), SERT density was believed to be affected in a variety of neuropsychiatric disorders. Several studies thus investigated the SERT using molecular imaging *in vivo* in relation to these disorders.

Interestingly, although SERT binding in depressive subjects has been intensely studied, no consensus has been reached on a potential increase or decrease of binding in this psychiatric disorder. Although initial findings pointed towards decreased density of SERTs in platelets and in post-mortem brain samples of depressed subjects and suicide victims (Briley et al, 1980; Paul et al, 1981; Perry et al, 1983; Stanley et al, 1982), others found no difference (for review see,

Stockmeier, 2003). These inconsistencies were ascribed mostly to methodological differences of studies, inconsistencies in the brain regions studied, medication history of the subjects or comorbid axis I psychiatric diseases (Meyer, 2007). Definite conclusions on SERT binding in MDD also in subsequent *in vivo* PET and SPECT studies have been elusive. Whereas Malison et al. (1998) observed a reduction of SERT binding using [^{123}I]β-CIT and SPECT, subsequent PET studies found either reduced (Parsey et al, 2006a; Selvaraj et al, 2011), elevated (Ichimiya et al, 2002), or the lack of a difference (Herold et al, 2006; Meyer et al, 2004a) compared to healthy controls. Interestingly, some studies tried to explain these inconsistencies by examining the variability of SERT binding within depressed subjects in relation to different depression symptomatology. Meyer et al. (2004a) observed that SERT binding was positively associated with negativistic dysfunctional attitudes, whereas a recent study by Miller et al. only observed reduced SERT binding in suicide attempters among their depressed study sample (Miller et al, 2013).

Similar inconsistencies can be found in the literature when SERT binding is investigated in other psychiatric disorders (without claim of completeness). This points towards the necessity of considering several mediating variables such as disease onset or sex when researching these disorders. Whereas Simpson et al. observed no difference in SERT binding between medication-free subjects with obsessive-compulsive disorder (OCD) and healthy controls (Simpson et al, 2003), a recent study found reduced SERT availability to be associated only with late but not with early onset of this disorder (Hesse et al, 2011). A study investigating panic disorder by Maron et al. reported regionally increased as well as decreased SERT binding in male patients compared to healthy control males, whereas no difference was observed for the female groups (Maron et al, 2011). Finally, divergent findings and the necessity of taking moderating variables into account, such as disease subtypes or 5-HTTLPR genotype does also not make a hold when moving to eating disorders (Bailer et al, 2007; Kuikka et al, 2001b; Lundgren et al, 2008; Pichika et al, 2012; Tauscher et al, 2001).

1.4.3. SERT occupancy measured with PET and its relation to treatment outcome

Imaging the SERT with SPECT and PET *in vivo* also provides the opportunity to study the percent reduction in binding potential after drug administration (referred to as "occupancy") and its relation to drug dosage and to treatment outcome. Of special note in this context is a study by Meyer et al. who measured 77 subjects before and 4 weeks after administration of five different SSRIs using PET and [^{11}C]DASB (Meyer et al, 2004b). Subjects included patients with MDD with or without comorbidities (OCD or panic disorder) and a group of healthy controls. Patients received citalopram, fluoxetine, sertraline, paroxetine, or venlafaxine at least at minimum therapeutic doses whereas healthy controls received no more than half of the minimum of recommended daily treatment dose. For the patient sample, the authors observed striatal SERT occupancies of about 80% for all SSRIs with minimum therapeutic treatment dose. In the case of citalopram, this meant that 20-40mg/day were necessary to achieve 80% striatal SERT occupancy, with the fitted regression line crossing the 80% mark at about 50ng/mL of citalopram plasma level. As a side note, a later study based on these findings confirmed that plasma levels less than 50ng/mL of citalopram were associated with an unfavorable treatment outcome (Ostad Haji et al, 2011). Interestingly, SERT occupancy in the study by Meyer et al. was not equally distributed throughout the brain regions studied. Whereas SERT occupancy was significantly higher in the midbrain and significantly lower in the thalamus (8%), the values in prefrontal cortex, anterior cingulate and cuneus were comparable to striatal SERT occupancies. Furthermore, the correlation between dosage or plasma concentrations and BP_{ND} including patients and controls were best fitted by a nonlinear relationship, showing a plateau of occupancy as plasma levels/dose increased for all five drugs. This nonlinear relationship had already been found in earlier studies (Ginovart et al, 2003; Kent et al, 2002; Meyer et al, 2001) and has been confirmed in several subsequent occupancy studies of SERT (Klein et al, 2006; Klein et al, 2007; Parsey et al, 2006a; Takano et al, 2006, among others).

However, Meyer et al. did not observe a relationship between SERT occupancy and symptom decline by means of percent reduction in the Hamilton Rating Scale for Depression (HAM-D) (Meyer et al, 2004b). This is also in line with several subsequent SPECT studies (Catafau et al,

2006; Cavanagh et al, 2006; Herold et al, 2006). Only one SPECT study indicated that SSRI induced occupancy in the diencephalon was associated with treatment outcome (Kugaya et al, 2004). This same study also showed that SERT availability before treatment could predict the antidepressant treatment response, a finding that has been replicated only by trend in a recent PET study focused on predictors of one-year remission in MDD (Miller et al, 2008).

1.5. Open questions

While the chapters above do not address all research topics pertaining to the SERT in psychiatry and molecular imaging, they intend to establish a thorough background for the publications arising from this thesis. As already stated in the introduction, the serotonergic system is implicated in a variety of cognitive and emotional functions. Most of these functions, however, seem to be lateralized with respect to their neural or behavioral correlates. Furthermore, not only the functions, but also their asymmetries have been linked to the serotonergic system, as SSRIs seem to affect this hemispheric specialization (e.g., Bar et al, 2003; Walsh et al, 2010). Several rodent studies suggest strong lateralization of 5-HT concentration, turnover and uptake (Andersen & Teicher, 1999; Rosen et al, 1984; Valdes et al, 1981). Furthermore, recent animal research even suggests an asymmetric expression of the SERT itself (Tellez et al, 2010), though so far no study has investigated this potential asymmetry in humans, neither *in vitro* nor *in vivo*. A hemispheric asymmetry in SERT distribution is also described in the context of sex steroid hormones. Sex steroids have been proposed to partly underlie the observed sex dimorphism in brain lateralization (Diamond, 1991; Draca, 2010) and it is known that sex steroids influence SERT expression and other components of the serotonergic system (Bethea et al, 2002). Finally, two temporarily separated androgen surges within pregnancy may underlie the sexual differentiation of the brain and that of the genitals. It was therefore proposed that a mismatch between these two processes may underlie transsexuality (Swaab & Garcia-Falgueras, 2009). However, so far no study has investigated SERT distribution or asymmetry in this population.

Heterogeneous SERT distribution among different brain regions has been thoroughly studied in depressed subjects and healthy controls (see section 1.4.1.). Several studies have been conducted also to study SERT occupancy by SSRIs. As mentioned earlier, Meyer et al. observed

higher SERT occupancy in the midbrain and lower values in the thalamus when compared to the striatum (Meyer et al, 2004b), indicating that SERT occupancy may be heterogeneous between brain regions. However, no study so far has investigated this potential heterogeneity in a systematic manner. Furthermore, the association between heterogeneous SERT distribution and SERT occupancy remains unknown. Finally, no consistent view has been reached concerning SERT distribution and occupancy in relation to treatment outcome among brain researchers. SERTs located in the raphe nuclei and in projection areas may have different effects on neural cell firing of 5-HT neurons and thus influence the extracellular levels of 5-HT in an inverse manner. Investigating a potential influence of SERT distribution on a systems level by comparing brainstem SERTs and those in terminal regions on antidepressant treatment has, however, not been pursued before.

II. AIMS OF THE THESIS

Based on the open issues mentioned in the last section, the overall aims of this thesis were three-fold: A first aim was to further increase our knowledge about the distribution of the SERT by investigating a potential asymmetry of SERT binding and its relation to gender identity. The first publication listed below deals with this issue. Elucidating the relation between regional SERT distribution and SERT occupancy by SSRIs was a second objective of this thesis. This is subject of the second publication. Finally, a third objective was to unveil the interregional relationship between SERTs in serotonergic nuclei and projection areas and its relation to antidepressant treatment outcome. This is subject of the third publication. The specific aims can thus be specified within five bullet points:

- To test whether SERT binding is asymmetrically distributed within the human brain using PET and the radioligand [^{11}C]DASB.
- To investigate SERT binding and SERT asymmetry in relation to gender identity by comparing healthy male and female control subjects to male-to-female transsexuals.
- To test whether SERT occupancy after acute and prolonged SSRI treatment is differently distributed within the human brain using PET and [^{11}C]DASB.
- To test whether regional SERT distribution before treatment affects SERT occupancy after acute and prolonged treatment with SSRIs.
- To investigate the potential of interregional relationship between SERTs in the raphe and in projection areas as a predictor of antidepressant treatment outcome.

III. RESULTS

3.1. First publication: Cerebral Serotonin Transporter Asymmetry in Females, Males and Male-to-Female Transsexuals measured by PET in vivo

Georg S. Kranz[1], Andreas Hahn[1], Pia Baldinger[1], Daniela Haeusler[2], Cecile Philippe[2], Ulrike Kaufmann[3], Wolfgang Wadsak[2], Markus Savli[1], Anna Hoeflich[1], Christoph Kraus[1], Thomas Vanicek[1], Markus Mitterhauser[2], Siegfried Kasper[1], Rupert Lanzenberger[1]*

[1]Department of Psychiatry and Psychotherapy,
[2]Department of Nuclear Medicine,
[3]Department of Obstetrics and Gynecology,
Medical University of Vienna
Waehringer Guertel 18-20
1090 Vienna, Austria

Published in:

Brain Structure and Function 2012 Dec 9. [Epub ahead of print]

[2011, IF: 5.628]

Correspondence to: Assoc. Prof. Rupert Lanzenberger, MD
Department of Psychiatry and Psychotherapy
Functional, Molecular & Translational Neuroimaging Lab
Medical University of Vienna
Waehringer Guertel 18-20
1090 Vienna, Austria
Ph.: +43 – 40400 3825
Fax: +43 – 40400 3099
Email: rupert.lanzenberger@meduniwien.ac.at
Web: http://www.meduniwien.ac.at/neuroimaging/

3.1.1. Abstract

The serotonergic system modulates brain functions that are considered to underlie affective states, emotion and cognition. Several lines of evidence point towards a strong lateralization of these mental processes, which indicates similar asymmetries in associated neurotransmitter systems. Here, our aim was to investigate a potential asymmetry of the serotonin transporter distribution using Positron Emission Tomography and the radioligand [^{11}C]DASB in vivo. As brain asymmetries may differ between sexes, we further aimed to compare serotonin transporter asymmetry between females, males and male-to-female transsexuals whose brains are considered to be partly feminized. Voxel-wise analysis of serotonin transporter binding in all groups showed both strong left and rightward asymmetries in several cortical and subcortical structures including temporal and frontal cortices, anterior cingulate, hippocampus, caudate and thalamus. Further, male controls showed a rightward asymmetry in the midcingulate cortex which was absent in females and male-to-female transsexuals. The present data support the notion of a lateralized serotonergic system, which is in line with previous findings of asymmetric serotonin-1A receptor distributions, extracellular serotonin concentrations, serotonin turnover and uptake. The absence of serotonin transporter asymmetry in the midcingulate in male-to-female transsexuals may be attributed to an absence of brain masculinization in this region.

Keywords

Serotonin transporter, cerebral asymmetry, lateralization, gender dysphoria, transsexual

3.1.2. Introduction

The essential role of the neurotransmitter serotonin (5-HT) in the realm of emotional and cognitive processing is well established and these psychological functions are considered to be lateralized. Lateralization of emotional processing has repeatedly been reported (Ley and Bryden 1979; Asthana and Mandal 2001; Alves et al. 2008). Negative stimuli seem to be processed in the right hemisphere, whereas positive stimuli are related to the left hemisphere (Otto et al. 1989; Stefanics et al. 2012; Nijboer and Jellema 2012; Alves et al. 2008). Lateralization of emotion processing was further linked to depressive personality traits (Biondi et al. 1993) and was shown to be influenced by treatment with selective serotonin reuptake inhibitors (SSRI) (Walsh et al. 2010). A higher pain threshold and pain tolerance was reported for the right hand (Chandramouli et al. 1993; Sarlani et al. 2003; Lugo et al. 2002).This finding seems to be further increased in patients with major depression (Bar et al. 2003; Schwier et al. 2010, although see Spernal et al. 2003) and similarly influenced by SSRI treatment (Bar et al. 2003). Furthermore, studies in rodents suggest asymmetric serotonergic modulation of brain regions and circuits. Serotonin concentrations where shown to be higher in left striatum and right accumbens and a greater 5-HT turnover was observed in the left than in the right accumbens (Rosen et al. 1984). Higher serotonin concentrations in the right amygdala were related to greater anxiety (Andersen and Teicher 1999), while expression of the serotonin transporter (SERT, 5-HTT) upon drug administration, as well as serotonin uptake via the SERT, were shown to be asymmetric (Valdes et al. 1981; Tellez et al. 2010).

In addition to the prominent role of serotonin in the modulation of emotions, there is strong evidence regarding a serotonergic role in cognitive control and flexibility (Clarke et al. 2004; Clarke et al. 2005; Clarke et al. 2007) and recently, cognitive flexibility was shown to be lateralized (Ocklenburg et al. 2012). Other strongly lateralized functions may also be influenced by serotonin, including hearing (Kahkonen et al. 2002) and handedness (Westergaard et al. 2003). The above mentioned studies therefore strongly point towards an asymmetric serotonergic system and associated functions, which complements asymmetries in other transmitter systems, including the dopaminergic (Martin-Soelch et al. 2011; Tomer et al. 2012) and noradrenergic system (Young and Williams 2010; Fitzgerald 2012).

Recently, we showed strong asymmetry of the human serotonin-1A (5-HT_{1A}) receptor, the major inhibitory receptor of the serotonergic system, especially in regions of auditory and language processing (Fink et al. 2009). Considering the lateralization of the human brain with respect to the serotonergic neurotransmitter system, the primary aim of the present study was to further examine a potential hemispheric asymmetry by investigating the SERT in vivo with positron emission tomography (PET) and the radioligand [^{11}C]DASB.

Although the neurotransmitter serotonin is most frequently associated with the mediation of emotion and cognitive processing, several studies have stressed its significance in embryonic brain development (Verney et al. 2002; Vitalis et al. 2007), neural cell migration (Riccio et al. 2009) and sexual brain differentiation (Dakin et al. 2008). Furthermore, it is well established that sex steroids exert a strong influence on the serotonergic system in early life and adulthood (Simerly et al. 1985; McQueen et al. 1997; Bethea et al. 2002; Lanzenberger et al. 2011; Witte et al. 2009; although see Stein et al. 2008). Sex steroids modulate brain development (McEwen 1992; McCarthy 2008) and prenatally present androgens and estrogen have permanent or "organizational" effects on sexual brain differentiation (Phoenix et al. 1959; Paus 2010; Wilson and Davies 2007; Bakker and Brock 2010). Sex steroids may also underlie the frequently observed sex dimorphism in brain lateralization i.e., brain structure and function of males seem to be more lateralized than that of females (Amunts et al. 2007; Amunts 2008; Diamond 1991; Draca 2010; Gur et al. 1999; Hausmann and Gunturkun 2000; Wisniewski 1998; although see Sommer et al. 2008; Takao et al. 2011). Since sexual differentiation of the brain and that of the genitals is temporarily separated within pregnancy, studies suggested that these two processes can be influenced independently and may eventually result in transsexuality (Swaab and Garcia-Falgueras 2009; Savic et al. 2010). This view is supported by post mortem studies, indicating atypical sexual differentiation of hypothalamic nuclei in male-to-female transsexuals (Garcia-Falgueras et al. 2011; Garcia-Falgueras and Swaab 2008; Kruijver et al. 2000; Zhou et al. 1995). The second aim of the present study was therefore to investigate brain asymmetry of the SERT in relation to prenatal brain differentiation by comparing SERT binding in healthy female (FC) and male control subjects (MC) to that of untreated male-to female (MtF) transsexuals.

3.1.3. Material and methods

Subjects

A total of 36 subjects aged 19-54 years, consisting of 9 female controls (FC), 13 male controls (MC) and 14 male-to-female transsexuals (MtF), were included in this study. Subjects age was comparable between groups (FC=29.0±9.9, MC=29.8±10.2, MtF=31.4±9.1 (mean±SD), p=0.84, ANOVA). All subjects were right-hand dominant, assessed with the Edinburgh Inventory (Oldfield 1971). To rule out physical, psychiatric and neurological disorders (except for transsexualism in MtF transsexuals) all subjects underwent standard medical examinations, electrocardiogram, routine laboratory tests and the Structural Clinical Interview (SCID) for DSM-IV disorders (American Psychiatric Association 2000). Further exclusion criteria were past or current substance abuse, intake of psychotropic medication, pregnancy and hormonal treatment (tested with multi-drug screen test panel and HCG (Human Chorionic Gonadotropin) pregnancy test at the screening visit and before the PET scan). Female controls were scanned randomly relative to their menstrual cycle. None of them used hormonal contraception and none were postmenopausal. Plasma hormone levels of MtF transsexuals were within the male range (testosterone: 4.2±1.5 [2.5-8.4 ng/ml], estrogen: 27.6±13.9 [14-60 pg/ml], progesterone: 0.6±0.2 [0.2-1.4 ng/ml]; mean±SD [male reference range]). Diagnostic assessment of transsexualism followed DSM-IV-TR and ICD-10 (World Health Organization, 1993) and was made after several semi-structured, socio-demographic, clinical and psychiatric interviews, based on legal requirements for cross-sex hormonal treatment in Austria. All MtF transsexuals were recruited from the Transgender outpatient-unit of the Department of Obstetrics and Gynecology, Medical University of Vienna, were naïve to steroid hormone treatment and wanted sex reassignment. All of them reported experiencing gender dysphoria at a relatively early age (before, or at puberty). Six MtF transsexuals had homosexual, seven heterosexual and one had a bisexual orientation, assessed using the Klein Grid (Klein et al. 1985). After complete description of the study to the subjects, written informed consent was obtained. The study was approved by the Ethics Committee of the Medical University of Vienna.

PET Imaging

All PET scans were performed in a GE Advance full-ring scanner (General Electric Medical Systems, Milwaukee, WI, USA) in 3D mode at the Department of Nuclear Medicine, Medical University of Vienna. A 5 min transmission scan was done using retractable ^{68}Ge rod sources for tissue attenuation correction (Lanzenberger et al. 2009; Hahn et al. 2012). Data acquisition started simultaneously with a bolus injection of [^{11}C]DASB measuring brain radioactivity in a series of 50 consecutive time frames. Mean injected dose and specific activity where not significantly different between groups (injected dose: FC=346.9±66.3, MC=349.8±53, MtF=352±59.9 MBq; specific activity: FC=26.9±27.9, MC=40.1±20.9, MtF=31.9±18.7µg; mean±SD, p>0.3, ANOVA). Total acquisition time was 90 minutes. Collected data were reconstructed in volumes consisting of 35 transaxial sections (128 x 128 matrix) using an iterative filtered back projection algorithm (FORE-ITER) with a spatial resolution of 4.36 mm full-width at half maximum (FWHM) 1 cm next to the center of the field of view. For radiotracer preparation and radiochemical variables, see (Lanzenberger et al. 2012; Haeusler et al. 2009).

SERT Quantification

The SERT binding potential (BP_{ND}) (Innis et al. 2007) was quantified using the multilinear reference tissue model (MRTM2) (Ichise et al. 2003). Following between-frame motion correction, individual summed PET images where spatially normalized to a custom symmetrical PET template in stereotactic Montreal Neurological Institute (MNI) space using SPM8 (Wellcome Trust Centre for Neuroimaging, London, UK; http://www.fil.ion.ucl.ac.uk/spm/). To minimize misalignment inherent to the normalization procedure, the PET template was created via T1-weighted MRI images (Meyer et al. 1999), which were available in a subsample (n=19). MRI images were spatially normalized using the "segment" option in SPM8. The obtained transformation matrix was then applied to the summed PET images after co-registration to the MRI scans. To this end, a tracer-specific template was flipped and averaged with the unflipped template (Takao et al. 2011). Whole-brain voxel-wise SERT BP_{ND} maps were computed. Cerebellar gray matter (excluding vermis and venous sinus) was used as reference region as recent post mortem and in vivo SERT quantification identified the cerebellar grey matter as optimal reference region for [^{11}C]DASB (Parsey et al. 2006; Meyer 2007). All modeling

calculations were performed using PMOD image analysis software, version 3.3 (PMOD Technologies Ltd, Zurich, Switzerland, www.pmod.com).

Asymmetry Processing and Statistical Analysis

Data were analyzed with SPM8 using repeated measures analyses of variance (ANOVA) with group as the between subjects factor, SERT asymmetry as repeated factor and group*asymmetry as the interaction term. Although contrasting asymmetry indexes is reported as being more sensitive in comparison to standard SPM analysis (Didelot et al. 2010; Soma et al. 2012), we refrained from comparing asymmetry indexes to avoid potential problems with ratio distributions for standard statistics (Coles 2008). In a second step, the potential confounding variables age and the radiochemical variables injected dose and specific activity were included in the analysis as variables of no interest. The alpha level was set at 0.05 false discovery rate (FDR) corrected at the cluster level following a voxel-level threshold of $p<0.001$ uncorrected with a spatial extent of $k\geq5$ voxel. Since the factor SERT asymmetry was assessed by comparing original with flipped images, voxel-wise comparisons for asymmetry and interaction effects were FDR corrected for only one hemisphere. Cohen's d was calculated for measuring effect sizes of significant peak voxels using original standard deviations. We refrained from using the standard deviation of change scores (which corrects for the amount of correlation between measures for the between-subjects comparisons) in order to avoid overestimation of the actual effect size (Dunlap et al. 1996) and because only the raw score approach is comparable with an effect size from an independent groups design.

3.1.4. Results

Voxel-wise analysis of SERT BPND differences between the left and right hemispheres (main effect of asymmetry including all 36 subjects) showed leftward, as well as rightward asymmetries in several cortical and subcortical areas (see Table1, Fig.1 and 2).

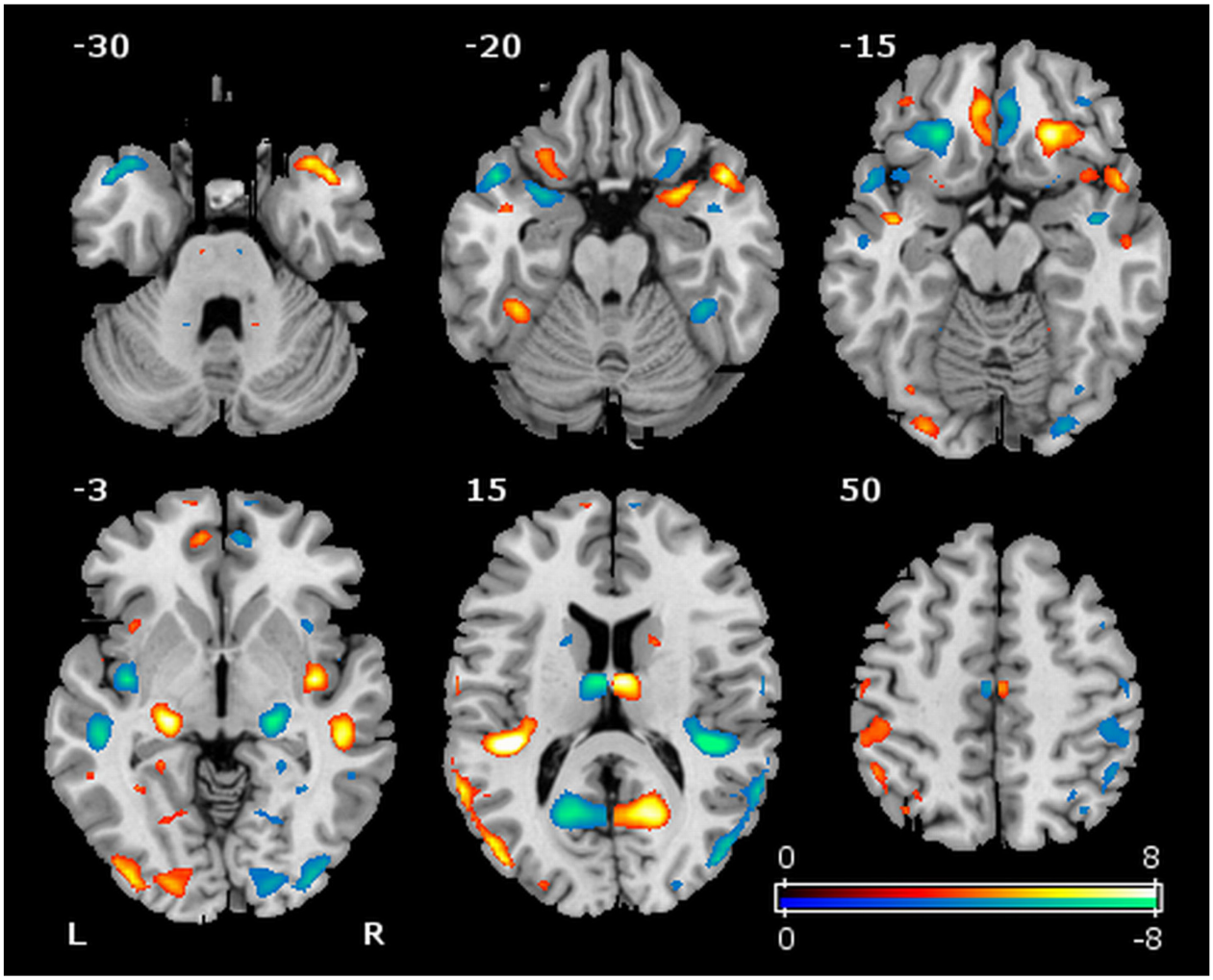

Fig 1. *Serotonin transporter asymmetries in 36 right-handed subjects (13 male controls, 14 male-to-female transsexuals and 9 female controls) aged 19-54 (P < 0.05, false discovery rate corrected at the cluster level). Numbers indicate z-coordinates of horizontal planes in mm MNI space (Montreal Neurological Institute). The color bars represent the t score at each voxel. Red-to-yellow indicates elevated, blue-to-green indicates reduced SERT* BP_{ND} *compared to the contralateral side. Left is left.*

Elevated left compared to right SERT binding i.e., leftward asymmetry, was found in planum temporale/superior temporal gyrus (Cohen's d=1.0), middle (d=0.9) and inferior orbitofrontal cortex (d=0.3), hippocampus (d=1.1), middle (d=0.7) and superior occipital gyrus (d=0.6), postcentral (d=0.6), angular (d=0.9) and fusiform gyrus (d=0.5), caudate (d=0.5) and insula (d=0.7), as well as in several other frontal and occipital regions (all p<0.05 corrected cluster). Elevated right compared to left SERT binding (rightward asymmetry) was detected in the middle temporal pole (d=0.7), anterior thalamus (d=0.9), posterior insula (d=0.9), posterior

hippocampus (d=1.1), superior orbitofrontal cortex (d=0.8), calcarine cortex (d=0.8), vermis (d=0.8), anterior cingulate cortex (d=0.7), supplementary motor area/midcingulate cortex (SMA/midCC, d=0.3) and caudate (d=0.7) among others (all p<0.05 corrected cluster, for a complete list of corrected and uncorrected peak values, see Table 1).

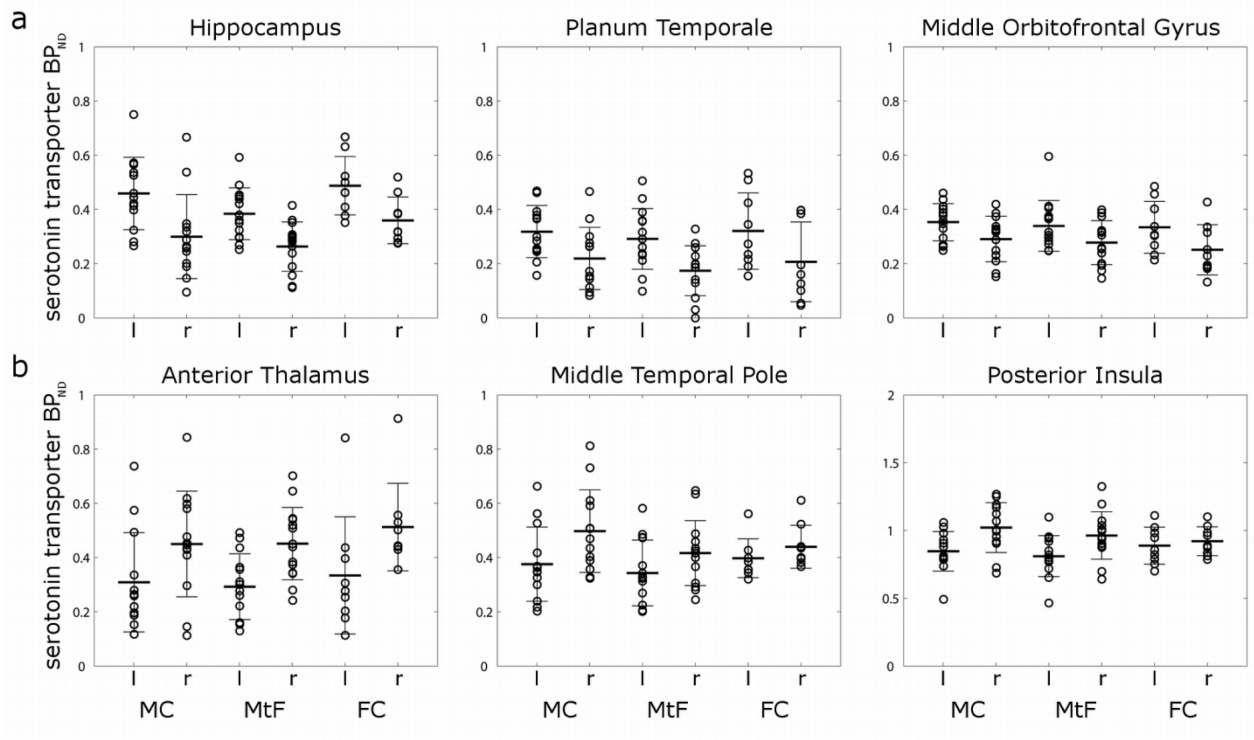

***Fig 2**. Scatter plots exemplarily illustrating (a) leftward and (b) rightward serotonin transporter asymmetries in 13 male controls (MC), 14 male-to-female transsexuals (MtF) and 9 female controls (FC). BP_{ND}, binding potential; l, left hemisphere; r, right hemisphere.*

Comparing SERT BP_{ND}, irrespective of asymmetry between FC, MC and MtF transsexuals (main effect of group), elevated SERT binding in the right calcarine gyrus in FC compared to MtF transsexuals was observed (d=3.2, p<0.05 corrected cluster). No differences in SERT binding was observed in other group comparisons that survived correction for multiple comparisons (for a complete list of uncorrected peak values, see Table 2).

There were, however, interactions between SERT asymmetry and group (see Table 3). For the comparison between MC and MtF transsexuals, an interaction was present in the midCC. Separate post hoc t-tests showed that midCC was rightward asymmetric in the MC group ($d=0.6$; $t=8.34$, $p<0.05$, corrected cluster) whereas no asymmetry was detected for MtF transsexuals in this region ($p>0.2$) (see Fig. 3). Interestingly, a similar interaction in midCC was observed when comparing MC with FC, with post hoc t-tests showing the above described rightward asymmetry in the MC group ($p<0.05$, corrected cluster) but not in the FC group ($p>0.7$). Other interactions were observed in the precentral gyrus, showing a numerical (but not significant) leftward asymmetry in the MC group and a numerically (but not significant) rightward asymmetry in the FC group; and a leftward asymmetry in the calcarine gyrus in FC ($d=1.5$; $t=4.84$, $p=0.0013$, uncorrected) but not in MtF transsexuals ($p>0.1$) (see Table 3 for a complete list of corrected and uncorrected peak values of interactions).

Including age and radiochemical variables into the analysis as variables of no interest did not change the main findings presented above.

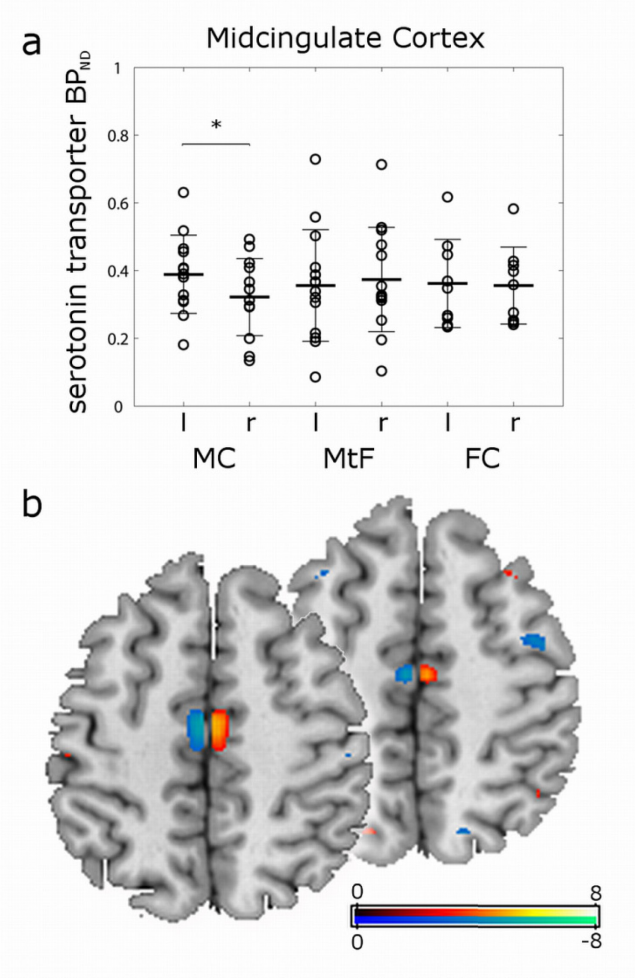

***Fig 3**. Serotonin transporter asymmetry in the midcingulate cortex comparing 13 healthy male controls (MC) with 14 male-to-female transsexuals (MtF) and 9 female controls (FC). (a) Scatterplot depicts absolute SERT BP_{ND} in the left and right midcingulate cortex. A signifcant difference in male controls (P<0.05, false discovery rate corrected at the cluster level) but not in male-to-female transsexuals and female controls is indicated by an asterisk. (b) Horizontal plane, z=51mm MNI space (Montreal Neurological Institute), showing the t-values of the interaction effect for MC (R>L) > MtF (R>L), left brain; and for MC (R>L) > FC (R>L), right brain. Left is left.*

3.1.5. Discussion

The results of this study demonstrate strong asymmetry of the SERT in a number of cortical and subcortical areas. Furthermore, SERT asymmetry is shown to differ between sex and gender in few regions. This is the case for a comparison between MC and MtF in the midCC, between FC and MC in the precentral gyrus, and between FC and MtF in the calcarine gyrus. The first part of our discussion will deal with SERT asymmetry per se, and the second part will include an analysis of SERT asymmetry and its relation to sexual identity.

As revealed in our study, SERT BP_{ND} asymmetry complements previous findings of asymmetry in several aspects of the serotonergic system and associated brain functions in the human and

rodent brain (e.g., Fink et al. 2009; Walsh et al. 2010; Bar et al. 2003; Ocklenburg et al. 2012; Rosen et al. 1984; Andersen and Teicher 1999; Valdes et al. 1981). Irrespective of sexual identity, we found elevated SERT BP_{ND} in the left hemisphere when compared to the right in planum temporale and middle occipital gyrus. The gray matter (GM) volumes in these regions have been repeatedly shown as also being leftward asymmetric (see e.g., Watkins et al. 2001; Good et al. 2001; Takao et al. 2011). Similarly, a rightward SERT and GM volume asymmetry were found in superior OFC, medial occipital cortex around calcarine sulcus, anterior cingulate cortex and cerebellum, and a leftward asymmetry in middle OFC and postcentral gyrus (Takao et al. 2011). SERT asymmetry in these regions may therefore reflect GM volume asymmetries, although see Underwood et al. (2012). This suggests that, when assuming that SERT BPND can be interpreted indicatory of SERT expression (Varnas et al. 2004; Hummerich et al. 2004), elevated SERT expression correlates with elevated GM volume. However, interpretations on SERT asymmetry in relation to gray matter volume must remain preliminary since no structural MR scans were available in this study. In any case, given that SERT immunostaining is repeatedly used as an index of serotonergic innervation (Nielsen et al. 2006; Vertes et al. 2010), our data may also suggest asymmetric serotonergic innervation for these regions.

However, SERT asymmetry did not always follow reported asymmetries in GM volume. For instance, a R>L GM volume asymmetry in the hippocampus is well-established (Pedraza et al. 2004, Shi et al. 2009). However, Woolard and Heckers (2012) showed in a considerable large sample of healthy subjects that this rightward asymmetry is limited to the anterior part of the hippocampus. In contrast, we found that, while the posterior hippocampus showed a strong rightward SERT asymmetry, a more anterior part showed SERT asymmetry to the left. The right posterior hippocampus is especially related to spatial memory and learning (Moser and Moser 1998; Shinohara et al. 2012). Our data may therefore indicate a serotonergic account in the functional specialization along the anterior-posterior axis (Moser and Moser 1998; Stern and Hasselmo 1999; Chua et al. 2007) and between right and left hippocampus (Belcheva et al. 2007; Shinohara et al. 2012; Hayes et al. 2010).

We found a leftward asymmetry of the anterior insula and a rightward asymmetry for the posterior insula, whereas GM volume for the posterior insula seems to be asymmetric to the left (Takao et al. 2011). However, SERT expression and SERT BP_{ND} signal-to-noise ratio are quite low in most cortical regions (except for the cingulate cortex) and our asymmetry findings in cortical regions must be interpreted with caution. This does, however, not apply for subcortical structures such as the midbrain, thalamus, hypothalamus, basal ganglia or hippocampus (Varnas et al. 2004). We detected strong SERT asymmetry to the left in caudate head and hippocampus, and to the right in the anterior thalamus and caudate body, regions which are known to have dense serotonergic innervations (Vertes et al. 2010; Vertes 1991). Interestingly, an early post-mortem human study investigating noradrenaline concentrations in the thalamus detected strong asymmetries. They were however, restricted mostly to middle and posterior sections (Oke et al. 1978). There is strong functional lateralization of the thalamus (Johnson and Ojemann 2000; Sapir et al. 2002) and it is plausible that neurotransmitter lateralization may play a role in such functionality. Similarly, dopamine D2/3 receptor asymmetry in the caudate and its decline with age has been reported and related to caudate function (Vernaleken et al. 2007), suggesting that SERT asymmetry in the caudate observed in our study may likewise contribute to its functional lateralization.

We will now turn to the comparison of SERT asymmetry between FC, MC and MtF transsexuals. Interestingly, in almost every brain region except for the midCC, the precentral gyrus and calcarine cortex, SERT asymmetries were very similar in all three groups. We therefore conclude that SERT asymmetry is largely unaffected by organizational effects of sex steroids on sexual brain differentiation in most regions. Although actual adult sex steroid levels were not obtained in male and female control subjects, one may assume differences in these levels between the two groups. Since most regions showed similar SERT asymmetry in male and female control subjects, it seems that assumed differences in adult hormonal levels did not profoundly affect SERT asymmetry. This, however, differs from studies indicating strong effects of sex steroids on serotonin function (Benmansour et al. 2012, Robichaud and Debonnel 2005, Rubinow et al. 1998). However, in the midCC our data show a rightward asymmetry for MC but not for FC and MtF transsexuals (see Fig.3). Although the midCC was traditionally ascribed mainly to process

cognitive functions, recent imaging studies indicated that the midCC (particularly its anterior part) is also involved in emotional, especially aversive processing (Shackman et al. 2011). This led to the conclusion that the midCC acts as a major hub linking cognitive control, negative affect and motivated behavior including emotional expression (Shackman et al. 2011). Interestingly, an ERP/MR study investigating sex differences in cognitive control demonstrated strong functional lateralization linked to the midCC which was only observed in males but not in females (Huster et al. 2011). Similarly, the observed SERT asymmetry in midCC in MC but not in FC and MtF transsexuals may indicate a gender-dimorphic organization of this structure and an altered masculinization in MtF transsexuals related to gender identity. However, as half of MtF transsexuals were homosexual and half of them heterosexual, differences between male controls and MtF transsexuals can be ascribed either to differences in sexual orientation or to gender identity. Still, given the strong modulatory role of serotonin in cognitive control and flexibility (Clarke et al. 2004; Clarke et al. 2005; Clarke et al. 2007), SERT asymmetry in the midCC observed in our study may thus add to the observed gender differences in cognitive control. On the other hand, SERT binding and asymmetry in the calcarine gyrus was shown to differ between FC and MtF transsexuals, whereas no such difference was observed in MC compared to MtF transsexuals. Furthermore, numerically different SERT asymmetry in the precentral gyrus was detected in MC compared to FC but not when both groups were compared to MtF transsexuals. Based on these results we conclude that MtF transsexuals exhibit SERT asymmetries that relate to both genetic sex, gender and a special feature of gender dysphoria. Still, since the female control group was relatively small, future studies with sufficiently large sample sizes should be conducted to confirm gender related differences in SERT binding and SERT asymmetry.

Limitations

This study includes limitations that compromise the interpretation of its results. Firstly, we were not able to properly address the relation between SERT BP_{ND} and gray matter volume asymmetries due to the absence of MR-scans from our subjects. We are therefore unable to relate SERT asymmetries to those of gray matter volume and individual differences in the sulci and lobes. Secondly, as normalization was done using a tracer specific PET template, we cannot

disambiguate SERT asymmetries caused by systematic local translocations from those caused by biologically-based differences in the size of corresponding anatomical regions. Thirdly, no information was obtained about menstrual cycle phase at the day of scanning from female controls and sex steroid levels from female and male control subjects were not assessed. We are therefore unable to infer any influence of adult sex steroids on our PET findings.

3.1.6. Conclusions

The present study supports the view of an asymmetric serotonergic system, which is in line with previous research focused on lateralized functions that are strongly modulated by serotonin. Asymmetry in SERT binding is in accord with asymmetry of other elements of the serotonergic system, such as 5-HT_{1A} receptor distribution, extracellular serotonin concentrations, turnover or uptake. The observed difference between males versus females and male-to-female transsexuals in the midcingulate cortex points towards a gender dimorphic serotonin transporter asymmetry and to the feminization / absence of masculinization of the midcingulate in male-to-female transsexuals in that region.

Acknowledgments

This research was funded by Austrian National Bank Grant P 13214 (to R. L.) and P 13675 (to M.M.). A. Hahn is a recipient of a DOC fellowship of the Austrian Academy of Sciences at the Department of Psychiatry and Psychotherapy. The authors are especially grateful to all transsexual subjects for participating in this study and to the clinical staff at the PET centre, the Department of Psychiatry and Psychotherapy for their technical and medical support and to Marie Spies for linguistic support.

Conflict of interest statement

The authors declare no conflict of interest related to this work.

3.1.7. References

Alves NT, Fukusima SS, Aznar-Casanova JA (2008) Models of brain asymmetry in emotional processing. Psychology & Neuroscience 1 (1):63-66.

Amunts K, Armstrong E, Malikovic A, Homke L, Mohlberg H, Schleicher A, Zilles K (2007) Gender-specific left-right asymmetries in human visual cortex. J Neurosci 27 (6):1356-1364.

Amunts VV (2008) Individual variability in the structural asymmetry of the dorsomedial nucleus of the thalamus in men and women. Neurosci Behav Physiol 38 (7):715-720.

Andersen SL, Teicher MH (1999) Serotonin laterality in amygdala predicts performance in the elevated plus maze in rats. Neuroreport 10 (17):3497-3500.

American Psychiatric Association (2000) Diagnostic and Statistical Manual of Mental Disorders DSM-IV-TR Fourth Edition (Text Revision). 4 edn. American Psychiatric Press, Washington, DC.

Asthana HS, Mandal MK (2001) Visual-field bias in the judgment of facial expression of emotion. J Gen Psychol 128 (1):21-29.

Bakker J, Brock O (2010) Early oestrogens in shaping reproductive networks: evidence for a potential organisational role of oestradiol in female brain development. J Neuroendocrinol 22 (7):728-735.

Bar KJ, Greiner W, Letsch A, Kobele R, Sauer H (2003) Influence of gender and hemispheric lateralization on heat pain perception in major depression. J Psychiatr Res 37 (4):345-353.

Belcheva I, Tashev R, Belcheva S (2007) Hippocampal asymmetry in serotonergic modulation of learning and memory in rats. Laterality 12 (6):475-486.

Benmansour S, Weaver RS, Barton AK, Adeniji OS, Frazer A (2012) Comparison of the effects of estradiol and progesterone on serotonergic function. Biol Psychiatry 71 (7):633-41.

Bethea CL, Lu NZ, Gundlah C, Streicher JM (2002) Diverse actions of ovarian steroids in the serotonin neural system. Front Neuroendocrinol 23 (1):41-100.

Biondi M, Parise P, Venturi P, Riccio L, Brunetti G, Pancheri P (1993) Frontal hemisphere lateralization and depressive personality traits. Percept Mot Skills 77 (3 Pt 1):1035-1042.

Chandramouli R, Kanchan BR, Ambadevi B (1993) Right-left asymmetry in tonic pain perception and its modification by simultaneous contralateral noxious stimulation. Neuropsychologia 31 (7):687-694.

Chua EF, Schacter DL, Rand-Giovannetti E, Sperling RA (2007) Evidence for a specific role of the anterior hippocampal region in successful associative encoding. Hippocampus 17 (11):1071-1080.

Clarke HF, Dalley JW, Crofts HS, Robbins TW, Roberts AC (2004) Cognitive inflexibility after prefrontal serotonin depletion. Science 304 (5672):878-880.

Clarke HF, Walker SC, Crofts HS, Dalley JW, Robbins TW, Roberts AC (2005) Prefrontal serotonin depletion affects reversal learning but not attentional set shifting. J Neurosci 25 (2):532-538.

Clarke HF, Walker SC, Dalley JW, Robbins TW, Roberts AC (2007) Cognitive inflexibility after prefrontal serotonin depletion is behaviorally and neurochemically specific. Cereb Cortex 17 (1):18-27.

Coles P (2008) Statistical errors and asymmetry indices. Proc Natl Acad Sci U S A 105 (45):E82; author reply E83.

Dakin CL, Wilson CA, Kallo I, Coen CW, Davies DC (2008) Neonatal stimulation of 5-HT(2) receptors reduces androgen receptor expression in the rat anteroventral periventricular nucleus and sexually dimorphic preoptic area. Eur J Neurosci 27 (9):2473-2480.

Diamond MC (1991) Hormonal effects on the development or cerebral lateralization. Psychoneuroendocrinology 16 (1-3):121-129.

Didelot A, Mauguière F, Redouté J, Bouvard S, Lothe A, Reilhac A, Hammers A, Costes N, Ryvlin P (2010) Voxel-based analysis of asymmetry index maps increases the specificity of 18F-MPPF PET abnormalities for localizing the epileptogenic zone in temporal lobe epilepsies. J Nucl Med 51(11):1732-1739.

Draca S (2010) Gender-specific functional cerebral asymmetries and unilateral cerebral lesion sequelae. Rev Neurosci 21 (6):421-425.

Dunlap WP, Cortina JM, Vaslow JB, Burke MJ (1996) Meta-analysis of experiments with matched groups or repeated measures designs. Psychological Methods 1 (2):170-177.

Fink M, Wadsak W, Savli M, Stein P, Moser U, Hahn A, Mien LK, Kletter K, Mitterhauser M, Kasper S, Lanzenberger R (2009) Lateralization of the serotonin-1A receptor distribution in language areas revealed by PET. Neuroimage 45 (2):598-605.

Fitzgerald PJ (2012) Whose side are you on: does serotonin preferentially activate the right hemisphere and norepinephrine the left? Med Hypotheses 79 (2):250-254.

Garcia-Falgueras A, Ligtenberg L, Kruijver FP, Swaab DF (2011) Galanin neurons in the intermediate nucleus (InM) of the human hypothalamus in relation to sex, age, and gender identity. J Comp Neurol 519 (15):3061-3084.

Garcia-Falgueras A, Swaab DF (2008) A sex difference in the hypothalamic uncinate nucleus: relationship to gender identity. Brain 131 (Pt 12):3132-3146.

Good CD, Johnsrude I, Ashburner J, Henson RN, Friston KJ, Frackowiak RS (2001) Cerebral asymmetry and the effects of sex and handedness on brain structure: a voxel-based morphometric analysis of 465 normal adult human brains. Neuroimage 14 (3):685-700.

Gur RC, Turetsky BI, Matsui M, Yan M, Bilker W, Hughett P, Gur RE (1999) Sex differences in brain gray and white matter in healthy young adults: correlations with cognitive performance. J Neurosci 19 (10):4065-4072.

Haeusler D, Mien LK, Nics L, Ungersboeck J, Philippe C, Lanzenberger RR, Kletter K, Dudczak R, Mitterhauser M, Wadsak W (2009) Simple and rapid preparation of [11C]DASB with high quality and reliability for routine applications. Appl Radiat Isot 67 (9):1654-1660.

Hahn A, Wadsak W, Windischberger C, Baldinger P, Hoflich AS, Losak J, Nics L, Philippe C, Kranz GS, Kraus C, Mitterhauser M, Karanikas G, Kasper S, Lanzenberger R (2012) Differential modulation of the default mode network via serotonin-1A receptors. Proc Natl Acad Sci U S A 109 (7):2619-2624.

Hausmann M, Gunturkun O (2000) Steroid fluctuations modify functional cerebral asymmetries: the hypothesis of progesterone-mediated interhemispheric decoupling. Neuropsychologia 38 (10):1362-1374.

Hayes SM, Baena E, Truong TK, Cabeza R (2010) Neural mechanisms of context effects on face recognition: automatic binding and context shift decrements. J Cogn Neurosci 22 (11):2541-2554.

Hummerich R, Reischl G, Ehrlichmann W, Machulla HJ, Heinz A, Schloss P (2004) DASB -in vitro binding characteristics on human recombinant monoamine transporters with regard to its potential as positron emission tomography (PET) tracer. J Neurochem 90 (5):1218-1226.

Huster RJ, Westerhausen R, Herrmann CS (2011) Sex differences in cognitive control are associated with midcingulate and callosal morphology. Brain Struct Funct 215 (3-4):225-235.

Ichise M, Liow JS, Lu JQ, Takano A, Model K, Toyama H, Suhara T, Suzuki K, Innis RB, Carson RE (2003) Linearized reference tissue parametric imaging methods: application to [11C]DASB positron emission tomography studies of the serotonin transporter in human brain. J Cereb Blood Flow Metab 23 (9):1096-1112.

Innis RB, Cunningham VJ, Delforge J, Fujita M, Gjedde A, Gunn RN, Holden J, Houle S, Huang SC, Ichise M, Iida H, Ito H, Kimura Y, Koeppe RA, Knudsen GM, Knuuti J, Lammertsma AA, Laruelle M, Logan J, Maguire RP, Mintun MA, Morris ED, Parsey R, Price JC, Slifstein M, Sossi V, Suhara T, Votaw JR, Wong DF, Carson RE (2007) Consensus nomenclature for in vivo imaging of reversibly binding radioligands. J Cereb Blood Flow Metab 27 (9):1533-1539.

Johnson MD, Ojemann GA (2000) The role of the human thalamus in language and memory: evidence from electrophysiological studies. Brain Cogn 42 (2):218-230.

Kahkonen S, Ahveninen J, Pennanen S, Liesivuori J, Ilmoniemi RJ, Jaaskelainen IP (2002) Serotonin modulates early cortical auditory processing in healthy subjects: evidence from MEG with acute tryptophan depletion. Neuropsychopharmacology 27 (5):862-868.

Klein F, Sepekoff B, Wolf TJ (1985) Sexual orientation: a multi-variable dynamic process. J Homosex 11 (1-2):35-49.

Kruijver FPM, Zhou JN, Pool CW, Hofman MA, Gooren LJG, Swaab DF (2000) Male-to-female transsexuals have female neuron numbers in a limbic nucleus. Journal of Clinical Endocrinology & Metabolism 85 (5):2034-2041.

Lanzenberger R, Kranz GS, Haeusler J, Akimova E, Savli M, Hahn A, Mitterhauser M, Spindelegger C, Philippe C, Fink M, Wadsak W, Karanikas G, Kasper S (2012) Prediction of SSRI treatment response in major depression based on serotonin transporter interplay between median raphe nucleus and projection areas. NeuroImage 63 (3):1091-1098.

Lanzenberger R, Mitterhauser M, Kranz GS, Spindelegger C, Wadsak W, Stein P, Moser U, Savli M, Kletter K, Kasper S (2011) Progesterone level predicts serotonin-1a receptor binding in the male human brain. Neuroendocrinology 94 (1):84-88.

Lanzenberger RR, Hahn A, Windischberger C, Wadsak W, Holik A, Gerstl F, Savli M, Moser U, Mien LK, Akimova E, Mitterhauser M, Kletter K, Moser E, Kasper S (2009) Serotonin-1A receptor binding and Reward-dependent Activation are associated within the Human Dorsal Raphe Nucleus as revealed by PET-fMRI. NeuroImage 47 (Supplement 1):S1-286.

Ley RG, Bryden MP (1979) Hemispheric differences in processing emotions and faces. Brain Lang 7 (1):127-138

Lugo M, Isturiz G, Lara C, Garcia N, Eblen-Zaijur A (2002) Sensory lateralization in pain subjective perception for noxious heat stimulus. Somatosens Mot Res 19 (3):207-212.

Martin-Soelch C, Szczepanik J, Nugent A, Barhaghi K, Rallis D, Herscovitch P, Carson RE, Drevets WC (2011) Lateralization and gender differences in the dopaminergic response to unpredictable reward in the human ventral striatum. Eur J Neurosci 33 (9):1706-1715.

McCarthy MM (2008) Estradiol and the developing brain. Physiol Rev 88 (1):91-124.

McEwen BS (1992) Steroid hormones: effect on brain development and function. Horm Res 37 Suppl 3:1-10.

McQueen JK, Wilson H, Fink G (1997) Estradiol-17 beta increases serotonin transporter (SERT) mRNA levels and the density of SERT-binding sites in female rat brain. Brain Res Mol Brain Res 45 (1):13-23.

Meyer JH (2007) Imaging the serotonin transporter during major depressive disorder and antidepressant treatment. J Psychiatry Neurosci 32 (2):86-102.

Meyer JH, Gunn RN, Myers R, Grasby PM (1999) Assessment of spatial normalization of PET ligand images using ligand-specific templates. Neuroimage 9 (5):545-553.

Moser MB, Moser EI (1998) Functional differentiation in the hippocampus. Hippocampus 8 (6):608-619.

Nielsen K, Brask D, Knudsen GM, Aznar S (2006) Immunodetection of the serotonin transporter protein is a more valid marker for serotonergic fibers than serotonin. Synapse 59 (5):270-276.

Nijboer TC, Jellema T (2012) Unequal impairment in the recognition of positive and negative emotions after right hemisphere lesions: a left hemisphere bias for happy faces. J Neuropsychol 6 (1):79-93.

Ocklenburg S, Gunturkun O, Beste C (2012) Hemispheric asymmetries and cognitive flexibility: an ERP and sLORETA study. Brain Cogn 78 (2):148-155.

Oke A, Keller R, Mefford I, Adams RN (1978) Lateralization of norepinephrine in human thalamus. Science 200 (4348):1411-1413.

Oldfield RC (1971) The assessment and analysis of handedness: the Edinburgh inventory. Neuropsychologia 9 (1):97-113.

Otto MW, Dougher MJ, Yeo RA (1989) Depression, pain, and hemispheric activation. J Nerv Ment Dis 177 (4):210-218.

Parsey RV, Kent JM, Oquendo MA, Richards MC, Pratap M, Cooper TB, Arango V, Mann JJ (2006) Acute occupancy of brain serotonin transporter by sertraline as measured by [11C]DASB and positron emission tomography. Biol Psychiatry 59 (9):821-828.

Paus T (2010) Sex differences in the human brain: a developmental perspective. In: Savic I (ed) Sex differences in the human brain, their underpinnings and implications, vol 186. Elsevier, Amsterdam, pp 13-28.

Pedraza O, Bowers D, Gilmore R (2004) Asymmetry of the hippocampus and amygdala in MRI volumetric measurements of normal adults. J Int Neuropsy Society 10 (5), 664–678.

Phoenix CH, Goy RW, Gerall AA, Young WC (1959) Organizing action of prenatally administered testosterone propionate on the tissues mediating mating behavior in the female guinea pig. Endocrinology 65:369-382.

Riccio O, Potter G, Walzer C, Vallet P, Szabo G, Vutskits L, Kiss JZ, Dayer AG (2009) Excess of serotonin affects embryonic interneuron migration through activation of the serotonin receptor 6. Mol Psychiatry 14 (3):280-290.

Rosen GD, Finklestein S, Stoll AL, Yutzey DA, Denenberg VH (1984) Neurochemical asymmetries in the albino rat's cortex, striatum, and nucleus accumbens. Life Sci 34 (12):1143-1148.

Robichaud M, Debonnel G (2005) Oestrogen and testosterone modulate the firing activity of dorsal raphe nucleus serotonergic neurones in both male and female rats. J Neuroendocrinol 17 (3):179-85.

Rubinow DR, Schmidt PJ, Roca CA (1998) Estrogen-serotonin interactions: implications for affective regulation. Biol Psychiatry 44 (9):839-50.

Sapir A, Rafal R, Henik A (2002) Attending to the thalamus: inhibition of return and nasal-temporal asymmetry in the pulvinar. Neuroreport 13 (5):693-697.

Sarlani E, Farooq N, Greenspan JD (2003) Gender and laterality differences in thermosensation throughout the perceptible range. Pain 106 (1-2):9-18.

Savic I, Garcia-Falgueras A, Swaab DF (2010) Sexual differentiation of the human brain in relation to gender identity and sexual orientation. In: Savic I (ed) Sex differences in the human brain, their underpinnings and implications, vol 186. Elsevier, Amsterdam, pp 41-61.

Schwier C, Kliem A, Boettger MK, Bar KJ (2010) Increased cold-pain thresholds in major depression. J Pain 11 (3):287-290.

Shackman AJ, Salomons TV, Slagter HA, Fox AS, Winter JJ, Davidson RJ (2011) The integration of negative affect, pain and cognitive control in the cingulate cortex. Nat Rev Neurosci 12 (3):154-167.

Shi F, Liu B, Zhou Y, Yu C, Jiang T (2009) Hippocampal volume and asymmetry in mild cognitive impairment and Alzheimer's disease: meta-analyses of MRI studies. Hippocampus 19 (11):1055–1064.

Shinohara Y, Hosoya A, Yamasaki N, Ahmed H, Hattori S, Eguchi M, Yamaguchi S, Miyakawa T, Hirase H, Shigemoto R (2012) Right-hemispheric dominance of spatial memory in split-brain mice. Hippocampus 22 (2):117-121.

Simerly RB, Swanson LW, Gorski RA (1985) Reversal of the sexually dimorphic distribution of serotonin-immunoreactive fibers in the medial preoptic nucleus by treatment with perinatal androgen. Brain Res 340 (1):91-98.

Soma T, Momose T, Takahashi M, Koyama K, Kawai K, Murase K, Ohtomo K (2012) Usefulness of extent analysis for statistical parametric mapping with asymmetry index using inter-ictal FGD-PET in mesial temporal lobe epilepsy. Ann Nucl Med 26(4):319-326.

Sommer IE, Aleman A, Somers M, Boks MP, Kahn RS (2008) Sex differences in handedness, asymmetry of the planum temporale and functional language lateralization. Brain Res 1206:76-88.

Spernal J, Krieg JC, Lautenbacher S (2003) Pain thresholds as a putative functional test for cerebral laterality in major depressive disorder and panic disorder. Neuropsychobiology 48 (3):146-151.

Stefanics G, Csukly G, Komlosi S, Czobor P, Czigler I (2012) Processing of unattended facial emotions: a visual mismatch negativity study. Neuroimage 59 (3):3042-3049.

Stein P, Savli M, Wadsak W, Mitterhauser M, Fink M, Spindelegger C, Mien LK, Moser U, Dudczak R, Kletter K, Kasper S, Lanzenberger R (2008) The serotonin-1A receptor distribution in healthy men and women measured by PET and [carbonyl-11C]WAY-100635. Eur J Nucl Med Mol Imaging 35 (12):2159-2168.

Stern CE, Hasselmo ME (1999) Bridging the gap: integrating cellular and functional magnetic resonance imaging studies of the hippocampus. Hippocampus 9 (1):45-53.

Swaab DF, Garcia-Falgueras A (2009) Sexual differentiation of the human brain in relation to gender identity and sexual orientation. Funct Neurol 24 (1):17-28.

Takao H, Abe O, Yamasue H, Aoki S, Sasaki H, Kasai K, Yoshioka N, Ohtomo K (2011) Gray and white matter asymmetries in healthy individuals aged 21-29 years: a voxel-based morphometry and diffusion tensor imaging study. Hum Brain Mapp 32 (10):1762-1773.

Tellez R, Rocha L, Castillo C, Meneses A (2010) Autoradiographic study of serotonin transporter during memory formation. Behav Brain Res 212 (1):12-26.

Tomer R, Slagter HA, Christian BT, Fox AS, King CR, Murali D, Davidson RJ (2012) Dopamine Asymmetries Predict Orienting Bias in Healthy Individuals. Cereb Cortex. Aug 31. [Epub ahead of print].

Underwood MD, Kassir SA, Bakalian MJ, Galfalvy H, Mann JJ, Arango V (2012) Neuron density and serotonin receptor binding in prefrontal cortex in suicide. Int J Neuropsychopharmacol 15 (4):435-447.

Valdes JJ, Mactutus CF, Cory RN, Cameron WR (1981) Lateralization of norepinephrine, serotonin and choline uptake into hippocampal synaptosomes of sinistral rats. Physiol Behav 27 (2):381-383.

Varnas K, Halldin C, Hall H (2004) Autoradiographic distribution of serotonin transporters and receptor subtypes in human brain. Hum Brain Mapp 22 (3):246-260.

Vernaleken I, Weibrich C, Siessmeier T, Buchholz HG, Rosch F, Heinz A, Cumming P, Stoeter P, Bartenstein P, Grunder G (2007) Asymmetry in dopamine D(2/3) receptors of caudate nucleus is lost with age. Neuroimage 34 (3):870-878.

Verney C, Lebrand C, Gaspar P (2002) Changing distribution of monoaminergic markers in the developing human cerebral cortex with special emphasis on the serotonin transporter. Anat Rec 267 (2):87-93.

Vertes RP (1991) A PHA-L analysis of ascending projections of the dorsal raphe nucleus in the rat. J Comp Neurol 313 (4):643-668.

Vertes RP, Linley SB, Hoover WB (2010) Pattern of distribution of serotonergic fibers to the thalamus of the rat. Brain Struct Funct 215 (1):1-28.

Vitalis T, Cases O, Passemard S, Callebert J, Parnavelas JG (2007) Embryonic depletion of serotonin affects cortical development. Eur J Neurosci 26 (2):331-344.

Walsh A, McDowall J, Grimshaw GM (2010) Hemispheric specialization for emotional word processing is a function of SSRI responsiveness. Brain Cogn 74 (3):332-340.

Watkins KE, Paus T, Lerch JP, Zijdenbos A, Collins DL, Neelin P, Taylor J, Worsley KJ, Evans AC (2001) Structural asymmetries in the human brain: a voxel-based statistical analysis of 142 MRI scans. Cereb Cortex 11 (9):868-877.

Westergaard GC, Chavanne TJ, Lussier ID, Houser L, Cleveland A, Suomi SJ, Higley JD (2003) Left-handedness is correlated with CSF monoamine metabolite and plasma cortisol concentrations, and with impaired sociality, in free-ranging adult male rhesus macaques (Macaca mulatta). Laterality 8 (2):169-187.

Wilson CA, Davies DC (2007) The control of sexual differentiation of the reproductive system and brain. Reproduction 133 (2):331-359.

Wisniewski AB (1998) Sexually-dimorphic patterns of cortical asymmetry, and the role for sex steroid hormones in determining cortical patterns of lateralization. Psychoneuroendocrinology 23 (5):519-547.

Witte AV, Floel A, Stein P, Savli M, Mien LK, Wadsak W, Spindelegger C, Moser U, Fink M, Hahn A, Mitterhauser M, Kletter K, Kasper S, Lanzenberger R (2009) Aggression is related to frontal serotonin-1A receptor distribution as revealed by PET in healthy subjects. Hum Brain Mapp 30 (8):2558-2570.

Woolard AA, Heckers S (2012) Anatomical and functional correlates of human hippocampal volume asymmetry. Psychiatry Res 201 (1):48-53.

Young EJ, Williams CL (2010) Valence dependent asymmetric release of norepinephrine in the basolateral amygdala. Behav Neurosci 124 (5):633-644.

Zhou JN, Hofman MA, Gooren LJ, Swaab DF (1995) A sex difference in the human brain and its relation to transsexuality. Nature 378 (6552):68-70.

Table 1. Serotonin transporter asymmetries in 9 female control, 13 male control and 14 male-to-female transsexuals (main effect: L vs. R).

Region		MNI coordinates (mm)			Peak	
Anatomical Region (AAL)	**BA**	**x**	**y**	**z**	**T value**	**Cluster Size (k)**
Leftward asymmetries (L > R)						
PlanumTemporale / Superior Temporal Gyrus	41	-40	-34	14	12.99*†‡	418
Middle Orbitofrontal Gyrus	11	-6	42	-12	8.33*†‡	347
	11	-12	64	-2	4.34*	14
		-36	42	-16	4.00*	5
Hippocampus		-24	-24	-6	8.15*†‡	201
Middle Occipital Gyrus	19	-44	-80	6	7.71*†‡	1377
Postcentral Gyrus	3	-58	-8	36	6.89*†‡	298
Angular Gyrus	40	-58	-50	34	6.55*†‡	42
	7	-34	-60	46	4.33*‡	26
Fusiform Gyrus	37	-38	-40	-24	5.93*†‡	59
	37	-28	-36	-24	3.90*	6
Superior Temporal Gyrus	20	-40	-6	-16	5.60*‡	39
Caudate head	25	-10	10	4	5.52*‡	39
Superior Occipital Gyrus	19	-24	-76	28	5.44*‡	33
Rolandic Operculum	48	-58	4	8	5.43*‡	53
Inferior Parietal Gyrus	40	-48	-50	50	5.33*‡	72
		-44	-36	52	4.85*‡	103
Olfactory Bulb	34	-24	6	-12	5.21*‡	81
Frontal Inferior Operculum	44	-42	8	26	5.04*	10
Anterior Insula	48	-32	16	6	4.73*‡	56
Anterior Cingulate Cortex	32	-12	20	32	4.71*	14
Precentral Gyrus	9	-44	8	48	4.64*‡	19
Rostral Pons	-	-4	-16	-28	4.61*	5
	-	-10	-18	-20	4.08*	6
Inferior Triangular Frontal Gyrus	45	-44	30	30	4.53*‡	21
Middle Temporal Gyrus	21	-52	-46	-6	4.32*	10
Inferior Orbitofrontal Gyrus	47	-38	36	0	4.29*‡	20
Hypothalamus	-	-8	-6	-12	4.13*	13
Precuneus	-	-4	-62	32	4.04*	7
Posterior Cingulate Cortex	23	-8	-48	24	3.95*	9
Superior Medial Frontal Gyrus	10	-10	64	14	3.93*	10
Lateral Thalamus	-	-20	-14	6	3.91*	12
Middle Frontal Gyrus	46	-36	42	26	3.90*	6
Rightward asymmetries (R > L)						
Middle Temporal Pole	38	44	14	-28	8.95*†‡	383
Anterior Thalamus	-	6	-8	14	7.88*†‡	135

Posterior Insula	48	38	-8	-4	7.78*†‡	278
Posterior Hippocampus	27	18	-36	8	7.71*‡	110
Superior Orbitofrontal Cortex	11	22	30	-16	7.59*†‡	198
Calcarine Cortex	17	18	-62	16	7.56*†‡	582
Cerebellar Vermis	-	12	-50	-42	6.60*†‡	168
	-	8	-40	-8	4.02*	10
Anterior Cingulate Cortex	11	10	34	8	5.42*†‡	31
	11	12	42	4	4.08*	12
Caudate Head	-	24	24	6	5.26*	9
	-	16	24	0	4.52*	9
SMA/midCC	-	4	-16	50	5.05*‡	20
	-	16	6	64	4.82*	11
Inferior Triangular Frontal Cortex	45	48	26	6	4.71*‡	36
Caudate	-	20	-2	22	4.58*‡	17
Putamen	48	20	4	12	4.51*	14
Precentral Gyrus	6	42	2	36	4.41*	16
Anterior Fusiform Gyrus	36	34	-6	-42	4.39*‡	26
Superior Frontal Gyrus	46	24	52	20	4.26*	7
Supramarginal Gyrus	48	50	-30	28	4.16*	5
Precentral Gyrus	4	14	-22	70	3.85*	8
Paracentral Gyrus	4	4	-32	74	3.85*	7
	4	10	-24	62	3.56*	7

*P< 0.001, uncorrected (voxel) with k ≥ 5 voxels (cluster). P < 0.05, FDR-corrected at †voxel and ‡cluster level. AAL, automated anatomical labeling; BA, brodmann area; midCC, midcingulate cortex; SMA, supplementary motor area.

Table 2. Differences in serotonin transporter binding between 13 male controls, 14 male-to-female transsexuals and 9 female controls.

Region		MNI coordinates (mm)			Peak	
Anatomical Region (AAL)	**BA**	**x**	**y**	**z**	**T value**	**Cluster Size (k)**
FC > MC						
Posterior Hippocampus L	-	-24	-36	8	5.41*	25
Supramarginal Gyrus R	7	24	-54	44	5.30*	7
Middle Occipital Gyrus L	17	-24	-100	0	5.02*	5
Cerebellar Vermis L	-	-12	-48	-32	4.99*	8
Parahippocampus L	30	-22	-28	-14	4.33*	8
Inferior Parietal Cortex R	3	44	-34	54	4.26*	8
	2	48	-36	50	3.96*	6
Calcarine Gyrus L	17	-2	-88	-10	4.16*	16
		-10	-92	-6	3.25*	6
Supramarginal Gyrus L	2	-58	-26	42	3.92*	7
MC > FC						
Gyrus Rectus	11	2	28	-16	3.85*	5
FC > MtF						
Calcarine Gyrus R	18	18	-78	10	7.55*†‡	95
Middle Temporal Gyrus L	37	-54	-66	12	5.20*	8
Precuneus R	29	6	-46	12	4.64*	16
Cuneus R	17	12	-100	10	4.44*	8
Superior Parietal Cortex L	7	-30	-68	52	4.33*	7
Hippocampus L	-	-22	-28	-6	4.15*	13
Angular Gyrus R	7	24	-54	44	4.10*	8
Calcarine Gyrus L	18	-4	-88	-12	3.90*	12
Middle Temporal Gyrus L	21	-64	-30	0	3.89*	7
MtF > FC						
Gyrus Rectus L	11	-6	28	-25	4.45*	11
Inferior Temporal Cortex	20	50	-2	-34	4.25*	9
Superior Ofbitofrontal Cortex	11	-10	52	-20	4.16*	5

*P< 0.001, uncorrected (voxel) with k ≥ 5 voxels (cluster). P < 0.05, FDR-corrected at †voxel and ‡cluster level. AAL, automated anatomical labeling; BA, brodmann area; FC, female controls; MC, male controls; MtF, male-to-female transsexuals.

Table 3. Serotonin transporter asymmetries in 13 males, 14 male-to-female transsexuals and 9 females (interaction: Group1 (R>L) > Group2 (R>L))

Region		MNI coordinates (mm)			Peak	
Anatomical Region (AAL)	**BA**	**x**	**y**	**z**	**T value**	**Cluster Size (k)**
MC vs. FC						
Leftward asymmetries (L > R)						
Precentral Gyrus	6	-40	-2	48	4.56*‡	23
Rightward asymmetries (R > L)						
Caudate	48	24	24	8	5.86*	8
Superior Temporal Pole	38	42	18	-30	5.04*	17
midCC	23	4	-16	50	4.78*	8
Middle Occipital Cortex	19	30	-68	30	4.50*	23
Rostral Pons	35	10	-22	-22	4.13*	6
MC vs. MtF						
Leftward asymmetries (L > R)						
Olfactory Gyrus	11	-22	14	-16	5.01*	11
Superior Orbitofrontal Cortex	11	-24	48	-14	4.20*	9
Middle Occipital Cortex	37	-52	-68	0	4.04*	5
Superior Frontal Cortex	32	-18	50	22	4.00*	7
Rightward asymmetries (R > L)						
midCC	23	2	-12	50	5.03*‡	30
Posterior Hippocampus	-	32	-32	6	4.89*	18
Inferior Orbitofrontal cortex	47	38	38	-8	4.79*	16
Heschl's Gyrus	48	34	-28	12	4.46*	8
Paracentral Gyrus	4	8	-24	70	4.07*	5
FC vs. MtF						
Leftward asymmetries (L > R)						
Calcarine Gyrus	18	-18	-80	8	5.99*‡	35
Middle Temporal Pole	38	-46	14	-30	4.83*	5
Gyrus Rectus	48	-20	14	-14	4.73*	5
Calcarine	18	-6	-84	16	3.89*	9
Rightward asymmetries (R > L)						
Superior Temporal Gyrus	22	62	-24	6	5.52*	6
Hypothalamus	-	2	0	-10	5.25*	11
Inferior Occipital Gyrus	19	38	-82	-6	5.01*	22
Middle Temporal Gyrus	21	62	-30	-4	4.56*	10

Lingual Gyrus	18	12	-88	-12	4.47*	8
Posterior Hippocampus	-	26	-34	4	4.14*	7
Precentral Gyrus	6	50	-8	44	3.91*	6

*P< 0.001, uncorrected (voxel) with k ≥ 5 voxels (cluster). P < 0.05, FDR-corrected at ‡cluster level. AAL, automated anatomical labeling; BA, brodmann area; FC, female controls; MC, male controls; midCC, midcingulate cortex; MtF, male-to-female transsexuals.

3.2. Second publication: Regional differences in SERT occupancy after acute and prolonged SSRI intake investigated by brain PET

Pia Baldinger[1]*, Georg S. Kranz[1]*, Daniela Haeusler[2], Markus Savli[1], Marie Spies[1], Cecile Philippe[2], Andreas Hahn[1], Anna Höflich[1], Wolfgang Wadsak[2], Markus Mitterhauser[2], Rupert Lanzenberger[1#], Siegfried Kasper[1]

**contributed equally*

[1]*Department of Psychiatry and Psychotherapy, Medical University of Vienna, Austria*

[2]*Department of Nuclear Medicine, Medical University of Vienna, Austria*

Submitted to

NEUROIMAGE (under review)

[2011, IF: 5.895]

Main article		
Word count	241	Abstract
	5040	Main section
Tables: 4, Figures: 5, References 55		
Appendices: 3 Tables		

[#]Correspondence to: Assoc. Prof. Rupert Lanzenberger, MD, PD
Functional, Molecular & Translational Neuroimaging Unit – PET & MRI
Department of Psychiatry and Psychotherapy
Medical University of Vienna
Waehringer Guertel 18-20
1090 Vienna, AUSTRIA
Tel: ++43-1-40400-3825
Email: rupert.lanzenberger@meduniwien.ac.at

3.2.1. Abstract

Blocking of the serotonin transporter (SERT) and reaching occupancy levels of approximately 80% in the striatum is considered to underlie the antidepressant effect of selective serotonin reuptake inhibitors (SSRIs). Interestingly, when compared to the striatum, higher SERT occupancy in the midbrain and lower values in the thalamus were reported. This indicates that occupancy might be differently distributed throughout the brain, which is mirrored by differences in relevance of brain regions in the recovery of depressive symptoms. The present study therefore aimed at investigating regional SERT occupancies with positron emission tomography and the radioligand [^{11}C]DASB in 19 depressed patients after acute and prolonged intake of oral doses of either 10mg/day escitalopram or 20mg/day citalopram. Compared to the mean occupancy across cortical and subcortical regions, we detected increased SERT occupancies in regions commonly associated with antidepressant response, such as the subgenual cingulate, amygdala and raphe nuclei. When acute and prolonged drug intake was compared, SERT occupancies increased in subcortical areas that are known to be rich in SERT. Moreover, SERT occupancy in subcortical brain areas after prolonged intake of antidepressants was predicted by plasma drug levels. Similarly, baseline SERT binding potential seems to impact SERT occupancy as regions rich in SERT showed greater binding reduction as well as higher residual binding. These findings suggest a region-specific distribution of SERT blockage by SSRIs and focus the postulated link between treatment response and SERT occupancy to certain brain regions such as the subgenual cingulate cortex.

ClinicalTrial / EudraCT Number: 2006-006576-38, https://eudract.ema.europa.eu/

Keywords: antidepressant, occupancy, PET, serotonin transporter, subgenual cingulate cortex

3.2.2. Introduction

In the last decades, neuroreceptor imaging studies using positron emission tomography (PET) have yielded new insights into psychiatric drug action, the neurobiological correlates of clinical response and the superiority of certain agents (Kasper et al., 2009; Talbot and Laruelle, 2002). Using the radioligand [^{11}C]DASB, Meyer et al. showed a significant decrease of striatal serotonin transporter (SERT) binding in depressed patients after four weeks treatment with SSRIs compared to healthy subjects; occupancy levels of SERT were around 80% after treatment with either 20mg/day of paroxetine (83%) or 20mg/day of citalopram (77%) (Meyer et al., 2001). Following several month long intake of antidepressant agents, comparable findings were described using [^{11}C]McN5652 for 10mg/day of clomipramine (81,1%) and 50mg/day of fluvoxamine (84,9%) (Suhara T and et al., 2003) as well as 20 to 40mg/day of paroxetine (82%) (Kent et al., 2002). However, when examining acute exposure to SSRIs, occupancy of SERT by 25 to 100mg/day of sertraline were shown to be lower than the values described earlier by Meyer et al. (Parsey et al., 2006a). This could be explained by a down-regulation of SERT after chronic SSRI intake and thereby apparently increased occupancy of the SERT by the administered antidepressant (Benmansour et al., 1999; Lesch et al., 1993). A more recent study conducted by Meyer et al., which investigated SERT occupancy in 77 subjects after a month long intake of citalopram, fluoxetine, sertraline, paroxetine and venlafaxine, consistently showed occupancy levels of approximately 80% in the striatum across all antidepressants applied at minimum therapeutic doses, thereby suggesting this value might be a necessary minimum for an adequate treatment of depressive episodes (Meyer et al., 2004). Interestingly, in addition to striatal SERT binding, this study also focused on occupancy levels in other brain regions, revealing a higher SERT occupancy in the midbrain (8% higher) and lower values in the thalamus (8% lower) when compared to the striatum. This data indicates that SERT occupancy might not be equally distributed throughout the brain.

Within the framework of major depression and antidepressant treatment, investigations into the regional distribution of SERT occupancy remain scarce. However, there is consistent evidence pointing toward a differentiated and specific regional involvement in mood disorders, e.g. role of the amygdala in emotion processing and the hippocampus and the anterior cingulate

cortex in cognitive performance in depression (Hoflich et al., 2012). Moreover, following the idea of regional selectivity (Lawler et al., 1999; Urban et al., 2007), one might suggest that SERT affinity and activity vary throughout the brain, as mechanisms regulating serotonin uptake, such as SERT internalization, may differ in their activity across brain areas. Furthermore, the expression of receptors and transporters within a given transmitter system are highly interrelated; it is well known from PET studies that binding and availability of SERT and serotonin receptors is differently distributed in various cortical and subcortical brain areas, e.g. high SERT binding potential in the thalamus, putamen and midbrain (Savli et al., 2012). Regarding serotonergic receptors, findings retrieved from animal studies emphasize regional differences in the coupling of serotonin-1A receptor to G proteins resulting in region-specific G protein subunits interacting with the receptor (Mannoury la Cour et al., 2006). Finally, there is evidence that serotonin levels differ throughout the brain with area-specific serotonin levels depending on related receptor distributions (Malagie et al., 2001; Pehrson et al., 2012). Pharmacological challenge studies suggest a topological difference in basal serotonin levels, as acute escitalopram infusion is accompanied by a serotonin increase that differs across regions, e.g. 6 to 7-fold increase in the frontal cortex and 20-fold increase in the dorsal raphe nucleus (DRN) compared to baseline (Tao et al., 2000). Regarding the distribution of SSRIs in the brain, Kugelberg et al. showed that citalopram concentrations differ between brain regions in a series of animal studies (Kugelberg et al., 2001; Kugelberg et al., 2003; Kugelberg et al., 2004). Citalopram concentrations were twofold higher in the cortex than in the midbrain of rats, which might be caused by regional differences in cerebral blood flow and lipophilicity (Fraser et al., 2010). Affinity of citalopram, on the other hand, seems to be a constant variable throughout brain regions, namely the brainstrem, the basal ganglia and the frontal cortex (Zeng et al., 2006a), although lipophilicity seems to partly determine tracer affinities (Laruelle et al., 2003).

In the context of personalized medicine, a highly contested topic is whether SERT or SERT related dimensions, e.g. the serotonin transporter promoter polymorphisms *5-HTTLPR*, might serve as predictive markers of treatment response in major depression (Holsboer, 2008). While several neuroimaging studies investigated pretreatment SERT availability and the outcome of SSRI treatment assessed by means of psychometric scales, the subject remains controversial

(Kugaya et al., 2004; Lanzenberger et al., 2012; Meyer et al., 2001; Meyer et al., 2004). However, as SERT occupancy of 80% was shown to represent a determining factor of treatment response (Meyer et al., 2004), one might suggest a certain connection between pretreatment SERT binding and the extent of SSRI mediated SERT blockage, particularly when investigating this across regions. Regarding the assessment of drug plasma levels, striatal SERT occupancy was shown to be correlated with citalopram plasma levels - with at least 50 ng/mL of citalopram necessary to achieve 80% SERT occupancy (Meyer et al., 2004). Plasma doses of less than 50 ng/mL of citalopram were associated with an unfavorable treatment outcome (Ostad Haji et al., 2011).

The present study is conducted to address several of the issues mentioned above. Whereas a recent study by our group focused on the influence of SERT pretreatment binding potential and occupancy levels on the clinical outcome after SSRI intake by investigating potential predictors of treatment response, the present longitudinal study focuses solely on occupancy data and aims to further illuminate a regional differentiation of SERT occupancies within a more basic neuropharmacological approach. Firstly, we aim at investigating whether SERT occupancy is equally distributed in the brain in vivo using [^{11}C]DASB in depressed subjects (**Q1**). A second objective is to substantiate differences in SERT occupancies between acute and chronic intake of SSRIs (**Q2**). Thirdly we aim to determine a potential relationship between baseline SERT expression and its change / reduction after treatment (**Q3**). Finally, the present study aims to clarify the association between regional SERT occupancies and SSRI plasma levels (**Q4**). Following both a region of interest (ROI) and a voxel-wise approach, our study benefits from the robustness and low disposition to noise within the ROI analysis, as well as a more detailed differentiation of occupancy by utilizing a voxel-wise processing of the PET data.

3.2.3. Methods

Participants

Nineteen out-patients suffering from major depression (13 females, 42.3±7.8 years (mean±sd)) were included in this study as described previously (Lanzenberger et al., 2012). Subject assessment included a Structured Clinical Interview (SCID) for DSM IV and the 17 item Hamilton Depression Rating Scale (HAM-D), physical and neurological examinations, routine blood tests, an electrocardiogram and a pregnancy test. Inclusion criteria were a HAM-D score of ≥16, no comorbid axis II disorder, major medical or neurological illness, no intake of antidepressant agents or other substances with high affinity for SERT for three months prior to scanning (four months for fluoxetine) and no history of drug abuse. All subjects gave written informed consent after detailed description of the study protocol. The study was approved by the Ethics Committee of the Medical University of Vienna.

Study design

Designed as a pooled longitudinal study, subjects received oral doses of either escitalopram (10 mg/day, 10 subjects) or citalopram (20 mg/day, 9 subjects) (Lundbeck A/S, Denmark), as described previously (Lanzenberger et al., 2012). Since no significant differences in SERT occupancy between citalopram and escitalopram were observed, the data was pooled for further analysis in order to increase statistical power. Briefly, patients underwent three [^{11}C]DASB PET scans: before treatment (PET 1), 6 hrs following the first SSRI dose (PET 2) and 6 hrs after the last dose, which was administered daily for a minimum of 3 weeks (24.73±3.3 days, PET 3).

Serum sampling

Blood samples were taken approximately 10 min before each PET scan and plasma was immediately separated by an experienced clinician. Plasma was then frozen at −20 °C and S-citalopram analysis of the plasma fraction was undertaken by Quintiles Bioanalytical Laboratory, Uppsala, Sweden (www.analytical-services.se).

Positron emission tomography (PET)

PET scans were performed at the Department of Nuclear Medicine, Medical University of Vienna with a GE Advance full-ring scanner (General Electric Medical Systems, Milwaukee, WI, USA) in 3D mode. Following a 5 min transmission scan using retractable ^{68}Ge rod sources for tissue attenuation correction, data acquisition started simultaneously with a bolus injection of [^{11}C]DASB. Brain radioactivity was measured in a series of 30 consecutive time frames with 90 min total acquisition time divided into fifteen 1 min frames and fifteen 5 min frames. Collected data were reconstructed in volumes consisting of 35 trans-axial sections (128x128 matrix) using an iterative filtered back-projection algorithm (FORE-ITER) with a spatial resolution of 4.36 mm full-width at half maximum 1cm next to the center of the field of view. For radiotracer preparation and radiochemical variables, see (Haeusler et al., 2009; Lanzenberger et al., 2012).

Serotonin transporter quantification and regions of interest

Following between-frame motion correction, individual summed PET images where spatially normalized to a PET template in stereotactic Montreal Neurological Institute (MNI) space using SPM8 (Wellcome Trust Centre for Neuroimaging, London, UK; http://www.fil.ion.ucl.ac.uk/spm/). Quantification of the SERT binding potential (BP_{ND}) (Innis et al., 2007) was done using the multilinear reference tissue model (MRTM2) (Ichise et al., 2003). Cerebellar gray matter (excluding vermis and venous sinus) was used as reference region as recent post mortem and *in vivo* SERT quantification identified the cerebellar grey matter as optimal reference region for [^{11}C]DASB (Meyer, 2007; Parsey et al., 2006b). All modeling calculations were performed using PMOD image analysis software, version 3.3 (PMOD Technologies Ltd, Zurich, Switzerland, www.pmod.com). SERT BP_{ND} was computed voxel-wise as well as in a ROI based approach. 22 ROIs were selected including subcortical structures such as the midbrain raphe nuclei, basal ganglia and thalamus, but also cortical regions with moderate to higher SERT binding such as the cingulate and temporal cortex (see Table 1 and Fig. 1 for the list of selected ROIs). Only regions and voxels with residual SERT $BP_{ND} \geq 0.05$ were included in subsequent analyses to avoid spurious occupancy values due to the low signal-to-noise ratio in

these regions. For similar reasons, only ROIs and voxels that showed a decrease in SERT BP_{ND} over time were included. Given that SSRIs are defined by blocking the SERT, only positive occupancy values should reflect accurate drug occupancies. SERT occupancy was derived using the equation: Occupancy(%)=(1−BP_{ND} treatment /BP_{ND} baseline)×100. In order to avoid bias induced by manual delineation, ROIs (except for DRN and median raphe nucleus, MRN) were taken from a standardized ROI atlas (Fink et al., 2009; Stein et al., 2008) based on the automated anatomical labeling (AAL) brain atlas (Tzourio-Mazoyer et al., 2002). SERT binding in the DRN and MRN was defined manually in two slices of the template comprising spheres of 3 mm radius (Kranz et al., 2012).

Statistical Analysis

To assess whether SERT occupancies show regional differences (**Q1**), mean occupancy values (across subjects) for each of the 8 subcortical ROIs were tested against an overall occupancy (across regions) representing the mean of these subcortical ROIs. The same procedure was done for the 14 cortical ROIs. To this end, one-sample t-tests were performed, using mean cortical and subcortical occupancy of M_{cort}=65.66 and M_{subc}=72.99 for PET 2, and M_{cort}=63.82 and M_{subc}=78.54 for PET 3 as test values. These values were also used to evaluate regional occupancy differences within the voxel-wise approach. Assessment of differences between SERT occupancies at PET 2 and PET 3 (**Q2**) for both the ROI- and voxel-based approach was done using repeated-measures ANOVA with either ROI or voxel and time (PET 2 and PET 3) as factors. Next, we assessed if SERT occupancies depend on pretreatment SERT binding (**Q3**). Simply correlating these two variables would produce a well-known statistical artifact, since correlations of any pretreatment value with changes of these values over time are mathematically inevitable (Gill et al., 1985). Two different approaches were adopted to solve this problem. First, regression analysis that predicted residual SERT BP_{ND} (PET 2 and 3, respectively) from baseline SERT BP_{ND} was computed. Second, correlation analysis between absolute SERT reduction and Oldham's transformation, i.e., (baseline BP_{ND}+residual BP_{ND})/2 (Oldham, 1962) was performed. Thus, whereas the first approach assesses the relationship between baseline and residual SERT BP_{ND}, the second approach gives an unbiased correlation between baseline SERT BP_{ND} and its change after treatment (Tu and Gilthorpe, 2007). Both

approaches were performed for each ROI and voxel to assess the strength of associations for a defined brain region (subjects as single values). In a second step, means of ROIs were entered into the analyses as single values to assess the strength of associations across the brain (ROIs as single values). Finally, to test whether individual SERT occupancies depend on escitalopram plasma levels (**Q4**), separate Pearson correlations were performed for each ROI and voxel. Correction for multiple comparisons was done using Bonferroni and family-wise error rate (FWE), for ROI and voxel-wise analyses, respectively. SPSS version 18.0 for Windows (SPSS Inc., Chicago, IL, www.spss.com) was used for computation within the ROI-based approach. Voxel-wise analysis was done using MATLAB and SPM8.

3.2.4. Results

Sample characteristics

Most subjects benefited from treatment, with eleven out of nineteen subjects being responders (showing at least a 50% reduction in HAM-D scores) and seven of these becoming remitters with final HAM-D scores ≤7, see (Lanzenberger et al., 2012) for more details. Injected doses and specific activities for [^{11}C]DASB did not differ between PET measurements (data not shown).

Regional serotonin transporter occupancies (Q1)

ROI based occupancy values approximately 6 hrs following the first SSRI dose (PET 2) ranged between 43.53±18.09% and 82.16±7.36%, with mean occupancy values of 65.66±10.60% for cortical, and 72.99±6.75% for subcortical regions. Testing the homogeneity of cortical occupancies using one-sample t-test (test value: 65.66) revealed that middle and inferior temporal cortex had significantly lowered occupancies, whereas the posterior (PCC) and subgenual cingulate cortex (sgCC) had significantly elevated occupancies ($p<0.05$, corrected). Likewise, subcortical regions such as the putamen and thalamus, exhibited decreased occupancies, whereas amygdala, DRN and MRN had elevated occupancy values (test value: 72.99, see Table 1, Fig. 1). Results were mostly reflected within the voxel-wise approach, showing elevated cortical occupancy values within clusters extending to the sgCC and inferior

orbitofrontal cortex and lowered cortical occupancies in temporal but also frontal, parietal and occipital regions (test value: 65.66). Analogous results within the voxel-wise analysis were also observed for subcortical regions (test value: 72.99). Interestingly, the voxel-wise approach also revealed occupancy differences within a single anatomical region. Whereas occupancy was elevated within a ventral posterior part of the thalamus, a more anterior part had significantly lowered occupancies bilaterally (for a complete list of corrected and uncorrected values, see Table 2.1).

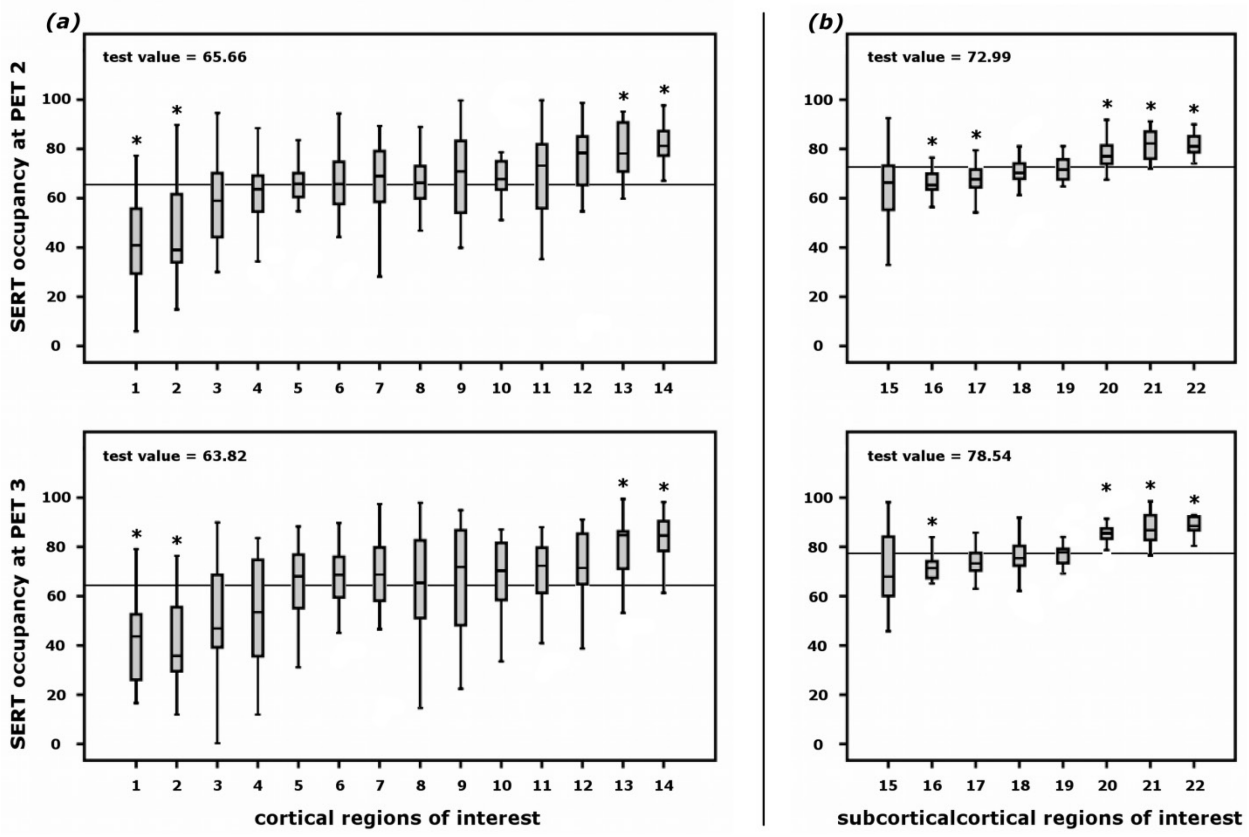

Fig 1: *Boxplots representing differential regional SERT occupancies after (upper row) single dosage (PET 2) and (bottom row) steady state (PET 3) SSRI intake when tested against mean occupancy values for (a) cortical and (b) subcortical regions. Significant regional SERT occupancy deviations from the mean (horizontal line within each boxplot) are indicated by an asterisk (see Table 1 for means, SD and t-values). Numbers on the x-axis indicate the selected regions of interest ordered by mean occupancy strength: 1 middle temporal gyrus; 2 inferior temporal gyrus; 3 precuneus, 4 superior temporal gyrus, 5 insula, 6 orbitofrontal gyrus, 7 cuneus, 8 gyrus rectus, 9 superior medial frontal cortex, 10 medial cingulate, 11 calcarine gyrus, 12 anterior cingulate, 13 posterior cingulate, 14 subgenual cingulate, 15 hippocampus,*

16 putamen, 17 thalamus, 18 olfactory bulb, 19 caudate, 20 median raphe nucleus, 21 amygdala, 22 dorsal raphe nucleus.

Similar data were obtained when investigating SERT occupancy after three weeks of treatment (PET 3). Occupancy values ranged between 41.84±18.34% and 84.12±9.16% with a mean of 63.82±12.21% for cortical and 78.54±7.52% for subcortical regions. Homogeneity of cortical occupancies was again not confirmed for the middle and inferior temporal cortex, which had significantly lowered occupancies, whereas the PCC and sgCC had significantly elevated occupancies ($p<0.05$, corrected, test value: 63.82). Similarly, occupancy values were different from the mean for several subcortical regions with the putamen having lowered occupancies, whereas amygdala, MRN and DRN had elevated occupancy values ($p<0.05$, corrected, test value: 78.54, see Table 1). ROI based results were mostly confirmed by the voxel-wise approach (see Table 2.2).

Serotonin transporter occupancies after acute and prolonged intake of SSRIs (Q2)

Repeated-measures ANOVA with ROI and time (PET 2 and PET 3) as factors revealed a main effect of ROI ($F_{(21,168)}=27.558$, $p<0.001$) but no main effect of time. Additionally, a significant ROI by time interaction ($F_{(21,168)}=3.627$, $p<0.001$) was present, with *post-hoc* comparisons suggesting changes in occupancy over time in some but not in all brain regions: an increased occupancy after three weeks of treatment was seen only in subcortical regions, namely in DRN ($T=-9.215$, $p<0.001$) and MRN ($T=-6.297$, $p<0.001$), the amygdala ($T=-3.806$, $p=0.001$) and thalamus ($T=-4.885$, $p<0.001$, all $p<0.05$ corrected), as well as a statistical trend in the caudate ($T=-3.118$, $p=0.006$). These results were mostly confirmed by the voxel-wise analysis, revealing significant clusters restricted to the midbrain raphe nuclei ($T=12.61$, 2/-22/-8 mm (x/y/z)), basal ganglia ($T=11.49$, -6/2/-8 mm) and bilateral thalamus ($T=9.72$, 2/-14/6 mm, $T=8.37$, -8/-22/4 mm, $p<0.05$ corrected, $k>5$ voxels).

Predictors of serotonin transporter occupancies (Q3 and Q4)

Assessing the predictive value of pretreatment SERT binding on residual binding for each brain region (at PET 2 and PET 3) only revealed a positive association for the sgCC (PET 2: R^2=0.43, β=0.68, T=3.73, p<0.05 corrected; PET 3: R^2=0.45, β=0.7, T=3.74, p<0.05 corrected), a borderline significance for the hippocampus (PET 3, R^2=0.41, β=0.67, T=3.6, p=0.002, uncorrected) and trends for orbitofrontal cortex and anterior cingulate (see Table A1 for a list of corrected and uncorrected values). Interestingly, voxel-wise analysis revealed partially different results. For PET 2, peak associations were found in the right caudate (T=9.39, R^2=0.83, 14/24/-2 mm); right anterior cingulate (T=8.74, R^2=0.81, 14/32/26 mm) and left temporal pole (T=7.24, R^2=0.75, -38/8/-20 mm) whereas for PET 3, associations were present in the sgCC (T=8.70, R^2=0.81, 2/20/-4 mm), right temporal pole (T=8.55, R^2=0.80, 40/12/-30 mm) and left middle occipital cortex (T=7.72, R^2=0.77, -44/-64/2 mm, all p<0.05 corrected, k>5 voxels). That is, subjects with higher pretreatment SERT binding in these regions also had significantly higher residual SERT binding after treatment.

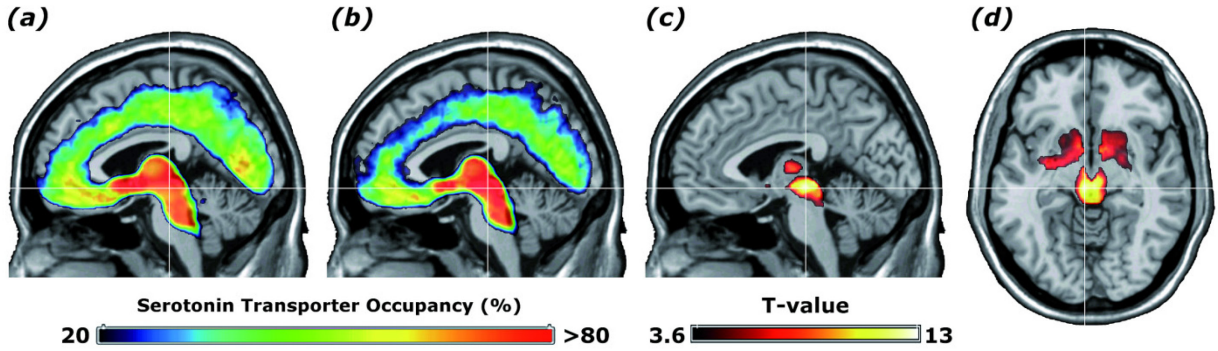

Fig 2. *Sagittal views of voxel-wise maps representing the averaged SERT occupancies after (a) single dosage (PET 2) and (b) steady state (PET 3) escitalopram or citalopram intake, overlaid onto structural MRI planes. Occupancy values are given in the color table. (c) and (d) show increased SERT occupancies at PET 3 compared to PET 2. Significant clusters are restricted to basal ganglia, thalamus and midbrain, p<0.05 corrected, k>5 voxels. Crosshair at -4/-23/-8 mm. Left is left.*

Assessing the association between the mean of baseline and residual SERT binding (Oldham's transformation) and absolute change after treatment within the ROI-based approach revealed

highly significant positive correlations for both PET 2 and PET 3 in most subcortical regions, as well as the PCC and sgCC (all p<0.05 corrected, see Table 3 and Fig. 3). Correlations were partly confirmed within the voxel-wise approach (see Table A2). These results therefore represent a strong and unbiased test for differential baseline effects of SERT BP_{ND} on change after both acute and prolonged SSRI treatment in these regions.

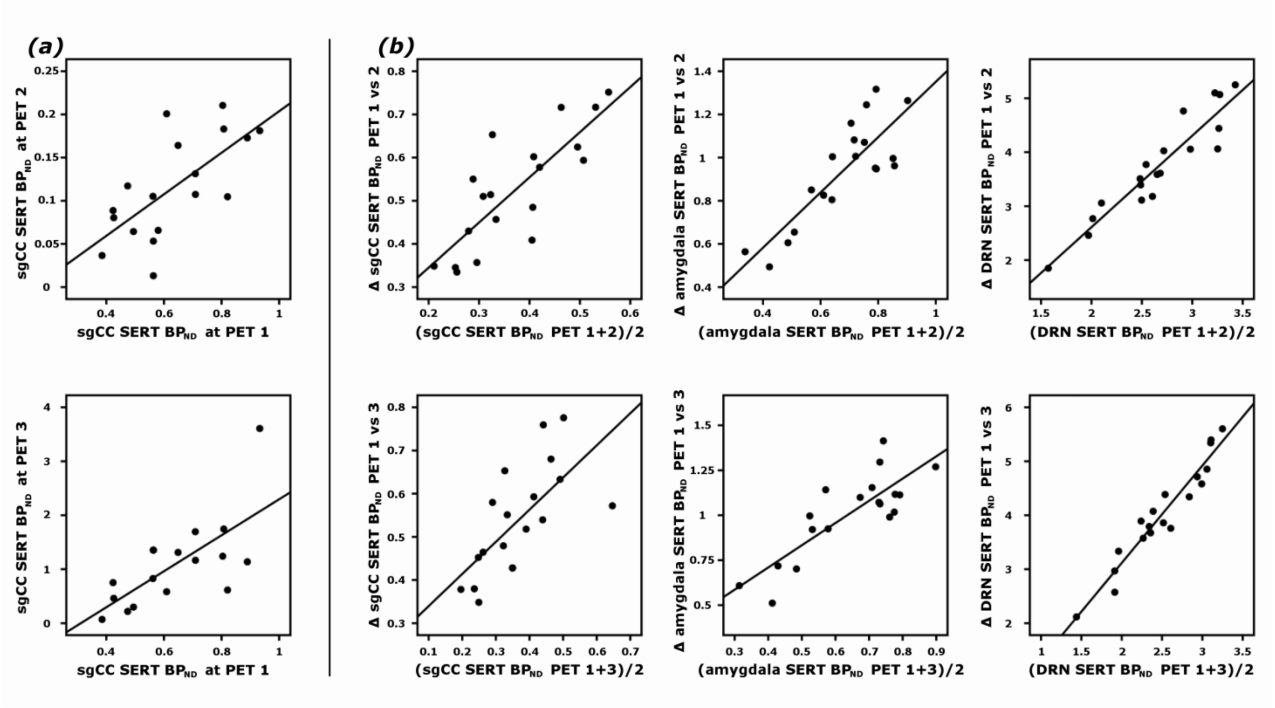

Fig 3. *Prediction of residual SERT binding and steepness of SERT decline at PET 2 (upper row) and PET 3 (bottom row) by pretreatment SERT binding. (a) Scatter plots representing the association between pretreatment and residual SERT binding in the subgenual cingulate cortex (sgCC). (b) Association between the mean of pretreatment and residual SERT binding and absolute reduction of SERT binding in the sgCC, amygdala and the dorsal raphe nucleus (DRN).*

Regression analysis across the brain using ROI means as single values revealed a strong positive effect of pretreatment SERT binding on residual SERT binding at PET 2 (R^2=0.92, β =0.96 T=15.10, p<0.001) and PET 3 (R^2=0.80, β =0.89 T=8.94, p<0.001). Thus, when averaged across subjects, regions with higher SERT binding before treatment had higher residual SERT binding after approximately six hours and three weeks of treatment. Similarly, high associations were found between Oldham's transformation and absolute change after treatment across brain regions, revealing highly significant positive correlations for both PET 2 and PET 3 (both r=0.99,

p<0.001). That is, regions with higher baseline SERT BP_{ND} were significantly more down-regulated / occupied by acute and prolonged SSRI treatment (see Fig. 4). Statistical assumptions of homoscedasticity and normal distribution of residuals were met.

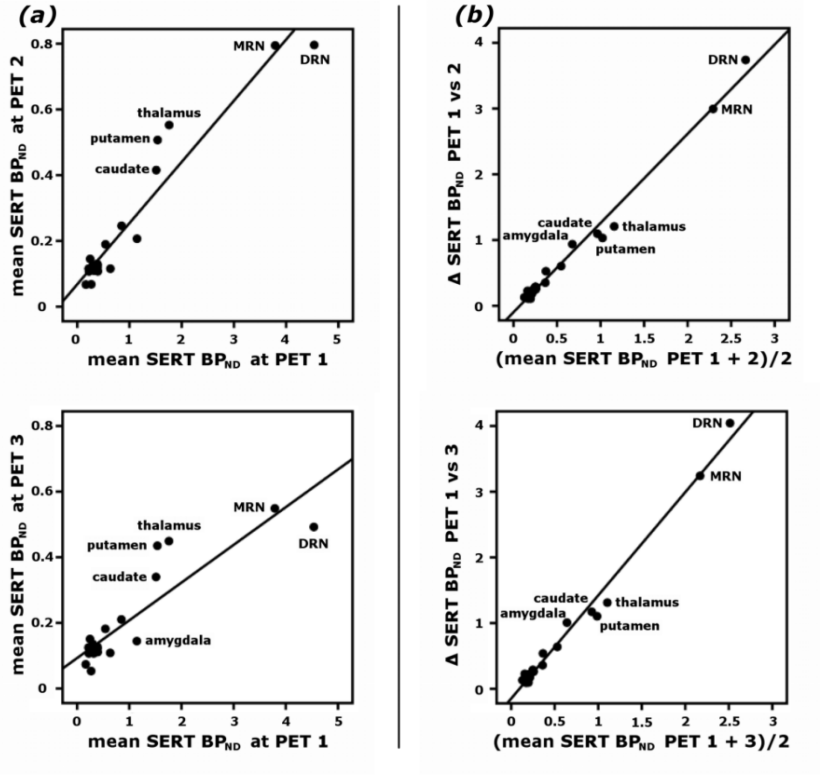

Fig 4*. Scatter plots representing the association between (a) regional SERT pretreatment binding and residual binding at PET 2 (upper row) and PET 3 (bottom row) and between (b) the mean of pretreatment and residual SERT binding and absolute reduction of SERT binding. Dots represent mean values for each region across subjects.*

Finally, correlation analysis between escitalopram plasma levels and occupancy at PET 2 revealed no significant associations for any ROI or voxel, not even when looking at uncorrected values. For PET 3, ROI analysis revealed significant correlations for caudate and putamen, thalamus and DRN (P<0.05, corrected, see Table 4, Fig. 5). These results were confirmed by the voxel-wise analysis, showing clusters mostly restricted to the midbrain and diencephalon, with two clusters in the basal ganglia surviving FWE correction (see Table A3). These findings imply that individual plasma levels of escitalopram affect SERT occupancy after continuous treatment

in the midbrain, thalamus and basal ganglia. However, they barely affect SERT occupancy after 6 hrs of drug intake.

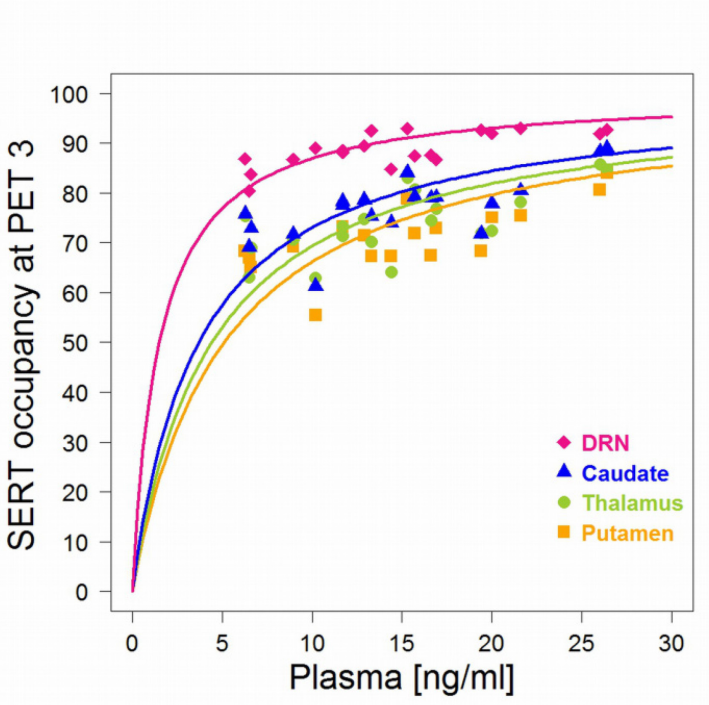

Fig 5: *Association between escitalopram plasma level and SERT occupancy at steady state treatment (PET 3) in the dorsal raphe nucleus (DRN, pink checkers), caudate (blue triangles), thalamus (green circles) and putamen (orange squares). Data were fitted by a hyperbolic curve of the form f(x)=a*x/(b+x), where f(x) refers to occupancy and x refers to escitalopram plasma level. Data are mostly restricted to the upper half of the curve above the bend which is due to the administration of a constant dosage of 20 mg of citalopram and 10 mg of escitalopram, respectively. Therefore, data are fitted better using a linear relationship. We thus used Pearson product-moment correlation analysis to assess the association between plasma and occupancy (see methods).*

3.2.5. Discussion

Using two different approaches, namely ROI based and voxel-wise computations, we detected an interregional divergence of SERT occupancy levels as well as a difference of SERT occupancy when comparing acute and prolonged citalopram/escitalopram intake. In addition, we found

two potent predictors of regional SERT occupancy, namely SERT binding potential at baseline and drug plasma levels. Each finding will be discussed below in detail.

Our first hypothesis investigated whether SERT occupancy levels were equally distributed throughout the brain and consequently if this applies to citalopram/escitalopram concentrations within brain regions (**Q1**). Assuming homogeneity of drug concentrations and supposing a brain-wide uniform affinity of the drug and the radiotracer [^{11}C]DASB (Zeng et al., 2006b), one might in fact imply similar SERT occupancies across all brain regions. That is, as occupancy refers to a relative measure, one might expect SERT occupancies of approximately 80% all over the brain for an effective dose of citalopram of 20mg daily (Meyer et al., 2004). However, if one of the above mentioned conditions is not satisfied, one would advocate for a topologically varying SERT occupancy, as is supported by the present study. We found elevated cortical SERT occupancies in PCC and sgCC and reduced values in the temporal cortex compared to the mean cortical occupancy level. Regarding subcortical ROIs, heightened SERT occupancies were detected in the amygdala, the MRN and DRN whereas subparts of the thalamus and putamen exhibited both lowered and elevated occupancy values (see Fig. 2, Table 1 and Table 2). These findings are in concordance with an earlier PET investigation showing higher SERT occupancy in the midbrain and lower occupancy in the thalamus compared to the striatum (Meyer et al., 2004). Furthermore, increased occupancies in the sgCC, amygdala and ventrocaudal thalamus near epithalamus are in accordance with the mechanistic explanation of our previous finding regarding the prediction of treatment efficacy by baseline SERT binding ratios (Lanzenberger et al., 2012). The above mentioned brain areas showing elevations from the mean occupancy values cortically and subcortically, as the midbrain raphe, the amygdala, the PCC and sgCC represent key structures in the pathobiology and treatment of major depression (Drevets et al., 2008; Hoflich et al., 2012; Johansen-Berg et al., 2008). Hence, the increased occupancy levels in these areas derived from our data strengthen the reported conceptual link between SERT occupancy and treatment of mood disorders (Lanzenberger et al., 2012; Mayberg, 2009). The assumption of an unequal regional occupancy distribution is in line with earlier animal studies postulating region-specific citalopram concentration (Kugelberg et al., 2001; Kugelberg et al., 2003; Kugelberg et al., 2004), although see (Kingback et al., 2011). A

possible causal mechanism suggested by Kugelberg et al. might be that a different degree of lipophilicity in various brain areas determines SERT occupancy by the SSRI (Kugelberg et al., 2001). By contrast, Takano et al. found no significant regional differences in SERT occupancy among the prefrontal cortex, the hippocampus, the amygdala, the thalamus and the striatum after administration of 50 mg of fluvoxamine in healthy subjects (Takano et al., 2006). However, one might mention that the population in this PET study was restricted to six participants (Takano et al., 2006). Nonetheless, the strong difference in means of SERT occupancy between cortical and subcortical brain regions - used as test values for the one-sample t-test (**Q1**) - supports the concept of regional variability of SERT occupancy and/or SSRI distribution. The fact that subcortical SERT occupancy was on average found to be higher in contrast to cortical SERT occupancy implies that occupancy levels might be determined by pretreatment SERT expression, given the consistently reported elevated SERT expression in subcortical compared to cortical regions (Savli et al., 2012).

In this context, the potential relationship between baseline SERT binding and SERT reduction / residual SERT binding after treatment was addressed (**Q3**). Individuals with higher baseline SERT binding levels exhibited elevated residual SERT binding in the sgCC, with statistical trends in hippocampus, anterior cingulate and orbitofrontal regions (see Table A1 and Fig. 3a). That is, as SERT BP_{ND} refers to both radiotracer affinity (K_D) and transporter availability (B_{max}), and given a consistent affinity throughout brain regions, one would expect residual SERT binding as being solely dependent on transporter availability. Thus, one would expect an association between pretreatment and residual SERT binding throughout the brain, though not restricted to only few regions, as observed in our study. Interestingly, we observed a strong correlation between pretreatment SERT binding potential and the extent of SERT binding reduction also only in few regions, namely the sgCC and subcortical regions (see Table 3 and Table A2, Fig. 3b). Given a uniform affinity for citalopram/escitalopram, SERT blockage by the drug should also dependent on pretreatment binding and one should – again – expect correlations throughout the brain, and not restricted to only few regions, as observed in our study. Hence, pretreatment SERT availability seems to be related to both residual SERT availability and SERT blockage by citalopram/escitalopram only for the sgCC, interestingly, a region that is known to be involved in

the treatment of mood disorders (Mayberg, 2009). To obtain a thorough understanding of SERT occupancy by SSRIs, regions of interest in SERT occupancy studies may therefore also include the sgCC in addition to striatum or putamen, which are typically used (Lundberg et al., 2012; Meyer et al., 2004). However, when averaged across subjects, regions with higher baseline SERT binding also exhibited higher residual binding and increased binding reduction (Fig. 4). This suggests that the dependence of residual SERT binding and binding reduction on pretreatment binding is also observed when potentially confounding or mediating variables such as subject's age or individual plasma levels of the drug are not considered.

On the other hand, within a given region, one might very well expect an influence of drug plasma levels on SERT occupancy (**Q4**). Hence, it is quite astonishing that we did not detect a significant correlation between SERT occupancy and escitalopram plasma levels 6 hrs after the first drug intake (PET 2). However, following approximately three weeks of SSRI administration, plasma levels correlated well with SERT occupancy in subcortical regions including the DRN, thalamus, caudate and putamen. Accordingly, several earlier PET studies determined this association between SERT occupancy after chronic intake of different antidepressant agents (amitryptiline, clomipramine, fluoxetine, citalopram, venlafaxine, sertraline, paroxetine) (Lundberg et al., 2012; Meyer et al., 2004). These findings imply that the region-specific impact of antidepressant agents on SERT occupancy only becomes evident after chronic SSRI intake. As the antidepressant effect of SSRI is known to begin after a certain latency period of several weeks (Blier and de Montigny, 1999; El Mansari et al., 2005), one may link plasma concentrations of the drug to treatment efficacy only after its effect on SERT occupancy has been established.

A further issue of the present study dealt with the comparison of SERT occupancies after acute and continuous SSRI treatment (**Q2**). We found significantly increased SERT occupancy in subcortical regions including the midbrain raphe region, basal ganglia, thalamus and the amygdala at PET 3 (see Fig. 1c). Indeed, this might be explained by a more pronounced SERT internalization after prolonged intake of antidepressants (Benmansour et al., 1999). Additionally, since SERT expression and activity seems to be usage-dependent (Ramamoorthy and Blakely, 1999; Steiner et al., 2008), one could expect an increased down-regulation of SERT

binding in brain regions originally exhibiting more SERT, such as the midbrain raphe region, the thalamus and basal ganglia, which matches well our findings. This would imply that prolonged – in contrast to acute – intake of citalopram/escitalopram exclusively impacts on subcortical regions which in turn challenges recent theoretical concepts of mechanisms for clinical response to SSRIs (Best et al., 2011). However, a study assessing the effects of prolonged exposure to various SSRIs on SERT availability using antibody detection showed that – besides SSRIs – serotonin by itself could induce SERT internalization while cocaine even elevated SERT surface expression despite exerting an effect similar to SSRIs (Kittler et al., 2010). Further long term treatment studies should be conducted to investigate a potential down-regulation of the SERT.

It is worth mentioning that our results are mostly in agreement, regardless of a ROI-based or a voxel-wise approach. However, some inconsistencies between both approaches remain, which may be attributed to inhomogeneity in SERT occupancy even within a defined brain region. As SERT occupancy depends on pretreatment binding, one might expect inhomogeneity in SERT expression also within an ROI. This is in accordance with previous findings using postmortem quantitative receptor autoradiography, showing that the distribution of serotonin receptors do not necessarily follow the common parcellations based on the cytoarchitecture defined in neuroanatomical atlases such as Brodmann's or AAL (Scheperjans et al., 2005; Zilles and Amunts, 2009). A further limitation to the study might be that no arterial blood sampling was available for this data set of 19 subjects. We were therefore not able to investigate differences in specific binding within the reference region (cerebellum) (Hinz et al., 2008; Parsey et al., 2006a). Here, the quantification of SERT binding potential relies on the reference model MRTM2 (Ichise et al., 2003), where computations are also based on unspecific SERT binding potential in the cerebellar gray. We cannot rule out that unspecific SERT binding potential differs between regions. However, this does not necessarily pose difficulties as the focus of this study is set on occupancy data, contrasting SERT binding before and after medication intake. We assume that the potential regional variability in unspecific binding might remain constant in all three PET scans. In order to provide a sufficiently large sample size in this PET study, all subjects were grouped despite differences in the study drug used, namely citalopram versus escitalopram. These were shown to exhibit different SERT occupancies in a previous study including eight

healthy male subjects using a different radiotracer (^{11}C[MADAM]) and solely comparing SERT occupancies after single-dose intake (Lundberg et al., 2012). Additionally, one might not leave unmentioned that the present study sample largely overlaps with the data set used in a previous investigation by our group centered on the prediction of SSRI treatment response by baseline SERT binding (Lanzenberger et al., 2012). However here, the focus is not set on the clinical outcome but on basic neuropharmacological issues regarding SERT occupancy levels following newly conducted extensive and highly complex data analyses according to other criterions (see methods sections).

3.2.6. Conclusion

The results of this study indicate regional differences in serotonin transporter occupancy by acute and prolonged treatment with SSRIs. Furthermore, our study reveals a strong but regionally restricted dependence of SERT blockage and residual availability on pretreatment transporter availability and drug plasma concentrations. These findings substantiate the postulated link between treatment response and SSRI blockage of the SERT while confining it to certain brain regions such as the subgenual cingulate cortex.

Role of funding source

Personal costs were partly funded by the Medical University of Vienna and Austrian national research funding agencies (FWF, OeNB) to R. Lanzenberger, PET measurements and treatment were supported by an investigator-initiated and unrestricted research grant from H. Lundbeck A/S, Denmark to S. Kasper. H. Lundbeck A/S, FWF and OeNB had no further role in study design; in the collection, analysis and interpretation of data; in the writing of the report and in the decision to submit the paper for publication.

Contributors

R. Lanzenberger and S. Kasper designed the main study. G.S. Kranz, P. Baldinger, M. Spies and A. Höflich established the details of analysis and study concept, M. Savli, G.S. Kranz and A. Hahn performed the data analyses. W. Wadsak, M. Mitterhauser, D. Haeusler and C. Philippe performed the radiotracer synthesis and supported the PET procedures. P. Baldinger and G.S. Kranz wrote the first draft of the manuscript. All authors contributed to and have approved the final manuscript.

Conflict of interest

S. Kasper declares that he has received grant/research support from Bristol Myers-Squibb, Eli Lilly, GlaxoSmithKline, Lundbeck, Organon, Sepracor and Servier; has served as a consultant or on advisory boards for AstraZeneca, Bristol-Myers Squibb, Eli Lilly, GlaxoSmithKline, Janssen, Lundbeck, Merck Sharp and Dome (MSD), Novartis, Organon, Pfizer, Schwabe, Sepracor, and Servier; and has served on speakers' bureaus for Angelini, AstraZeneca, Bristol Myers-Squibb, Eli Lilly, Janssen, Lundbeck, Pfizer, Pierre Fabre, Schwabe, Sepracor, and Servier. R. Lanzenberger received travel grants and conference speaker honoraria from AstraZeneca and Lundbeck A/S. M. Mitterhauser and W. Wadsak received speaker honoraria from Bayer. A. Hahn was recipient of a DOC-fellowship of the Austrian Academy of Sciences at the Department of Psychiatry and Psychotherapy. The authors G.S. Kranz, D. Haeusler, C. Philippe, P. Baldinger, A. Höflich, M. Spies and M. Savli report no financial relationships with commercial interests.

Acknowledgments

The authors are grateful to U. Moser, E. Akimova, C. Spindelegger, M. Fink, M. Willeit, G. Karanikas, K. Kletter and the clinical staff at the PET centre for their medical support, and H. Sitte for advisory service. We are especially indebted to G. Wagner, B. Reiterits, I. Leitinger, and R. Bartosch for technical support during the PET scans.

3.2.7. References

Benmansour, S., Cecchi, M., Morilak, D.A., Gerhardt, G.A., Javors, M.A., Gould, G.G., Frazer, A., 1999. Effects of chronic antidepressant treatments on serotonin transporter function, density, and mRNA level. J Neurosci 19, 10494-10501.

Best, J., Nijhout, H.F., Reed, M., 2011. Bursts and the efficacy of selective serotonin reuptake inhibitors. Pharmacopsychiatry 44 Suppl 1, S76-83.

Blier, P., de Montigny, C., 1999. Serotonin and drug-induced therapeutic responses in major depression, obsessive-compulsive and panic disorders. Neuropsychopharmacology 21, 91S-98S.

Drevets, W.C., Savitz, J., Trimble, M., 2008. The subgenual anterior cingulate cortex in mood disorders. CNS Spectr 13, 663-681.

El Mansari, M., Sanchez, C., Chouvet, G., Renaud, B., Haddjeri, N., 2005. Effects of acute and long-term administration of escitalopram and citalopram on serotonin neurotransmission: an in vivo electrophysiological study in rat brain. Neuropsychopharmacology 30, 1269-1277.

Fink, M., Wadsak, W., Savli, M., Stein, P., Moser, U., Hahn, A., Mien, L.-K., Kletter, K., Mitterhauser, M., Kasper, S., Lanzenberger, R., 2009. Lateralization of the serotonin-1A receptor distribution in language areas revealed by PET. Neuroimage 45, 598-605.

Fraser, T., Tayler, H., Love, S., 2010. Fatty Acid Composition of Frontal, Temporal and Parietal Neocortex in the Normal Human Brain and in Alzheimer's Disease. Neurochemical Research 35, 503-513.

Gill, J.S., Beevers, D.G., Zezulka, A.V., Davies, P., 1985. Relation between initial blood pressure and its fall with treatment. The Lancet 325, 567-569.

Haeusler, D., Mien, L.K., Nics, L., Ungersboeck, J., Philippe, C., Lanzenberger, R.R., Kletter, K., Dudczak, R., Mitterhauser, M., Wadsak, W., 2009. Simple and rapid preparation of [11C]DASB with high quality and reliability for routine applications. Appl Radiat Isot 67, 1654-1660.

Hinz, R., Selvaraj, S., Murthy, N.V., Bhagwagar, Z., Taylor, M., Cowen, P.J., Grasby, P.M., 2008. Effects of citalopram infusion on the serotonin transporter binding of [lsqb]11C[rsqb]DASB in healthy controls. J Cereb Blood Flow Metab 28, 1478-1490.

Hoflich, A., Baldinger, P., Savli, M., Lanzenberger, R., Kasper, S., 2012. Imaging treatment effects in depression. Rev Neurosci 23, 227-252.

Holsboer, F., 2008. How can we realize the promise of personalized antidepressant medicines? Nat Rev Neurosci 9, 638-646.

Ichise, M., Liow, J.-S., Lu, J.-Q., Takano, A., Model, K., Toyama, H., Suhara, T., Suzuki, K., Innis, R.B., Carson, R.E., 2003. Linearized Reference Tissue Parametric Imaging Methods[colon] Application to [lsqb]11C[rsqb]DASB Positron Emission Tomography Studies of the Serotonin Transporter in Human Brain. J Cereb Blood Flow Metab 23, 1096-1112.

Innis, R.B., Cunningham, V.J., Delforge, J., Fujita, M., Gjedde, A., Gunn, R.N., Holden, J., Houle, S., Huang, S.-C., Ichise, M., Iida, H., Ito, H., Kimura, Y., Koeppe, R.A., Knudsen, G.M., Knuuti, J., Lammertsma, A.A., Laruelle, M., Logan, J., Maguire, R.P., Mintun, M.A., Morris, E.D., Parsey, R., Price, J.C., Slifstein, M., Sossi, V., Suhara, T., Votaw, J.R., Wong, D.F., Carson, R.E., 2007. Consensus nomenclature for in vivo imaging of reversibly binding radioligands. J Cereb Blood Flow Metab 27, 1533-1539.

Johansen-Berg, H., Gutman, D.A., Behrens, T.E.J., Matthews, P.M., Rushworth, M.F.S., Katz, E., Lozano, A.M., Mayberg, H.S., 2008. Anatomical Connectivity of the Subgenual Cingulate Region Targeted with Deep Brain Stimulation for Treatment-Resistant Depression. Cerebral Cortex 18, 1374-1383.

Kasper, S., Sacher, J., Klein, N., Mossaheb, N., Attarbaschi-Steiner, T., Lanzenberger, R., Spindelegger, C., Asenbaum, S., Holik, A., Dudczak, R., 2009. Differences in the dynamics of serotonin reuptake transporter occupancy may explain superior clinical efficacy of escitalopram versus citalopram. Int Clin Psychopharmacol 24, 119-125.

Kent, J., Coplan, J., Lombardo, I., Hwang, D.-R., Huang, Y., Mawlawi, O., Van Heertum, R., Slifstein, M.,Abi-Dargham, A., Gorman, J., Laruelle, M., 2002. Occupancy of brain serotonin transporters during treatment with paroxetine in patients with social phobia: a positron emission tomography study with [11C]McN 5652. Psychopharmacology 164, 341-348.

Kingback, M., Carlsson, B., Ahlner, J., Bengtsson, F., Kugelberg, F.C., 2011. Cytochrome P450-dependent disposition of the enantiomers of citalopram and its metabolites: in vivo studies in Sprague-Dawley and Dark Agouti rats. Chirality 23, 172-177.

Kittler, K., Lau, T., Schloss, P., 2010. Antagonists and substrates differentially regulate serotonin transporter cell surface expression in serotonergic neurons. Eur J Pharmacol 629, 63-67.

Kranz, G.S., Hahn, A., Savli, M., Lanzenberger, R., 2012. Challenges in the differentiation of midbrain raphe nuclei in neuroimaging research. Proceedings of the National Academy of Sciences 109, E2000.

Kugaya, A., Sanacora, G., Staley, J.K., Malison, R.T., Bozkurt, A., Khan, S., Anand, A., van Dyck, C.H., Baldwin, R.M., Seibyl, J.P., Charney, D., Innis, R.B., 2004. Brain serotonin transporter availability predicts treatment response to selective serotonin reuptake inhibitors. Biological Psychiatry 56, 497-502.

Kugelberg, F.C., Apelqvist, G., Carlsson, B., Ahlner, J., Bengtsson, F., 2001. In vivo steady-state pharmacokinetic outcome following clinical and toxic doses of racemic citalopram to rats. Br J Pharmacol 132, 1683-1690.

Kugelberg, F.C., Carlsson, B., Ahlner, J., Bengtsson, F., 2003. Stereoselective single-dose kinetics of citalopram and its metabolites in rats. Chirality 15, 622-629.

Kugelberg, F.C., Druid, H., Carlsson, B., Ahlner, J., Bengtsson, F., 2004. Postmortem redistribution of the enantiomers of citalopram and its metabolites: an experimental study in rats. J Anal Toxicol 28, 631-637.

Lanzenberger, R., Kranz, G.S., Haeusler, D., Akimova, E., Savli, M., Hahn, A., Mitterhauser, M., Spindelegger, C., Philippe, C., Fink, M., Wadsak, W., Karanikas, G., Kasper, S., 2012. Prediction of SSRI treatment response in major depression based on serotonin transporter interplay between median raphe nucleus and projection areas. Neuroimage 63, 874-881.

Laruelle, M., Slifstein, M., Huang, Y., 2003. Relationships between radiotracer properties and image quality in molecular imaging of the brain with positron emission tomography. Mol Imaging Biol 5, 363-375.

Lawler, C.P., Prioleau, C., Lewis, M.M., Mak, C., Jiang, D., Schetz, J.A., Gonzalez, A.M., Sibley, D.R., Mailman, R.B., 1999. Interactions of the Novel Antipsychotic Aripiprazole (OPC-14597) with Dopamine and Serotonin Receptor Subtypes. Neuropsychopharmacology 20, 612-627.

Lesch, K.P., Aulakh, C.S., Wolozin, B.L., Tolliver, T.J., Hill, J.L., Murphy, D.L., 1993. Regional brain expression of serotonin transporter mRNA and its regulation by reuptake inhibiting antidepressants. Brain Res Mol Brain Res 17, 31-35.

Lundberg, J., Tiger, M., Landén, M., Halldin, C., Farde, L., 2012. Serotonin transporter occupancy with TCAs and SSRIs: a PET study in patients with major depressive disorder. The International Journal of Neuropsychopharmacology 15, 1167-1172.

Malagie, I., Trillat, A.C., Bourin, M., Jacquot, C., Hen, R., Gardier, A.M., 2001. 5-HT1B Autoreceptors limit the effects of selective serotonin re-uptake inhibitors in mouse hippocampus and frontal cortex. J Neurochem 76, 865-871.

Mannoury la Cour, C., El Mestikawy, S., Hanoun, N., Hamon, M., Lanfumey, L., 2006. Regional Differences in the Coupling of 5-Hydroxytryptamine-1A Receptors to G Proteins in the Rat Brain. Molecular Pharmacology 70, 1013-1021.

Mayberg, H.S., 2009. Targeted electrode-based modulation of neural circuits for depression. J Clin Invest 119, 717-725.

Meyer, J.H., 2007. Imaging the serotonin transporter during major depressive disorder and antidepressant treatment. J Psychiatry Neurosci 32, 86-102.

Meyer, J.H., Wilson, A.A., Ginovart, N., Goulding, V., Hussey, D., Hood, K., Houle, S., 2001. Occupancy of serotonin transporters by paroxetine and citalopram during treatment of depression: a [(11)C]DASB PET imaging study. Am J Psychiatry 158, 1843-1849.

Meyer, J.H., Wilson, A.A., Sagrati, S., Hussey, D., Carella, A., Potter, W.Z., Ginovart, N., Spencer, E.P., Cheok, A., Houle, S., 2004. Serotonin transporter occupancy of five selective serotonin reuptake inhibitors at different doses: an [11C]DASB positron emission tomography study. Am J Psychiatry 161, 826-835.

Oldham, P.D., 1962. A note on the analysis of repeated measurements of the same subjects. J Chronic Dis 15, 969-977.

Ostad Haji, E., Tadic, A., Wagner, S., Dragicevic, A., Muller, M.J., Boland, K., Rao, M.L., Fric, M., Laux, G., Hiemke, C., 2011. Association between citalopram serum levels and clinical improvement of patients with major depression. J Clin Psychopharmacol 31, 281-286.

Parsey, R.V., Kent, J.M., Oquendo, M.A., Richards, M.C., Pratap, M., Cooper, T.B., Arango, V., Mann, J.J., 2006a. Acute Occupancy of Brain Serotonin Transporter by Sertraline as Measured by [11C]DASB and Positron Emission Tomography. Biological Psychiatry 59, 821-828.

Parsey, R.V., Ojha, A., Ogden, R.T., Erlandsson, K., Kumar, D., Landgrebe, M., Van Heertum, R., Mann, J.J., 2006b. Metabolite Considerations in the In Vivo Quantification of Serotonin Transporters Using 11C-DASB and PET in Humans. Journal of Nuclear Medicine 47, 1796-1802.

Pehrson, A.L., Cremers, T., Betry, C., van der Hart, M.G., Jorgensen, L., Madsen, M., Haddjeri, N., Ebert, B., Sanchez, C., 2012. Lu AA21004, a novel multimodal antidepressant, produces regionally selective increases of multiple neurotransmitters-A rat microdialysis and electrophysiology study. Eur Neuropsychopharmacol.

Ramamoorthy, S., Blakely, R.D., 1999. Phosphorylation and sequestration of serotonin transporters differentially modulated by psychostimulants. Science 285, 763-766.

Savli, M., Bauer, A., Mitterhauser, M., Ding, Y.-S., Hahn, A., Kroll, T., Neumeister, A., Haeusler, D., Ungersboeck, J., Henry, S., Isfahani, S.A., Rattay, F., Wadsak, W., Kasper, S., Lanzenberger, R., 2012. Normative database of the serotonergic system in healthy subjects using multi-tracer PET. Neuroimage 63, 447-459.

Scheperjans, F., Grefkes, C., Palomero-Gallagher, N., Schleicher, A., Zilles, K., 2005. Subdivisions of human parietal area 5 revealed by quantitative receptor autoradiography: a parietal region between motor, somatosensory, and cingulate cortical areas. Neuroimage 25, 975-992.

Stein, P., Savli, M., Wadsak, W., Mitterhauser, M., Fink, M., Spindelegger, C., Mien, L.-K., Moser, U., Dudczak, R., Kletter, K., Kasper, S., Lanzenberger, R., 2008. The serotonin-1A receptor distribution in healthy men and women measured by PET and [carbonyl-11C]WAY-100635. European Journal of Nuclear Medicine and Molecular Imaging 35, 2159-2168.

Steiner, J.A., Carneiro, A.M., Blakely, R.D., 2008. Going with the flow: trafficking-dependent and -independent regulation of serotonin transport. Traffic 9, 1393-1402.

Suhara T, T.A.S.Y., et al., 2003. HIgh levels of serotonin transporter occupancy with low-dose clomipramine in comparative occupancy study with fluvoxamine using positron emission tomography. Archives of General Psychiatry 60, 386-391.

Takano, A., Suhara, T., Ichimiya, T., Yasuno, F., Suzuki, K., 2006. Time course of in vivo 5-HTT transporter occupancy by fluvoxamine. J Clin Psychopharmacol 26, 188-191.

Talbot, P.S., Laruelle, M., 2002. The role of in vivo molecular imaging with PET and SPECT in the elucidation of psychiatric drug action and new drug development. European Neuropsychopharmacology 12, 503-511.

Tao, R., Ma, Z., Auerbach, S.B., 2000. Differential Effect of Local Infusion of Serotonin Reuptake Inhibitors in the Raphe versus Forebrain and the Role of Depolarization-Induced Release in Increased Extracellular Serotonin. Journal of Pharmacology and Experimental Therapeutics 294, 571-579.

Tu, Y.K., Gilthorpe, M.S., 2007. Revisiting the relation between change and initial value: a review and evaluation. Stat Med 26, 443-457.

Tzourio-Mazoyer, N., Landeau, B., Papathanassiou, D., Crivello, F., Etard, O., Delcroix, N., Mazoyer, B., Joliot, M., 2002. Automated anatomical labeling of activations in SPM using a macroscopic anatomical parcellation of the MNI MRI single-subject brain. Neuroimage 15, 273-289.

Urban, J.D., Clarke, W.P., von Zastrow, M., Nichols, D.E., Kobilka, B., Weinstein, H., Javitch, J.A., Roth, B.L., Christopoulos, A., Sexton, P.M., Miller, K.J., Spedding, M., Mailman, R.B., 2007. Functional Selectivity and Classical Concepts of Quantitative Pharmacology. Journal of Pharmacology and Experimental Therapeutics 320, 1-13.

Zeng, Z., Chen, T.-B., Miller, P.J., Dean, D., Tang, Y.S., Sur, C., Williams Jr, D.L., 2006a. The serotonin transporter in rhesus monkey brain: comparison of DASB and citalopram binding sites. Nuclear Medicine and Biology 33, 555-563.

Zeng, Z., Chen, T.B., Miller, P.J., Dean, D., Tang, Y.S., Sur, C., Williams, D.L., Jr., 2006b. The serotonin transporter in rhesus monkey brain: comparison of DASB and citalopram binding sites. Nucl Med Biol 33, 555-563.

Zilles, K., Amunts, K., 2009. Receptor mapping: architecture of the human cerebral cortex. Curr Opin Neurol 22, 331-339.

Table 1: Regional SERT occupancy levels compared to mean cortical and subcortical SERT occupancies (test values given in the table) in 14 cortical and 8 subcortical regions of interest. *p<0.05 Bonferroni corrected.

	PET 2					PET 3				
	mean	**SD**	**t**	**df**	**p**	**mean**	**SD**	**t**	**df**	**p**
cortical ROI	test value = 65.66					test value = 63.82				
middle temporal gyrus	43.53	18.09	-5.19	17	**<0.001***	41.84	18.34	-5.09	17	**<0.001***
inferior temporal gyrus	47.4	20.67	-3.76	17	**0.002***	43.53	20.65	-4.17	17	**0.001***
precuneus	58.5	18.43	-1.76	15	0.141	50.1	26.49	-2.14	16	0.049
superior temporal gyrus	60.54	16.08	-1.35	17	0.194	54.83	22.16	-1.72	17	0.103
insula	64.54	11.12	-0.44	18	0.666	66.08	13.86	0.71	18	0.487
orbitofrontal cortex	66.12	16.5	0.12	18	0.904	65.69	14.7	0.54	17	0.597
cuneus	67.21	16.85	0.37	15	0.717	67.56	20.82	0.74	16	0.469
gyrus rectus	67.44	11.65	0.67	18	0.514	68.59	15.19	1.37	18	0.188
superior medial frontal cortex	68.53	18.33	0.61	14	0.554	66.28	23.78	0.37	12	0.716
medial cingulate	70.53	12.41	1.67	17	0.114	66.26	20.28	0.52	18	0.607
calcarine gyrus	71.45	16.14	1.52	17	0.146	67.68	15.76	1.01	16	0.328
anterior cingulate	72.8	20.7	1.5	18	0.152	72.34	14.12	2.56	17	0.02
posterior cingulate	78.49	11.65	4.12	13	**0.001***	78.55	16.27	3.51	14	**0.003***
subgenual cingulate	82.16	7.36	9.51	17	**<0.001***	84.12	9.16	9.14	16	**<0.001***
subcortical ROI	test value = 72.99					test value = 78.54				
hippocampus	65.01	15.33	-2.27	18	0.036	70.06	15.9	-2.26	17	0.037
putamen	66.71	5.27	-5.19	18	**<0.001***	71.1	6.32	-5.12	18	**<0.001***
thalamus	67.92	6.46	-3.42	18	0.003*	73.83	6.72	-3.05	18	0.007
olfactory bulb	70.4	8.14	-1.39	18	0.182	74.84	8.67	-1.86	18	0.079
caudate	72.1	5.14	-0.76	18	0.458	77	6.42	-1.04	18	0.311
median raphe	78.14	6.16	3.641	18	0.002*	85.13	4.75	6.04	18	**<0.001***
amygdala	81.78	6.48	5.909	18	**<0.001***	87.58	6.74	5.69	17	**<0.001***
dorsal raphe	81.88	4.52	8.57	18	**<0.001***	88.78	3.56	12.56	18	**<0.001***

Table 2.1: Regional SERT occupancy levels compared to mean cortical and subcortical SERT occupancies (test values given in the table 1) at PET 2 following a voxel-wise approach. *p<0.05 FWE corrected voxel-level, p<0.001 uncorrected voxel-level, cluster extent treshhold k>5 voxel, MNI coordinates in mm, L left, R right.

Anatomical Region (AAL)	MNI Coordinates						
	BA	x	y	z	t	p	Cluster Size
	regional occupancy > mean cortical occupancy at PET 2						
inferior orbitofrontal cortex L	38	-24	16	-20	8.37	**<0.001***	41
subgenual cingulate cortex L	11	-2	30	-10	6.29	<0.001	-
lingual gyrus L	19	-16	-50	-4	5.82	<0.001	24
middle cingulate R	24	4	14	32	5.76	<0.001	93
parahippocampal gyrus L	35	-20	-18	-22	5.28	<0.001	7
heschl gyrus R	48	38	-20	12	4.75	<0.001	30
middle cingulate gyrus	23	0	-18	34	4.52	<0.001	10
anterior cingulate L	24	-6	32	20	4.46	<0.001	22
anterior cingulate	24	0	36	12	4.35	<0.001	17
superior temporal gyrus L	48	-42	0	-12	4.11	<0.001	7
middle cingulate L	23	-2	-4	38	4.03	<0.001	9
	regional occupancy < mean cortical occupancy at PET 2						
middle temporal gyrus R	37	44	-70	14	12.24	**<0.001***	4576
middle frontal gyrus L	46	-34	52	20	8.87	**<0.001***	1865
middle temporal gyrus L	37	-56	-54	4	8.62	**<0.001***	5100
middle orbitofrontal gyrus R	11	28	60	-8	7.75	**<0.001***	1070
precuneus R	7	6	-70	48	6.46	<0.001	537
inferior triangular frontal gyrus L	45	-46	24	4	6.20	<0.001	256
cuneus R	-	6	-70	28	5.44	<0.001	90
precuneus L	-	-8	-50	36	4.93	<0.001	22
inferior triangular frontal gyrus L	44	-38	16	32	4.62	<0.001	33
parahippocampal gyrus R	20	30	-30	-12	4.61	<0.001	15
middle frontal gyrus R	6	36	-2	58	4.61	<0.001	35
insula R	48	46	10	6	4.50	<0.001	39
inferior triangular frontal gyrus R	48	42	20	30	4.41	<0.001	8
insula R	48	42	18	4	4.34	<0.001	29
superior orbitofrontal cortex L	11	-14	36	-20	4.32	<0.001	8
middle frontal gyrus L	46	-36	28	40	4.29	<0.001	11
middle frontal gyrus L	8	-26	28	50	4.26	<0.001	31
precentral gyrus L	6	-34	0	62	4.26	<0.001	16
fusiform gyrus R	19	26	-62	10	4.24	<0.001	8
precentral gyrus R	44	44	10	34	4.11	<0.001	27
inferior occipital gyrus L	18	-28	-90	-10	4.10	<0.001	12
precuneus R	7	2	-68	56	4.09	<0.001	6
precentral gyrus L	6	-42	2	48	3.95	<0.001	6
inferior orbitofrontal cortex R	47	38	40	-8	3.95	<0.001	7
	regional occupancy > mean subcortical occupancy at PET 2						
midbrain (tectum)	-	2	-30	-4	14.35	**<0.001***	952

midbrain (DRN)		0	-26	-6	13.41	**<0.001***	-
thalamus R	-	6	-28	4	8.56	**<0.001***	
amygdala L	34	-20	0	-20	8.10	**<0.001***	107
caudate R	-	8	14	0	7.86	**<0.001***	-
amygdala R	35	14	-8	-16	7.56	<0.001	109
caudate L	-	-12	8	10	5.63	<0.001	-
pons L	-	-6	-26	-32	5.12	<0.001	14
	regional occupancy < mean subcortical occupancy at PET 2						
thalamus R	-	-12	-10	6	10.43	**<0.001***	-
thalamus L	-	10	-14	4	9.16	**<0.001***	-
putamen R	-	-10	-22	-14	8.98	**<0.001***	-
putamen L	-	10	-24	-14	7.34	<0.001	-
amygdala R	-	34	4	0	6.27	<0.001	-
hippocampus L	-	-28	4	-4	5.81	<0.001	-

Table 2.2: Regional SERT occupancy levels compared to mean cortical and subcortical SERT occupancies (test values given in the table 1) at PET 3 following a voxel-wise approach. *p<0.05 FWE corrected voxel-level, p<0.001 uncorrected voxel-level, cluster extent treshhold k>5 voxel, MNI coordinates in mm, L left, R right.

Anatomical Region (AAL)	MNI Coordinates						
	BA	x	y	z	t	p	Cluster Size
	regional occupancy > mean cortical occupancy at PET 3						
middle cingulate gyrus L	24	-4	2	40	6.66	<0.001	154
lingual gyrus R	17	2	-80	4	5.57	<0.001	87
lingual gyrus L	18	-14	-56	-2	5.31	<0.001	36
calcarine gyrus	17	0	-84	0	4.93	<0.001	7
fusiform gyrus L	30	-28	-22	-28	4.57	<0.001	6
superior temporal pole L	38	-40	20	-28	4.53	<0.001	8
supplementary motor area L	6	-8	-16	56	4.39	<0.001	6
anterior cingulate L	24	-6	30	22	4.35	<0.001	15
lingual gyrus R	18	14	-56	-4	4.31	<0.001	6
supplementary motor area R	-	6	-4	50	4.15	<0.001	13
anterior cingulate R	24	6	26	24	3.96	<0.001	6
middle cingulate gyrus R	24	6	12	36	3.95	<0.001	10
	regional occupancy < mean cortical occupancy at PET 3						
middle temporal gyrus R	37	54	-58	16	10.68	**<0.001***	3860
middle temporal gyrus L	37	-54	-60	16	9.16	**<0.001***	4708
middle frontal gyrusL	10	-30	62	0	6.95	<0.001	1287
middle frontal gyrus R	46	36	54	14	6.22	<0.001	618
inferior frontal operculum L	48	-48	12	0	6.06	<0.001	311
superior frontal gyrus L	10	-18	50	10	4.75	<0.001	18
precuneus R	-	10	-48	50	4.56	<0.001	18
precuneus L	-	-8	-58	34	4.63	<0.001	68
middle frontal gyrus L	46	-20	46	18	4.63	<0.001	7
rolandic operculum R	48	52	10	6	4.58	<0.001	30
inferior frontal operculum R	44	42	16	30	4.51	<0.001	26
precentral gyrus L	6	-40	0	50	4.45	<0.001	12
fusiform gyrus R	20	44	-28	-26	4.41	<0.001	12
middle frontal gyrus R	6	30	-2	56	4.38	<0.001	9
middle frontal gyrus R	45	42	30	32	4.34	<0.001	12
superior orbitofrontal cortex L	11	-14	64	-12	4.32	<0.001	9
precuneus L	-	-2	-70	34	4.31	<0.001	28
cuneus R	-	8	-70	28	4.24	<0.001	9
precuneus R	-	6	-66	50	4.21	<0.001	16
precuneus L	-	-6	-66	50	4.19	<0.001	17
inferior frontal operculum R	48	42	12	8	4.14	<0.001	28
middle frontal gyrus R	8	30	24	44	4.00	<0.001	8
	regional occupancy > mean subcortical occupancy at PET 3						
midbrain (tectum)	-	0	-30	-6	15.21	**<0.001***	888
thalamus R	-	8	-30	2	7.21	<0.001	-

caudate L	-	-6	14	-6	6.85	<0.001	-
caudate R	-	10	16	0	5.76	<0.001	-
midbrain (median raphe nucleus)	-	0	-32	-18	4.62	<0.001	8
	regional occupancy < mean subcortical occupancy at PET 3						
thalamus R	-	12	-14	2	13.76	**<0.001***	-
thalamus L	-	-12	-12	6	12.14	**<0.001***	-
putamen R	-	32	12	4	9.42	**<0.001***	-
putamen L	-	-30	4	6	8.12	**<0.001***	-
amygdala R	-	34	-2	-22	5.38	<0.001	17
hippocampus L	-	-24	-10	-22	4.65	<0.001	-

Table 3: Correlation analysis between absolute SERT reduction and Oldham's transformation at PET 2 and PET 3 (baseline BP_{ND} + residual BP_{ND})/2 in 22 regions of interest. *p<0.05 Bonferroni corrected.

ROI	PET 2		PET 3	
	r	p	r	p
middle temporal gyrus	0.03	0.894	0.14	0.563
inferior temporal gyrus	0.16	0.523	0.01	0.978
precuneus	0.37	0.119	0.34	0.16
superior temporal gyrus	0.3	0.205	0.08	0.747
insula	0.62	0.005	0.39	0.102
orbitofrontal cortex	0.47	0.044	0.43	0.066
cuneus	0.48	0.036	0.41	0.078
gyrus rectus	0.56	0.013	0.37	0.121
superior medial frontal cortex	0.49	0.064	0.28	0.348
medial cingulate	0.6	0.006	0.57	0.011
calcarine gyrus	0.61	0.005	0.6	0.007
anterior cingulate	0.54	0.016	0.64	0.003
posterior cingulate	0.72	**0.001***	0.79	**<0.001***
subgenual cingulate	0.81	**<0.001***	0.68	**0.002***
hippocampus	0.49	0.035	0.23	0.345
putamen	0.82	**<0.001***	0.83	**<0.001***
thalamus	0.86	**<0.001***	0.82	**<0.001***
olfactory bulb	0.8	**<0.001***	0.73	**<0.001***
caudate	0.88	**<0.001***	0.82	**<0.001***
median raphe	0.91	**<0.001***	0.93	**<0.001***
amygdala	0.84	**<0.001***	0.83	**<0.001***
dorsal raphe	0.94	**<0.001***	0.96	**<0.001***

Table 4: Correlation analysis between escitalopram plasma levels and SERT occupancy at PET 2 and PET 3 in 22 regions of interest. *p<0.05 Bonferroni corrected.

ROI	PET 2		PET 3	
	r	p	r	p
middle temporal gyrus	0.03	0.894	0.14	0.563
inferior temporal gyrus	0.16	0.523	0.01	0.978
precuneus	0.37	0.119	0.34	0.16
superior temporal gyrus	0.3	0.205	0.08	0.747
insula	0.62	0.005	0.39	0.102
orbitofrontal cortex	0.47	0.044	0.43	0.066
cuneus	0.48	0.036	0.41	0.078
gyrus rectus	0.56	0.013	0.37	0.121
superior medial frontal cortex	0.49	0.064	0.28	0.348
medial cingulate	0.6	0.006	0.57	0.011
calcarine gyrus	0.61	0.005	0.6	0.007
anterior cingulate	0.54	0.016	0.64	0.003
posterior cingulate	0.72	**0.001***	0.79	**<0.001***
subgenual cingulate	0.81	**<0.001***	0.68	**0.002***
hippocampus	0.49	0.035	0.23	0.345
putamen	0.82	**<0.001***	0.83	**<0.001***
thalamus	0.86	**<0.001***	0.82	**<0.001***
olfactory bulb	0.8	**<0.001***	0.73	**<0.001***
caudate	0.88	**<0.001***	0.82	**<0.001***
median raphe	0.91	**<0.001***	0.93	**<0.001***
amygdala	0.84	**<0.001***	0.83	**<0.001***
dorsal raphe	0.94	**<0.001***	0.96	**<0.001***

3.2.8. Appendices

Table A1: Regression analysis of residual SERT binding on pretreatment SERT binding in 22 regions of interest. *p<0.05 Bonferroni corrected, values are given as corrected r^2 and standardized β.

ROI	PET 1-2				PET 1-3			
	r^2	β	t	p	r^2	β	t	p
middle temporal gyrus	0.27	0.56	2.76	0.013	0.28	0.57	2.86	0.011
inferior temporal gyrus	0.04	0.3	1.3	0.212	0.06	0.34	1.46	0.161
precuneus	0.25	0.54	2.52	0.024	0.05	0.33	1.37	0.191
superior temporal gyrus	0.13	0.42	1.93	0.07	0.05	0.33	1.39	0.184
insula	0.26	0.55	2.73	0.014	0.12	0.41	1.83	0.085
orbitofrontal cortex	0.3	0.58	2.97	0.009	0.18	0.48	2.17	0.046
cuneus	0.16	0.46	1.99	0.066	0.06	0.34	1.4	0.183
gyrus rectus	0.32	0.6	3.08	0.007	0.32	0.6	3.05	0.007
superior medial frontal cortex	0.01	0.27	1.05	0.311	0.01	0.29	1.09	0.295
medial cingulate	0.1	0.39	1.76	0.1	0.12	0.41	1.86	0.081
calcarine gyrus	0.14	0.43	1.98	0.065	-0.01	0.23	0.92	0.374
anterior cingulate	0.31	0.59	3.03	0.008	0.32	0.6	3.03	0.008
posterior cingulate	0.07	0.37	1.42	0.179	0.07	0.36	1.41	0.183
subgenual cingulate	0.43	0.68	3.73	**0.002***	0.45	0.7	3.74	**0.002***
hippocampus	0.25	0.54	2.67	0.016	0.41	0.67	3.6	0.002
putamen	0.23	0.52	2.53	0.021	-0.04	0.12	0.48	0.635
thalamus	0.1	0.39	1.73	0.101	-0.03	0.17	0.72	0.48
olfactory bulb	0.25	0.54	2.66	0.017	0.15	0.44	2.04	0.057
caudate	0.28	0.56	2.8	0.012	0.03	0.29	1.26	0.225
median raphe	0.003	0.24	1.03	0.319	0.01	0.25	1.08	0.294
amygdala	0.15	0.45	2.07	0.054	0.2	0.5	2.31	0.035
dorsal raphe	0.02	0.28	1.19	0.252	-0.004	0.23	0.96	0.35

Table A2: Correlation analysis between absolute SERT reduction and Oldham's transformation at PET 2 and PET 3 (baseline BP_{ND}+residual BP_{ND})/2 using the voxel-wise approach. All p<0.05 FWE corrected voxel level, cluster extent threshold k>5 voxel, MNI coordinates in mm, L left, R right.

Anatomical Region (AAL)	MNI Coordinates							
	BA	x	y	z	t	p	r^2	Cluster Size
					PET 2			
midbrain	-	2	-28	-6	30.65	**<0.001**	0.98	119410
lingual gyrus L	17	-2	-80	4	12.55	**<0.001**	0.90	1176
insula R	48	40	-2	4	11.95	**<0.001**	0.89	128
fusiform gyrus L	36	-24	-2	-36	11.49	**<0.001**	0.88	149
middle cingulate gyrus L	23	-2	-10	40	11.48	**<0.001**	0.88	6
middle orbitofrontal cortex R	11	2	26	-14	10.16	**<0.001**	0.83	8
middle cingulate cortex L	23	-4	-16	42	9.98	**<0.001**	0.85	9
subgenual cingulate L	38	-2	38	-8	9.92	**<0.001**	0.85	63
fusiform gyrus R	36	26	2	-38	9.79	**<0.001**	0.85	12
thalamus R	-	20	-26	12	9.16	**0.001**	0.81	7
calcarine R	23	2	-66	20	8.84	**0.001**	0.83	10
inferior temporal gyrus L		-42	-22	-30	8.79	**0.001**	0.83	8
middle temporal pole L	38	-44	14	-28	8.25	**0.003**	0.79	6
calcarine L	17	-16	-58	8	8.16	**0.004**	0.79	21
calcarine R	12	6	-74	12	8.12	**0.004**	0.79	8
middle cingulate cortex	-	0	-30	46	8.04	**0.005**	0.78	16
					PET 3			
midbrain (DRN) R	-	4	-26	-10	28.72	**<0.001**	0.98	4603
inferior orbitofrontal gyrus L	11	-24	28	-18	11.22	**<0.001**	0.88	17
calcarine R	17	8	-80	6	10.77	**<0.001**	0.86	255
putamen R	48	36	-4	2	10.61	**<0.001**	0.86	167
inferior orbitofrontal gyrus L	38	-26	16	-20	10.12	**<0.001**	0.86	6
insula R	48	38	12	-4	9.85	**<0.001**	0.85	6
fusiform gyrus R	20	34	-32	-26	9.85	**<0.001**	0.85	16
lingual gyrus L	18	-14	-52	2	9.73	**<0.001**	0.85	88
putamen L	48	-28	0	14	9.56	**<0.001**	0.85	12
middle cingulate cortex R	23	4	-30	36	9.49	**<0.001**	0.85	38
middle temporal pole R	36	30	14	-36	8.80	**0.001**	0.83	16
middle temporal pole L	20	-34	18	-34	8.65	**0.002**	0.81	12
inferior orbitofrontal gyrus L	11	-20	20	-18	8.45	**0.003**	0.81	9
calcarine R	17	14	-66	10	7.96	**0.006**	0.79	6
pallidum R	-	22	6	4	7.18	**0.023**	0.76	7

Table A3: Voxel-wise regression analysis between escitalopram plasma levels and SERT occupancy at PET 3. *p<0.05 FWE corrected, p<0.001 uncorrected voxel-level, cluster extent threshold k>5 voxel, MNI coordinates in mm, L left, R right.

Anatomical Region (AAL)	MNI Coordinates							
	BA	x	y	z	t	p	r^2	Cluster Size
putamen L	48	-16	6	-8	8.12	**<0.001***	0.80	596
caudate R	-	14	18	0	7.98	**<0.001***	0.79	87
rostral midbrain R	-	4	-18	-10	7.61	<0.001	0.77	367
putamen R	-	26	-2	8	5.88	<0.001	0.67	33
middle temporal cortex L	21	-56	-48	-4	5.82	<0.001	0.66	16
caudate R	25	14	10	-10	5.11	<0.001	0.61	138
thalamus R		12	-20	6	4.99	<0.001	0.59	133
brainstem R		2	-36	-32	4.16	<0.001	0.51	9
middle occipital gyrus R	19	32	-78	36	4.15	<0.001	0.51	11
inferior temporal cortex L	37	-54	-52	-18	3.79	<0.001	0.48	11

3.3. Third publication: Prediction of SSRI treatment response in major depression based on serotonin transporter interplay between median raphe nucleus and projection areas

R. Lanzenberger[1], G.S. Kranz[1], D. Haeusler[2], E. Akimova[1], M.Savli[1], A. Hahn[1], M. Mitterhauser[2], C. Spindelegger[1], C. Philippe[2], M. Fink[1], W. Wadsak[2], G. Karanikas[2], S. Kasper[1,*]

[1]*Department of Psychiatry and Psychotherapy, Medical University of Vienna, Austria*

[2]*Department of Nuclear Medicine, Medical University of Vienna, Austria*

Published in:

NEUROIMAGE 2012 Nov 1; 63(2):874-81

[2011, IF: 5.895]

[*]Correspondence to: Siegfried Kasper, MD, Dr.h.c.mult., Prof.
Head: Department of Psychiatry and Psychotherapy
Medical University of Vienna
Waehringer Guertel 18-20, A-1090 Wien, AUSTRIA
Tel: ++43-1-40400-3568
Email: sci-biolpsy@meduniwien.ac.at

3.3.1. Abstract

Recent mathematical models suggest restored serotonergic burst-firing to underlie the antidepressant effect of selective serotonin reuptake inhibitors (SSRI), resulting from down-regulated serotonin transporters (SERT) in terminal regions. This mechanism possibly depends on the interregional balance between SERTs in the raphe nuclei and in terminal regions before treatment. To evaluate these hypotheses on a systems level in humans *in vivo*, we investigated SERT availability and occupancy longitudinally in patients with major depressive disorder using positron emission tomography (PET) and the radioligand [^{11}C]DASB. Measurements were performed before and after a single oral dose, as well as after three weeks (mean 24.73±3.3 days) of continuous oral treatment with either escitalopram (10mg/day) or citalopram (20mg/day). Data were analyzed using voxel-wise linear regression and ANOVA to evaluate SERT binding, occupancy and binding ratios (SERT binding of the entire brain compared to SERT binding in the dorsal and median raphe nuclei) in relation to treatment outcome. Regression analysis revealed that treatment response was predicted by pre-treatment SERT binding ratios, i.e., SERT binding in key regions of depression including bilateral habenula, amygdala–hippocampus complex and subgenual cingulate cortex in relation to SERT binding in the median but not dorsal raphe nucleus ($p<0.05$ FDR-corrected). Similar results were observed in the direct comparison of responders and non-responders. Our data provide a first proof-of-concept for recent modeling studies and further underlie the importance of the habenula and subgenual cingulate cortex in the etiology of and recovery from major depression. These findings may indicate a promising molecular predictor of treatment response and stimulate new treatment approaches based on regional differences in SERT binding.

Keywords: prediction, antidepressant, SSRI, serotonin transporter, PET

3.3.2. Introduction

The mechanism of selective serotonin reuptake inhibitors' (SSRIs) antidepressant effects and research approaches to develop predictors for treatment response are matters of vivid debate (Holsboer, 2008; Papakostas, 2011). SSRIs are defined by their selective blockage of the serotonin transporter (SERT) and a substantial body of research has been conducted to investigate the SERT in unmedicated patients and under the influence of SSRIs (Cannon et al., 2007; Catafau et al., 2006; Cavanagh et al., 2006; Herold et al., 2006; Meyer et al., 2001; Meyer et al., 2004; Miller et al., 2008). Although profound knowledge exists about the biological effects of SSRIs, psychiatrists still lack accurate tools to predict the clinical response to these antidepressants. Moreover, the reason for their delayed onset of therapeutic efficacy remains puzzling. Attempts to explain this latency are manifold and embrace downstream adaptive changes including neurogenesis (Anacker et al., 2011; Boldrini et al., 2009; Santarelli et al., 2003). Most theories, however, assume that the sustained blockage of the SERT causes a reorganization of the serotonergic (5-HT) system, involving up- or down-regulations and modifications in the sensitivity of certain 5-HT receptors such as the serotonin-1A ($5\text{-}HT_{1A}$) receptor (Hahn et al., 2010; Hervas et al., 2001; Richardson-Jones et al., 2010; Spindelegger et al., 2009), or the SERT itself (Benmansour et al., 2002; Lau et al., 2008).

In a recent comprehensive simulation study, Best et al., (2011) demonstrated a normalized phasic increase in 5-HT level in response to burst-firing of 5-HT neurons as the potential underlying mechanism of SSRI response, caused by a reduction of SERTs in terminal regions (Best et al., 2011). A variety of empirical research is in agreement with the assumptions of this model, and down-regulated SERTs due to long-term SSRI treatment in rodents has been consistently shown both *in vivo* and *in vitro* (Benmansour et al., 2002; Lau et al., 2008; Pineyro et al., 1994). A second major issue covered in Best et al.'s (2010a, 2011, 2010b) recent work concerns the association between SERT function in the raphe nuclei and SERT availability in projection areas. Blockage of raphe SERTs raises local extracellular 5-HT levels and reduces tonic firing rates via increased $5\text{-}HT_{1A}$-mediated autoinhibition (Blier et al., 1998). This in turn reduces the extracellular 5-HT levels at nerve terminals in projection areas. Blockage of SERTs in projection areas, though, increases the extracellular 5-HT in these regions (Best et al., 2011). On

the other hand, availability of SERTs in projection areas is adjusted to the tonic firing rate of 5-HT neurons (Best et al., 2010b). Therefore, on a systems level, the interplay between SERT availability in the raphe nuclei and SERT availability in serotonergic projection areas may be an important indicator of serotonergic transmission.

Molecular neuroimaging such as positron emission tomography (PET) and single photon emission computed tomography (SPECT) has provided neuroscientists with the unique opportunity to study the SERT before and during SSRI treatment in humans *in vivo*. Several imaging studies have since been performed, relating the SERT with antidepressant treatment outcome. For example, a SPECT study found that higher pretreatment SERT availability in diencephalon (and with a trend in brainstem) predicted treatment response of depressed patients (Kugaya et al., 2004). In addition, higher SSRI induced occupancy of diencephalic SERTs predicted treatment response. Conversely, most SPECT (Catafau et al., 2006; Cavanagh et al., 2006; Herold et al., 2006) and PET (Meyer et al., 2001; Meyer et al., 2004; Miller et al., 2008) studies reported either no relationship (Catafau et al., 2006; Cavanagh et al., 2006; Herold et al., 2006; Meyer et al., 2001; Meyer et al., 2004) or only a trend towards a positive correlation between treatment response and SERT pretreatment availability or occupancy after medication. Some of the inconsistency may be explained by the poor power of these studies or by the different methodological approaches used, such as the use of different radiotracers having different imaging qualities such as SERT affinity, specific-to-nonspecific binding ratios and uptake kinetics. However, to our knowledge, no study has so far investigated the ratio between SERTs located in the midbrain raphe and those located in serotonergic projection areas in relation to treatment response on a systems level.

The primary objective of the present study was therefore to investigate SERT ratios before treatment as a potential predictor of treatment outcome. Following the PET and SPECT studies stated above, our second aim was to investigate SERT binding and SERT occupancy (acute and subchronic) in relation to treatment outcome. We used [^{11}C]-3-amino-4-(2-dimethylaminomethyl-phenylsulfanyl)-benzonitrile ([^{11}C]DASB), which is currently one of the most reliable PET radiotracers showing a high affinity and selectivity for the SERT (Ichise et al.,

2003). Transporter availability was measured before and after a single oral dose, as well as after 3 weeks of continuous oral SSRI treatment in subjects suffering from major depressive disorder (MDD). We used escitalopram and citalopram, both widely prescribed (Kasper et al., 2009), containing an equimolar-dose of the s-enantiomer of citalopram, which is mostly responsible for inhibiting serotonin reuptake activity (Sanchez et al., 2004).

Surprisingly, when investigating somatodendritic SERT, studies frequently refer to "the midbrain", without differentiating the various subregions. The median (MRN) and dorsal raphe nucleus (DRN) comprise the ascending serotonergic neurons projecting to the forebrain. However, MRN and DRN differ in several respects, including the number, density and distribution of 5-HT containing neurons (Baker et al., 1991), autoreceptor function (Hopwood and Stamford, 2001) and their projection sites and patterns (Vertes, 1991; Vertes et al., 1999). Therefore, our analysis of SERT binding in the raphe region consisted of separate quantifications for MRN and DRN (see Supplementary Text and Figure S1 for the separation of the two nuclei from each other).

3.3.3. Methods

Subjects

22 out-patients (aged 24-54 years.), suffering from major depression, were recruited. Subjects were assessed using a Structured Clinical Interview (SCID) for DSM-IV and the 17-item Hamilton Depression Rating Scale (HAM-D), physical and neurological examinations, routine blood tests, an electrocardiogram, and a pregnancy test. For study inclusion, a HAM-D score of $\geq$16 was required. None had a comorbid axis II disorder. Only patients who had been medication-free for three months prior scanning (four months for fluoxetine), were included and none have had a past history of drug abuse (except for nicotine abuse, 6 subjects). 19 subjects (13 F, 42.3±7.8 years of age (mean±SD)) were included in the final data analysis as three patients were excluded due to compliance failure and excessive head movement during the PET scan. After complete

description of the study to the subjects, written informed consent was obtained. The study was approved by the Ethics Committee of the Medical University of Vienna.

Study Design and Treatment Protocol

The study was designed longitudinally with subjects receiving an equivalent amount of the enantiomer S-citalopram, i.e., they were administered oral doses of either escitalopram (S-citalopram, 10mg/day, 10 subjects) or citalopram (R,S-citalopram, 20mg/day, 9 subjects) (Lundbeck A/S, Denmark). We previously reported differences in the dynamics of SERT occupancy after multiple dose administration of escitalopram vs. citalopram using [^{123}I]ADAM SPECT (Kasper et al., 2009; Klein et al., 2007). However, none of the subjects of the current sample were part of any previous publications, and since we observed no significant differences in SERT availability or occupancy between citalopram and escitalopram (data not shown) using [^{11}C]DASB PET, which is superior in terms of specificity and sensitivity compared to [^{123}I]ADAM SPECT, the data was pooled for further analysis in order to increase statistical power. Each patient underwent three [^{11}C]DASB PET scans, the first before treatment (PET1), the second 6 h following the first SSRI dose (PET2) as occupancy was considered to be at maximum according to our molecular imaging data. The final PET scan was conducted 6 h after the last dose of study medication which was administered daily for a minimum of 3 weeks (24.73±3.3 days) (PET3). Treatment duration was based upon Kugaya et al. (2004), who showed strong correlation between pretreatment SERT availability and treatment response after 4 but *not* after 6 weeks of treatment.

Serum Sampling

Blood samples were drawn ~10 min prior to each PET scan and plasma was immediately separated by an experienced clinician. Samples were then frozen at -20°C and S-citalopram analysis of the plasma fraction was undertaken by Quintiles Bioanalytical Laboratory, Uppsala, Sweden (www.analytical-services.se).

PET Measurement

All PET scans were performed in an advance full-ring scanner (General Electric Medical Systems, Milwaukee, WI, USA) in 3D mode at the Department of Nuclear Medicine of the Medical University of Vienna. A 5 min transmission scan was done using a retractable ^{68}Ge ring source for tissue attenuation correction. Data acquisition started simultaneously with a bolus injection of [^{11}C]DASB measuring brain radioactivity in a series of 30 consecutive time frames. Total acquisition time was 90 min, divided into fifteen 1 min frames and fifteen 5 min frames. Collected data were reconstructed in volumes consisting of 35 transaxial sections (128 x 128 matrix) using an iterative filtered backprojection algorithm (FORE-ITER) with a spatial resolution of 4.36 mm full-width at half maximum (FWHM) at the centre of the field of view. For radiotracer preparation and radiochemical variables, see Supplementary Information.

Serotonin Transporter Quantification and Regions of Interest

The SERT binding potential (BP_{ND}) (Innis et al., 2007) was quantified using the multilinear reference tissue model (MRTM2) (Ichise et al., 2003). Following between-frame motion correction individual summed PET images where normalized to a tracer-specific template in stereotactic Montreal Neurological Institute (MNI) space using SPM8 (Wellcome Trust Centre for Neuroimaging, London, UK; http://www.fil.ion.ucl.ac.uk/spm/) and whole-brain voxel-wise SERT BP_{ND} maps were computed. Independently, to determine local SERT binding in the MRN and DRN, two regions of interest (ROI) comprising spheres of 3 mm radius (14 voxels each) were defined manually in two slices of the template (for details see Spindelegger et al., 2009). Despite a relatively low spatial resolution in PET (FWHM=4.36) compared to MRI, careful delineation of ROIs for the DRN and MRN allowed to reliably separate the two nuclei from each other (see Supplementary Text and Figure S1). Furthermore, the striatum was taken from a ROI-atlas (Spindelegger et al., 2009) to provide exemplary estimates of SERT availability and occupancy (Meyer et al., 2004). SERT drug occupancy was derived using the equation: Occupancy(%)=(1–BP_{ND} treatment/BP_{ND} baseline)x100. Cerebellar gray matter (excluding vermis and venous sinus) was used as a reference region because recent *post mortem* and *in vivo* SERT quantification identified the cerebellar grey matter as an optimal reference region for [^{11}C]DASB during SSRI administration (Parsey et al., 2006). All modelling calculations were performed using PMOD

image analysis software, version 3.3 (PMOD Technologies Ltd, Zurich, Switzerland, www.pmod.com).

Statistical Analysis

Treatment efficacy (absolute reduction in HAM-D values) was analysed using a general linear mixed model containing a fixed term for time, age as covariate and a random term for subject. SPSS version 18.0 for Windows (SPSS Inc., Chicago, IL, www.spss.com) was used for computation. Voxel-wise SERT occupancy was analysed using a general linear model within SPM8. In a second step, associations between treatment efficacy and SERT pretreatment binding, treatment efficacy and SERT occupancy, as well as between treatment efficacy and binding ratios (SERT binding in projection areas divided by SERT binding in raphe nuclei) were evaluated. The computation of binding ratios can be seen as an adjustment of terminal SERT binding to individual levels of raphe SERT availability. It may also eliminate potentially confounding effects of the reference region, since it contributes to both the terminal SERT region and to the raphe nuclei. To this end, voxel-wise linear regression analyses were performed in SPM8 for PET1, PET2 and PET3 separately. For computational reasons, the reduction in HAM-D scores served as the regressor, and the whole-brain SERT binding maps (or the binding ratios) served as the dependent variable, controlling for age. Given the sample size, no further covariates were included into the model to avoid over-fitting. The resulting *t* maps were corrected for multiple comparisons ($p<0.05$ voxel-level) using the false discovery rate (FDR). Although whole-brain voxel-wise analyses clearly require correction for multiple comparisons, they imply major advantages over ROI-based evaluation, namely independence of choice, size and location of regions of interest.

To compare treatment remitters, responders and non-responders, we performed a one-way ANOVA (1 factor with 3 levels, controlled for age for an overall comparison (F-test)) and post-hoc t-tests between groups. The binding ratios were used as dependent variables. Again, the resulting *t* maps were corrected for multiple comparisons ($p<0.05$) using FDR.

3.3.4. Results

Clinical outcome

HAM-D scores ranged between 16 and 28 with a mean of 21.0±3.2 at screening visit, and 20.2±3.9 at PET1 before treatment. SSRI treatment had a significant effect on depressive symptoms over time ($F(3,54)=44.74$, $P<0.001$), with post-hoc *t*-tests revealing significant reductions at PET3 (HAM-D: 9.0±4.7) compared to screening visit, PET1 and PET2 (HAM-D: 18.37±3.82, all Ps<0.001, corrected, see Figure 1). Eleven out of nineteen subjects (2 males, 9 females) showed at least a 50% reduction in HAM-D scores and were considered as responders (57.9%). Of these, seven (36.8% of the entire group) became remitters with final scores of ≤7.

Plasma concentration of S-citalopram and SERT occupancy

The plasma concentration of S-citalopram was 6.92±2.25 ng/ml (range 1–12 ng/ml) at PET2 and 14.76±6.02 ng/ml (range 6–26 ng/ml) at PET3. In line with previous studies (Meyer et al., 2001), SSRI treatment caused a considerable reduction in SERT availability ($F(2,24.83)=452.33$, $P<0.001$). A single dose of SSRIs (PET2) led to a significant reduction in striatal SERT availability, resulting in occupancies with a mean of 69.8%±4.9 (range 60%–78%) compared to baseline values (PET1) (SERT BP_{ND}: 1.56±0.25 vs. 0.46±0.08, $P<0.001$, PET1 vs. PET2).

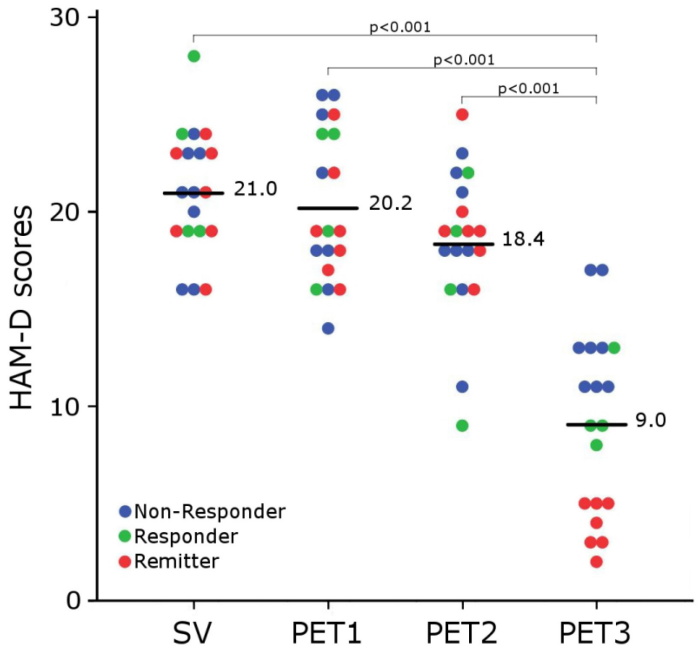

Figure 1. *Individual Hamilton Depression Rating Scale (HAM-D) scores before and after treatment with escitalopram or citalopram. HAM-D scores are given for screening visit (SV), baseline positron emission tomography (PET) scan before treatment (PET1), second PET scan after 6h of the first drug intake (PET2), and third PET scan after a minimum of 3 weeks continuous treatment (PET3). Bars indicate mean HAM-D scores. HAM-D scores at PET3 differ significantly to prior interview scores (SV, PET1 and PET2, all p<0.001). Green filled circles indicate responders, showing a 50% or greater reduction relative to initial scores, blue filled circles indicate non-responders (below 50% reduction). All responders displaying a final HAM-D score (PET3) of ≤ 7 are marked as filled red circles (remitters).*

Prolonged SSRI treatment further raised occupancies to 75.3%±4.4 on average (range 70%–86%) at PET3 (SERT BP_{ND}: 1.56±0.25 vs. 0.38±0.06, P<0.001, PET1 vs. PET3). For illustration, SERT BP_{ND} regional distributions at baseline are shown in Figure 2 (bottom row). Radiochemical variables such as injected dose, radiochemical purity, specific activity, unlabelled DASB or dose per weight did not differ significantly between PET measurements (data not shown).

Association of treatment response and pretreatment SERT binding ratios between median raphe nucleus and serotonergic projection areas

The predictive potential of SERT binding ratios at baseline on treatment response was investigated. When evaluating terminal SERT binding adjusted to individual MRN SERT binding

(terminal BP_{ND}/MRN BP_{ND}), binding ratios were positively correlated with treatment response (absolute reduction in HAM-D scores, PET1-PET3) for several cortical and subcortical regions ($p<0.05$ FDR-corrected, Figure 2 and 3). That is, the more SERT binding in terminal regions in relation to MRN SERT binding, the better the treatment outcome. Peak values were found bilaterally in the amygdala–anterior hippocampus complex (e.g., t=7.95 for the left side), in the habenula (part of the epithalamus, t=7.86), putamen (t=5.82), orbitofrontal cortex (OFC, t=4.56), the subgenual and anterior cingulate cortex (t=5.21, see Table and Figure 2, upper row, and Figure 3). Using different statistical evaluations of $p<0.001$ uncorrected voxel-level with $p<0.05$ FDR- or FWE-corrected cluster-level did not change the abovementioned findings.

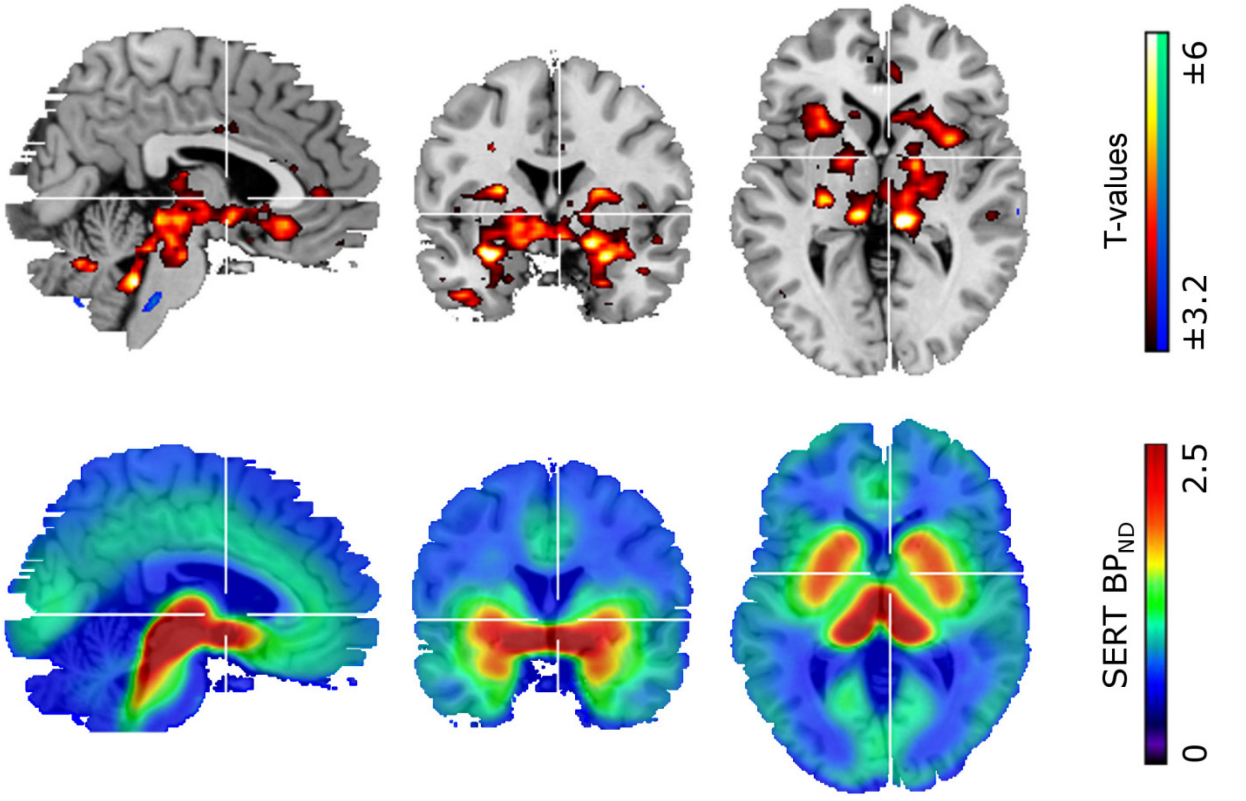

Fig 2. *Brain areas showing significant associations between pretreatment serotonin transporter (SERT) binding ratios and treatment response. The terminal SERT binding in the whole brain was adjusted to SERT binding in the median raphe nucleus by calculating the ratios between these areas. (**Upper row**) Significant clusters are overlaid onto sagittal, coronal and axial structural MRI planes. The highest peaks were found in the habenulae (epithalamus), amygdala-hippocampus complex, anterior insula, subgenual anterior cingulate cortex (sgACC), striatum, midbrain and cerebellar vermis (color table: t ranging from ±*

*3.2 to ≥ ±6) t-values for peaks are given in the table). (**Bottom row**) Voxel-wise maps representing the averaged baseline SERT distribution, overlaid onto structural MRI planes. The planes correspond to the upper row. Binding potential (BP_{ND}) values are given in the colour table. The SERT density in projection areas depends on tonic firing that is modulated by the SERT binding in the raphe nuclei. Comparing the upper and bottom row shows that significant clusters are independent of the local SERT binding distribution, e.g. the SERT binding is high all over the thalamus and striatum; however the associations to treatment response are restricted to specific areas as the epithalamus (habenula). The habenula and amygdala are indicated in Fig. 3 by white crosshairs. Left is right.*

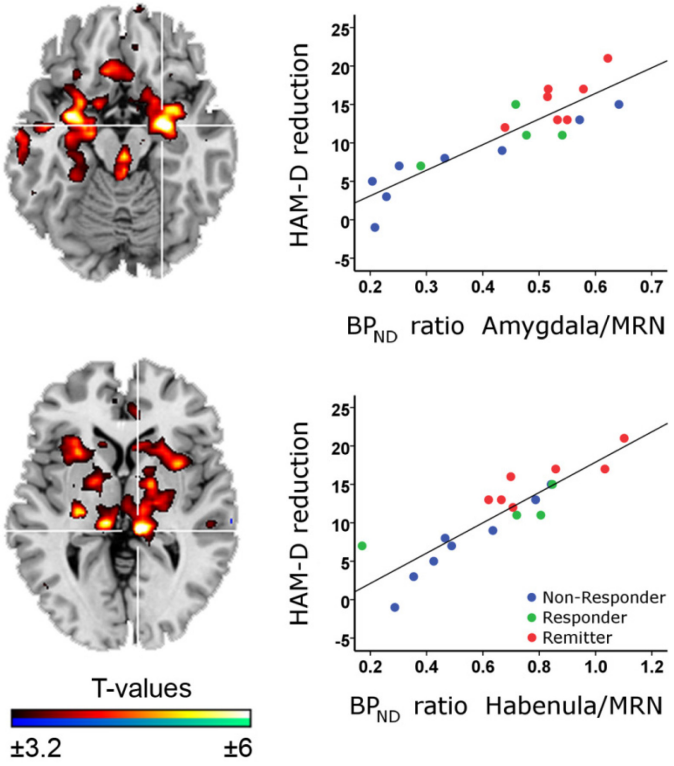

Figure 3. *Significant associations between pretreatment SERT binding ratios in amygdala and habenula and treatment response T-values are given in the color table. (Left) Statistical parametric maps (SPM) showing highest associations in both amygdalae (upper row) and in both habenulae / epithalami (bottom row), for coordinates, see Table. (Right) Scatterplots depicting the relationship between absolute HAM-D reduction and pretreatment SERT binding ratios at the peak voxel (see crosshair in SPM images, left). Colored circles are given corresponding to Figure 1. Significance corresponds to a FDR threshold P<0.05, corrected for multiple comparisons at the voxel level. Left is right. Note that these are results of voxel-wise whole-brain analysis where no regions were defined a priori (except raphe region).*

Including baseline HAM-D as covariate (which is equivalent to investigating the relative change in HAM-D scores) yielded slightly lower t-values (e.g., amydala: t=6.62, habenulae: t=6.04, subgenual ACC: t=4.5), which surviveed correction for multiple comparisons on a cluster level ($p<0.05$ FDR corrected), except for the subgenual ACC. Including citalopram/escitalopram as covariate did not change our findings, i.e., results are still significant at $p<0.05$ FDR-corrected. When evaluating terminal SERT binding, adjusted to SERT binding in the DRN (terminal BP_{ND}/DRN BP_{ND}), no associations were found to survive FDR correction for multiple comparisons.

Differences between treatment remitters or responders and non-responders

The ANOVA revealed group differences between remitters, responders and non-responders in regional SERT BP_{ND} adjusted to SERT BP_{ND} in the MRN. Compared to non-responders both remitters and responders showed higher SERT binding ratios between projection areas and MRN. Significant clusters were found in the sgACC and OFC, habenula, amygdala, anterior insula, striatum and midbrain ($p<0.05$ FDR-corrected, Figure 4).

Association between treatment response and pretreatment SERT availability and occupancy

When investigating whether pretreatment SERT binding itself predicts treatment response, no associations were found that survived whole-brain FDR correction for multiple comparisons. Also, no associations with treatment response were found for residual SERT binding at PET2 and PET3, and for SERT binding ratios between terminal projection regions and raphe at PET2 and PET3. No associations were found between treatment response and SERT occupancy after a single dose (PET2) or after three weeks of SSRI treatment (PET3) after FDR correction. Furthermore, no associations were found for occupancy ratios with either MRN or DRN as the denominator that survived FDR correction.

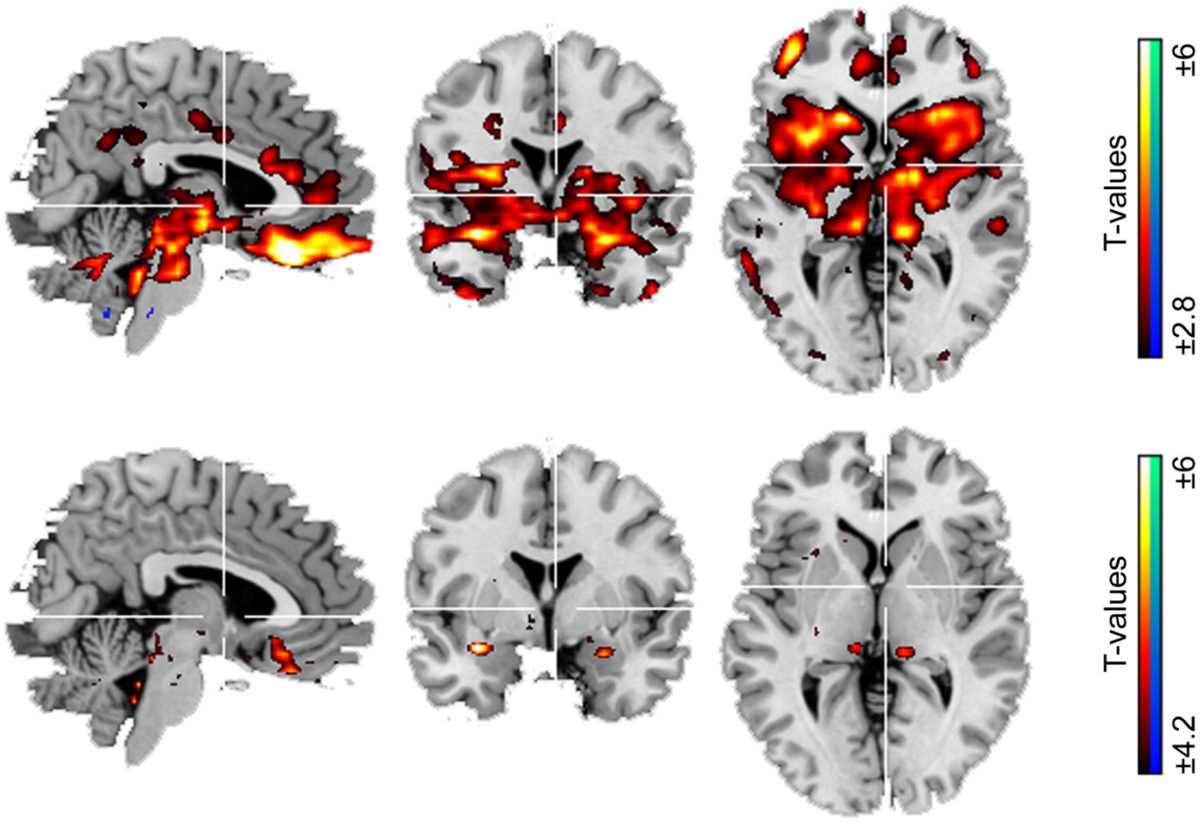

Figure 4. *Brain areas showing significant differences between responders (n=11) and non-responders (n=8) (upper row) and between remitters (n=7) and non-responders (bottom row) for SERT binding ratios. T-values are given in the color table. All p-values are FDR corrected (p<0.05, cluster size ≥30 voxels, model corrected for age). Treatment responders had a 50% or greater reduction relative to initial HAM-D scores and remitters displayed a final HAM-D score of ≤ 7. The highest peaks were found in the sgACC and orbitofrontal cortex, habenulae, amygdalae, anterior insula, striatum and midbrain.*

For completeness, we investigated the ratios of terminal to MRN SERT binding before and after SSRIs with a repeated measures ANOVA and post-hoc t-tests (p<0.05 FDR-corrected). Comparing PET1 (baseline) with PET2 (single dose SSRI) showed increased binding ratios almost throughout the entire cortex as well as subcortical regions, such as the striatum and thalamus. At PET3 (multiple doses SSRI), this effect was only observed in the inferior and middle temporal, orbitofrontal and insular cortices. Subsequent assessment of mean occupancy images showed that this was attributable to a more pronounced decrease of SERT binding in the raphe than in sub-/cortical brain regions.

3.3.5. Discussion

The results of this study indicate that SERT binding ratios before treatment can predict treatment response after a minimum treatment period of three weeks with escitalopram or citalopram in preliminary unmedicated patients with major depression. Lower SERT binding in the MRN (origin of serotonergic neurons) compared to SERT binding in terminal projection regions of serotonergic neurons (habenula, sgACC or the amygdala–anterior hippocampus complex) predicted beneficial treatment outcome, strongly supporting recent mathematical simulation studies (Best et al., 2011; Best et al., 2010b).

As Best et al. (2011) point out in their model, SSRI treatment reduces the rate of tonic firing of 5-HT neurons. Because SERTs are not only blocked in terminal regions but also in the raphe, extracellular serotonin is also raised in the raphe area and 5-HT neural firing via inhibitory autoreceptors is dampened (Pineyro and Blier, 1999). Reduced neural firing of serotonin neurons counteracts the SSRI induced elevation of extracellular 5-HT levels in terminal regions. Elevations of extracellular 5-HT in terminal regions are therefore smaller than those in the raphe region. Furthermore, *a priori* lowered SERT density in the raphe nuclei should equally decrease neuronal firing due to increased activation of inhibitory autoreceptors. Indeed, electrophysiological studies showed that SERT knockout mice exhibit reduced firing of serotonergic cells due to an increased activation of 5-HT_{1A} autoreceptors (Gobbi et al., 2001). Consequently, attenuated SERT function by SSRIs in the midbrain under already lowered SERT conditions in the raphe nuclei all the more dampens tonic firing rate of serotonin neurons.

According to Best et al., lowered tonic firing of 5-HT neurons result in a down-regulation of SERTs in terminal regions because the tonic firing rate of 5-HT neurons determines SERT density in projection areas (Best et al., 2010b). This seems to be reasonable because SERT expression in the presynaptic membrane is usage dependent (Ramamoorthy and Blakely, 1999). Serotonin reuptake inhibits SERT phosphorylation and internalization, whereas when the SERT is blocked by SSRIs, phosphorylation and internalization accelerates (Ramamoorthy and Blakely, 1999). An internalization of SERTs in the presence of SSRIs will thus be more pronounced when elevations

of extracellular 5-HT in terminal regions are smaller, due to lowered tonic firing of 5-HT neurons, and high SERT density in projection areas. Lowered raphe SERT binding in comparison to terminal SERT binding would therefore lead to a more pronounced internalization of terminal SERT after prolonged SSRI administration. According to Best *et al.* this would lead to reduced *tonic* serotonergic firing, whereas the 5-HT level in response to *phasic* neuronal firing has returned back to normal. Since this mechanism was recently proposed to underlie a beneficial effect of SSRIs (Best et al., 2011), and in accordance with our results, lowered raphe SERT binding in comparison to terminal SERT binding should be associated with a better treatment outcome.

Antidepressant response

We found significant differences between remitters and non-responders, and between responders and non-responders in cortical and subcortical SERT binding adjusted to SERT BP_{ND} in the MRN. Both remitters and responders showed higher adjusted SERT binding in the sgACC, the OFC, the habenula, the amygdala–anterior hippocampus complex, the anterior insula, striatum and midbrain (Figure 4). As expected, the spatial pattern of significant brain regions was very similar when using two different statistical approaches (see Figures 2 and 4). However, the comparison between responders and non-responders highlighted a dominant cluster including the sgACC and OFC (Figure 4, upper row), which has been frequently linked to alterations and treatment in depression (Mayberg, 2009; Price and Drevets, 2009). In a recent fMRI study, Lisiecka et al. reported OFC-coupling with caudate and thalamus to be positively associated with antidepressant response (Lisiecka et al., 2011). With regard to our results, this suggests that the functionality of modulatory neurotransmitters such as the 5-HT system might at least partly underlie the functional connectivity between brain regions. Mayberg et al. reported changes in glucose metabolism or blood flow with antidepressant response using different treatment options (Mayberg, 2009). For instance, a decrease in the sgACC was found following SSRI treatment and electroconvulsive therapy in depression. Therefore, our molecular results of the serotonergic system provide further data emphasizing the central role of the sgACC and OFC in the pathogenesis and treatment of depression.

SERT occupancy

We were not able to demonstrate an association between treatment response and SERT binding or SERT occupancy after 3 weeks of SSRI administration. This is, however, in line with recent imaging studies (Catafau et al., 2006; Cavanagh et al., 2006; Herold et al., 2006; Meyer et al., 2001). A simple explanation might be that SERT availability at PET 3 is too low and therefore the signal-to-noise ratio too small to demonstrate significant effects. Furthermore, a reduction of SERT availability is caused by a combination of the high affinity of S-citalopram to SERTs (fewer SERTs available for [^{11}C]DASB binding) and true SERT reduction. SERT occupancy after prolonged SSRI administration should therefore reflect both a blockade and a down-regulation of SERTs. Our data indicate occupancy rates of 70% after short term administration, and an increase by 5% to 75% after three weeks of SSRI treatment. Animal studies, however, suggest SERT down-regulation of only 25% during the first days of treatment, compared to more than 70% after 15 days of SSRI treatment (difference=45%) (Benmansour et al., 1999; Benmansour et al., 2002). Definitive answers will provide future PET studies investigating SERT binding after discontinuation of medication for a defined washout period disentangling occupancy by medication from real down-regulation of SERTs.

Dorsal and median raphe nuclei

Our data indicate lower SERT binding in the MRN compared to SERT binding in projection areas to be beneficial for treatment efficacy. Analog results were, however, not obtained for the DRN, suggesting that this is not a general feature of SERT balance per se, but rather specific to the MRN (see Supplementary Text and Figure S1 for the separation of the two nuclei). MRN and DRN project to essentially non-overlapping regions in the forebrain (Lechin et al., 2006). Whereas the DRN projects e.g., to the frontal and parietal cortex, ventral hippocampus, amygdala, striatum and lateral septum, the MRN projects preferably to the temporal cortex, mammillary bodies, dorsal hippocampus and medial septum. Notably, early analyses of raphe projections indicate that the MRN projects abundantly to the lateral habenula (LHb) (Azmitia and Segal, 1978; Vertes et al., 1999), whereas DRN projections to the LHb are much sparser and were found to be mainly non-serotonergic (Michelsen et al., 2007; Vertes, 1991). In addition, functional studies with patients remitted from MDD indicate that with experimentally reduced

serotonin-levels (tryptophan depletion) the neuronal activation in the habenulae markedly increases (Morris et al., 1999). Assuming that MRN projections upon LHb are serotonergic (Kohler and Steinbusch, 1982), this suggests an inhibitory influence of MRN on LHb neuronal firing. On the other hand, neurons of the LHb project to MRN and DRN and exert strong inhibitory influence on serotonergic neurons, possibly via intermediate GABA cells (Hikosaka et al., 2008). This indicates a tight interconnection between ascending serotonergic raphe neurons and LHb neurons controlling these modulatory pathways, where the MRN seems to play a prominent role in this reciprocal network. The inhibitory influence of LHb neurons upon MRN and DRN should thus be high, when the inhibitory power of MRN projections upon LHb neurons is small, and vice versa. With regard to our data, this would suggest that lowered SERT availability in the MRN compared to projection areas (e.g., LHb) increases the inhibitory influence of LHb neurons upon DRN and MRN, and by that further reduces tonic firing of serotonergic cells. As outlined above, lowered *tonic* firing results in a down-regulation of SERTs in terminal regions that brings 5-HT levels in response to *phasic* serotonergic burst-firing back to normal. This is proposed to be an important underlying mechanism of antidepressant response to SSRIs (Best et al., 2010b).

Limitations of this study

The treatment period of our study sample was 24.73 ± 3.3 days, and no HAM-D scores during long-term treatment (e.g., half year) are available. Due to the lack of longer observation periods, we cannot distinguish a predictor of early treatment response from a predictor of continuous treatment response. Although animal research suggests robust down-regulation of the SERT within 15-20 days of continuous treatment (Benmansour et al., 2002), further long-term treatment studies are necessary. In addition, we did not collect information about previous episodes, making it impossible to evaluate a potential influence of the number of previous episodes on treatment response or our PET-results.

A methodological limitation of our study pertains to the PET-to-PET normalization given the absence of individual magnetic resonance images. This is particularly prone to miss-registrations of small nuclei such as MRN and DRN. Special caution was therefore laid upon the correct position of the raphe ROIs by visual inspection of the summed individual PET images (across

time) and time activity curves within the modeling procedures. Given the small ROIs for MRN and DRN, partial volume (PV)-effects may have influenced our result, which poses an additional limitation. However, in contrast to the serotonin-1A receptor within midbrain, which is highly expressed in DRN and MRN compared to the surrounding brain areas, the SERT is also highly concentrated in the surrounding midbrain, rendering partial volume effects less likely. Moreover, a potential PV-effect is expected to be constant across subjects since no comparisons across different population groups were carried out. Alterations would therefore not necessarily change the association per se but only shift the regression line. Finally, calculation with and without PV correction even for serotonin-1A BP_{ND} in the DRN, as recently performed by our group, did not significantly change our results (Hahn et al., 2012). Since no arterial blood sampling was available, we were not able to investigate differences in specific binding within the reference region (Hinz et al., 2008; Parsey et al., 2006). However, previous studies identified the cerebellar gray matter as optimal reference region for [11C]DASB occupancy studies (Meyer, 2007; Parsey et al., 2006) and estimated the maximum influence to be only 7% in target regions by entire blockade of specific cerebellar SERT binding (Kish et al., 2005).

3.3.6. Conclusions

The results of this study strongly indicate a pivotal role of the balance between baseline SERT binding in the MRN and baseline SERT binding in key areas within the depression circuits to serve as a strong predictor of treatment response (for a distinction between predictors, moderators and mediators, see Papakostas *et al.*, 2011). Among those key areas, the habenulae, the sgACC and the OFC, and the amygdala-hippocampus complex have been consistently linked to major depression and antidepressant treatment response (Mayberg, 2009; Sartorius et al., 2010). In contrast to other studies neglecting the MRN, our data support the distinction between the MRN and DRN in PET studies, emphasizing the central role of the MRN in association with the habenulae.

Disclosures and acknowledgments

S. Kasper declares that he has received grant/research support from Bristol Myers-Squibb, Eli Lilly, GlaxoSmithKline, Lundbeck, Organon, Sepracor and Servier; has served as a consultant or on advisory boards for AstraZeneca, Bristol-Myers Squibb, Eli Lilly, GlaxoSmithKline, Janssen, Lundbeck, Merck Sharp and Dome (MSD), Novartis, Organon, Pfizer, Schwabe, Sepracor, and Servier; and has served on speakers' bureaus for Angelini, AstraZeneca, Bristol Myers-Squibb, Eli Lilly, Janssen, Lundbeck, Pfizer, Pierre Fabre, Schwabe, Sepracor, and Servier. R. Lanzenberger received travel grants and conference speaker honoraria from AstraZeneca and Lundbeck A/S. M. Mitterhauser and W. Wadsak received speaker honoraria from Bayer. A. Hahn is recipient of a DOC-fellowship of the Austrian Academy of Sciences at the Department of Psychiatry and Psychotherapy. The authors G.S. Kranz, D. Haeusler, E. Akimova, M. Savli, C. Spindelegger, C. Philippe, M. Fink, and G. Karanikas report no financial relationships with commercial interests.

The authors are grateful to U. Moser, M. Willeit, K. Kletter and clinical staff at the PET centre for their medical support, and A. Saulin for her assistance in editing this article. We are especially indebted to G. Wagner, B. Reiterits, I. Leitinger, and R. Bartosch for technical support during the PET scans.

Grant Support

Personal costs were partly funded by the Medical University of Vienna and Austrian national research funding agencies (FWF, OeNB) to R. Lanzenberger, PET measurements and treatment were supported by an investigator-initiated and unrestricted research grant from H. Lundbeck A/S, Denmark to S. Kasper. A. Hahn is recipient of a DOC-fellowship of the Austrian Academy of Sciences at the Department of Psychiatry and Psychotherapy

3.3.7. References

Anacker, C., Zunszain, P.A., Cattaneo, A., Carvalho, L.A., Garabedian, M.J., Thuret, S., Price, J., Pariante, C.M., 2011. Antidepressants increase human hippocampal neurogenesis by activating the glucocorticoid receptor. Mol Psychiatry 16, 738-750.

Azmitia, E.C., Segal, M., 1978. An autoradiographic analysis of the differential ascending projections of the dorsal and median raphe nuclei in the rat. J Comp Neurol 179, 641-667.

Baker, K.G., Halliday, G.M., Hornung, J.P., Geffen, L.B., Cotton, R.G.H., Tork, I., 1991. Distribution, Morphology and Number of Monoamine-Synthesizing and Substance P-Containing Neurons in the Human Dorsal Raphe Nucleus. Neuroscience 42, 757-775.

Benmansour, S., Cecchi, M., Morilak, D.A., Gerhardt, G.A., Javors, M.A., Gould, G.G., Frazer, A., 1999. Effects of chronic antidepressant treatments on serotonin transporter function, density, and mRNA level. J Neurosci 19, 10494-10501.

Benmansour, S., Owens, W.A., Cecchi, M., Morilak, D.A., Frazer, A., 2002. Serotonin clearance in vivo is altered to a greater extent by antidepressant-induced downregulation of the serotonin transporter than by acute blockade of this transporter. J Neurosci 22, 6766-6772.

Best, J., Nijhout, H.F., Reed, M., 2010a. Serotonin synthesis, release and reuptake in terminals: a mathematical model. Theor Biol Med Model 7, 34.

Best, J., Nijhout, H.F., Reed, M., 2011. Bursts and the efficacy of selective serotonin reuptake inhibitors. Pharmacopsychiatry 44 Suppl 1, S76-83.

Best, J., Reed, M., Nijhout, H.F., 2010b. Models of dopaminergic and serotonergic signaling. Pharmacopsychiatry 43 Suppl 1, S61-66.

Blier, P., Pineyro, G., el Mansari, M., Bergeron, R., de Montigny, C., 1998. Role of somatodendritic 5-HT autoreceptors in modulating 5-HT neurotransmission. Ann N Y Acad Sci 861, 204-216.

Boldrini, M., Underwood, M.D., Hen, R., Rosoklija, G.B., Dwork, A.J., John Mann, J., Arango, V., 2009. Antidepressants increase neural progenitor cells in the human hippocampus. Neuropsychopharmacology 34, 2376-2389.

Cannon, D.M., Ichise, M., Rollis, D., Klaver, J.M., Gandhi, S.K., Charney, D.S., Manji, H.K., Drevets, W.C., 2007. Elevated serotonin transporter binding in major depressive disorder assessed using positron emission tomography and [11C]DASB; comparison with bipolar disorder. Biol Psychiatry 62, 870-877.

Catafau, A.M., Perez, V., Plaza, P., Pascual, J.C., Bullich, S., Suarez, M., Penengo, M.M., Corripio, I., Puigdemont, D., Danus, M., Perich, J., Alvarez, E., 2006. Serotonin transporter occupancy induced by paroxetine in patients with major depression disorder: a 123I-ADAM SPECT study. Psychopharmacology (Berl) 189, 145-153.

Cavanagh, J., Patterson, J., Pimlott, S., Dewar, D., Eersels, J., Dempsey, M.F., Wyper, D., 2006. Serotonin transporter residual availability during long-term antidepressant therapy does not differentiate responder and nonresponder unipolar patients. Biol Psychiatry 59, 301-308.

Gobbi, G., Murphy, D.L., Lesch, K., Blier, P., 2001. Modifications of the serotonergic system in mice lacking serotonin transporters: an in vivo electrophysiological study. J Pharmacol Exp Ther 296, 987-995.

Hahn, A., Lanzenberger, R., Wadsak, W., Spindelegger, C., Moser, U., Mien, L.K., Mitterhauser, M., Kasper, S., 2010. Escitalopram enhances the association of serotonin-1A autoreceptors to heteroreceptors in anxiety disorders. J Neurosci 30, 14482-14489.

Hahn, A., Wadsak, W., Windischberger, C., Baldinger, P., Hoflich, A.S., Losak, J., Nics, L., Philippe, C., Kranz, G.S., Kraus, C., Mitterhauser, M., Karanikas, G., Kasper, S., Lanzenberger, R., 2012. Differential modulation of the default mode network via serotonin-1A receptors. Proc Natl Acad Sci U S A 109, 2619-2624.

Herold, N., Uebelhack, K., Franke, L., Amthauer, H., Luedemann, L., Bruhn, H., Felix, R., Uebelhack, R., Plotkin, M., 2006. Imaging of serotonin transporters and its blockade by citalopram in patients with major depression using a novel SPECT ligand [123I]-ADAM. J Neural Transm 113, 659-670.

Hervas, I., Vilaro, M.T., Romero, L., Scorza, M.C., Mengod, G., Artigas, F., 2001. Desensitization of 5-HT(1A) autoreceptors by a low chronic fluoxetine dose effect of the concurrent administration of WAY-100635. Neuropsychopharmacology 24, 11-20.

Hikosaka, O., Sesack, S.R., Lecourtier, L., Shepard, P.D., 2008. Habenula: crossroad between the basal ganglia and the limbic system. J Neurosci 28, 11825-11829.

Hinz, R., Selvaraj, S., Murthy, N.V., Bhagwagar, Z., Taylor, M., Cowen, P.J., Grasby, P.M., 2008. Effects of citalopram infusion on the serotonin transporter binding of [11C]DASB in healthy controls. J Cereb Blood Flow Metab 28, 1478-1490.

Holsboer, F., 2008. How can we realize the promise of personalized antidepressant medicines? Nat Rev Neurosci 9, 638-646.

Hopwood, S.E., Stamford, J.A., 2001. Multiple 5-HT(1) autoreceptor subtypes govern serotonin release in dorsal and median raphe nuclei. Neuropharmacology 40, 508-519.

Ichise, M., Liow, J.S., Lu, J.Q., Takano, A., Model, K., Toyama, H., Suhara, T., Suzuki, K., Innis, R.B., Carson, R.E., 2003. Linearized reference tissue parametric imaging methods: application to [11C]DASB positron emission tomography studies of the serotonin transporter in human brain. J Cereb Blood Flow Metab 23, 1096-1112.

Innis, R.B., Cunningham, V.J., Delforge, J., Fujita, M., Gjedde, A., Gunn, R.N., Holden, J., Houle, S., Huang, S.C., Ichise, M., Iida, H., Ito, H., Kimura, Y., Koeppe, R.A., Knudsen, G.M., Knuuti, J., Lammertsma, A.A., Laruelle, M., Logan, J., Maguire, R.P., Mintun, M.A., Morris, E.D., Parsey, R., Price, J.C., Slifstein, M., Sossi, V., Suhara, T., Votaw, J.R., Wong, D.F., Carson, R.E., 2007. Consensus nomenclature for in vivo imaging of reversibly binding radioligands. J Cereb Blood Flow Metab 27, 1533-1539.

Kasper, S., Baldwin, D.S., Larsson Lonn, S., Boulenger, J.P., 2009. Superiority of escitalopram to paroxetine in the treatment of depression. Eur Neuropsychopharmacol 19, 229-237.

Kish, S.J., Furukawa, Y., Chang, L.J., Tong, J., Ginovart, N., Wilson, A., Houle, S., Meyer, J.H., 2005. Regional distribution of serotonin transporter protein in postmortem human brain: is the cerebellum a SERT-free brain region? Nucl Med Biol 32, 123-128.

Klein, N., Sacher, J., Geiss-Granadia, T., Mossaheb, N., Attarbaschi, T., Lanzenberger, R., Spindelegger, C., Holik, A., Asenbaum, S., Dudczak, R., Tauscher, J., Kasper, S., 2007. Higher serotonin transporter occupancy after multiple dose administration of escitalopram compared to citalopram: an [123I]ADAM SPECT study. Psychopharmacology (Berl) 191, 333-339.

Kohler, C., Steinbusch, H., 1982. Identification of serotonin and non-serotonin-containing neurons of the mid-brain raphe projecting to the entorhinal area and the hippocampal formation. A combined immunohistochemical and fluorescent retrograde tracing study in the rat brain. Neuroscience 7, 951-975.

Kugaya, A., Sanacora, G., Staley, J.K., Malison, R.T., Bozkurt, A., Khan, S., Anand, A., Van Dyck, C.H., Baldwin, R.M., Seibyl, J.P., Charney, D., Innis, R.B., 2004. Brain serotonin transporter availability predicts treatment response to selective serotonin reuptake inhibitors. Biol Psychiatry 56, 497-502.

Lau, T., Horschitz, S., Berger, S., Bartsch, D., Schloss, P., 2008. Antidepressant-induced internalization of the serotonin transporter in serotonergic neurons. FASEB J 22, 1702-1714.

Lechin, F., van der Dijs, B., Hernandez-Adrian, G., 2006. Dorsal raphe vs. median raphe serotonergic antagonism. Anatomical, physiological, behavioral, neuroendocrinological, neuropharmacological and clinical evidences: relevance for neuropharmacological therapy. Prog Neuropsychopharmacol Biol Psychiatry 30, 565-585.

Lisiecka, D., Meisenzahl, E., Scheuerecker, J., Schoepf, V., Whitty, P., Chaney, A., Moeller, H.J., Wiesmann, M., Frodl, T., 2011. Neural correlates of treatment outcome in major depression. Int J Neuropsychopharmacol 14, 521-534.

Mayberg, H.S., 2009. Targeted electrode-based modulation of neural circuits for depression. J Clin Invest 119, 717-725.

Meyer, J.H., 2007. Imaging the serotonin transporter during major depressive disorder and antidepressant treatment. J Psychiatry Neurosci 32, 86-102.

Meyer, J.H., Wilson, A.A., Ginovart, N., Goulding, V., Hussey, D., Hood, K., Houle, S., 2001. Occupancy of serotonin transporters by paroxetine and citalopram during treatment of depression: a [(11)C]DASB PET imaging study. Am J Psychiatry 158, 1843-1849.

Meyer, J.H., Wilson, A.A., Sagrati, S., Hussey, D., Carella, A., Potter, W.Z., Ginovart, N., Spencer, E.P., Cheok, A., Houle, S., 2004. Serotonin transporter occupancy of five selective serotonin reuptake inhibitors at different doses: an [11C]DASB positron emission tomography study. Am J Psychiatry 161, 826-835.

Michelsen, K.A., Schmitz, C., Steinbusch, H.W., 2007. The dorsal raphe nucleus--from silver stainings to a role in depression. Brain Res Rev 55, 329-342.

Miller, J.M., Oquendo, M.A., Ogden, R.T., Mann, J.J., Parsey, R.V., 2008. Serotonin transporter binding as a possible predictor of one-year remission in major depressive disorder. Journal of Psychiatric Research 42, 1137-1144.

Morris, J.S., Smith, K.A., Cowen, P.J., Friston, K.J., Dolan, R.J., 1999. Covariation of activity in habenula and dorsal raphe nuclei following tryptophan depletion. Neuroimage 10, 163-172.

Papakostas, G.I., 2011. Surrogate markers of treatment outcome in major depressive disorder. Int J Neuropsychopharmacol, 1-14.

Parsey, R.V., Kent, J.M., Oquendo, M.A., Richards, M.C., Pratap, M., Cooper, T.B., Arango, V., Mann, J.J., 2006. Acute occupancy of brain serotonin transporter by sertraline as measured by [11C]DASB and positron emission tomography. Biol Psychiatry 59, 821-828.

Pineyro, G., Blier, P., 1999. Autoregulation of serotonin neurons: role in antidepressant drug action. Pharmacol Rev 51, 533-591.

Pineyro, G., Blier, P., Dennis, T., de Montigny, C., 1994. Desensitization of the neuronal 5-HT carrier following its long-term blockade. J Neurosci 14, 3036-3047.

Price, J.L., Drevets, W.C., 2009. Neurocircuitry of Mood Disorders. Neuropsychopharmacology. 35(1):192-216.

Ramamoorthy, S., Blakely, R.D., 1999. Phosphorylation and sequestration of serotonin transporters differentially modulated by psychostimulants. Science 285, 763-766.

Richardson-Jones, J.W., Craige, C.P., Guiard, B.P., Stephen, A., Metzger, K.L., Kung, H.F., Gardier, A.M., Dranovsky, A., David, D.J., Beck, S.G., Hen, R., Leonardo, E.D., 2010. 5-HT1A autoreceptor levels determine vulnerability to stress and response to antidepressants. Neuron 65, 40-52.

Sanchez, C., Bogeso, K.P., Ebert, B., Reines, E.H., Braestrup, C., 2004. Escitalopram versus citalopram: the surprising role of the R-enantiomer. Psychopharmacology (Berl) 174, 163-176.

Santarelli, L., Saxe, M., Gross, C., Surget, A., Battaglia, F., Dulawa, S., Weisstaub, N., Lee, J., Duman, R., Arancio, O., Belzung, C., Hen, R., 2003. Requirement of hippocampal neurogenesis for the behavioral effects of antidepressants. Science 301, 805-809.

Sartorius, A., Kiening, K.L., Kirsch, P., von Gall, C.C., Haberkorn, U., Unterberg, A.W., Henn, F.A., Meyer-Lindenberg, A., 2010. Remission of major depression under deep brain stimulation of the lateral habenula in a therapy-refractory patient. Biol Psychiatry 67, e9-e11.

Spindelegger, C., Lanzenberger, R., Wadsak, W., Mien, L.K., Stein, P., Mitterhauser, M., Moser, U., Holik, A., Pezawas, L., Kletter, K., Kasper, S., 2009. Influence of escitalopram treatment on 5-HT 1A receptor binding in limbic regions in patients with anxiety disorders. Mol Psychiatry 14, 1040-1050.

Vertes, R.P., 1991. A PHA-L analysis of ascending projections of the dorsal raphe nucleus in the rat. J Comp Neurol 313, 643-668.

Vertes, R.P., Fortin, W.J., Crane, A.M., 1999. Projections of the median raphe nucleus in the rat. J Comp Neurol 407, 555-582.

Table

Table: Regional peak T-values of significant positive associations between treatment response and SERT BP_{ND} ratios (SERT BP_{ND} in the whole brain adjusted to SERT BP_{ND} in the MRN).

MNI					
X	*Y*	*Z*	*t-value*	*L/R*	*Region*
-26	-6	-16	7.95	L	Amygdala / anterior hippocampus
30	0	-18	6.99	R	Amygdala
-10	-32	2	7.86	L	Habenula (part of epithalamus)
6	-32	-4	6.59	R	Habenula
62	-12	-14	5.96	R	Medial temporal lobe
-50	-22	-12	4.81	L	Medial temporal lobe
-32	4	8	5.82	L	Putamen
24	-4	12	5.80	R	Putamen
8	26	-18	5.21	R	Subgenual cingulate cortex / OFC
-10	66	-14	4.56	L	Medial OFC
-8	40	4	4.55	L	Anterior cingulate cortex
-6	-20	-24	5.87	L	Anterior midbrain
46	-66	28	4.10	R	Angular gyrus
-10	-66	-32	8.51	L	Cerebellar vermis / white matter

All p-values are FDR corrected ($p<0.05$ voxel-level, cluster size ≥30 voxels). Only the highest peak within an anatomical region is included in the case of several peaks. Model corrected for age; MNI, Montreal Neurological Institute stereotactic space coordinates (X/Y/Z mm); L, left; R, right; BP_{ND}, binding potential; OFC, orbitofrontal cortex.

3.3.8. Supplementary Information

Delineation of regions of interest (ROIs) for the dorsal (DRN) and median (MRN) raphe nuclei

From rostral to caudal, the DRN extends at the level of the accessory oculomotor nucleus to the level of the isthmus (referring to B7 (Dahlstrom and Fuxe, 1964)), having its characteristic fountain shaped appearance. This part of the DRN also contains the majority of 5-HT neurons (Baker et al., 1991b). Further caudally, the DRN narrows its lateral wings and extends as two staves until 14 mm below the level of the isthmus (referring to B6, Baker et al., 1990). In contrast, the rostro-caudal extension of the MRN in the pontine tegmentum starts at the level of the decussation of the superior cerebellar peduncle (1mm above the level of the isthmus) and extends until the level of the motor trigeminal nucleus 19 mm below the level of the isthmus (Baker et al., 1991a). Most of the about 64.000 5-HT neurons of MRN lie within the first 10mm below the level of the isthmus (Baker et al., 1991a).

A reliable differentiation between DRN and MRN was therefore realized by delineating the ROI for the DRN in two PET image slices at the level between superior and inferior culliculus, and by delineating the ROI for the MRN in two slices within the rostral third of the pons (slice thickness = 2mm). Hence, the two raphe ROIs covered 4mm each in z-direction with an in-between gap of 6mm (see Figure S1), see also Kranz et al., 2012.

Radiotracer preparation

The radioligand [^{11}C]DASB (3-amino-4-[N-methyl-N-[^{11}C]methyl-amino-methyl-phenylsulfanyl]-benzonitrile) was synthesized in a fully-automated ^{11}C-methylation synthesizer (GE Medical Systems, Uppsala, Sweden) at the Department of Nuclear Medicine of the Medical University of Vienna, according to a previously published method (Haeusler et al., 2009). Briefly, freshly prepared [^{11}C]methyl iodide was trapped online in the reaction mixture containing 1 mg of precursor (MASB; desmethyl-DASB; obtained from ABX, Radeberg, Germany) in 500 µL of dimethylsulfoxide (DMSO). The reaction mixture was heated to 100°C for 2 min, diluted with 1 mL of HPLC eluent and subsequently transferred to the semi-preparative HPLC system (column: Supelco ABZ+ 5 µm, 250 x 10 mm) for purification.

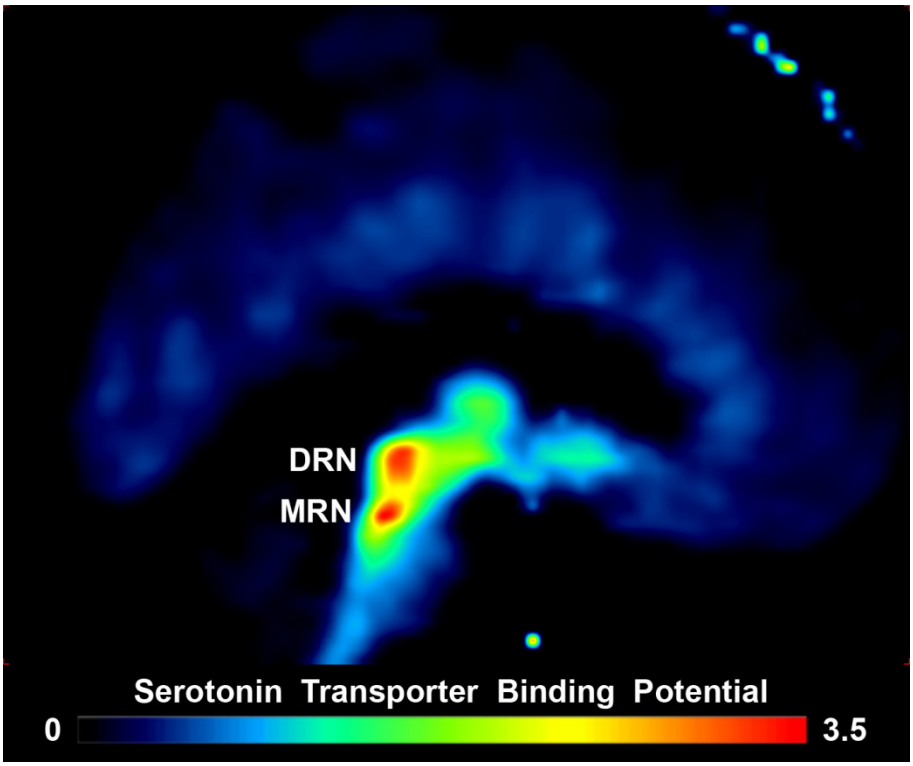

Figure S1: *Sagittal view at x=0mm (M.N.I. coordinate) of the voxel-wise serotonin transporter binding measured with PET and [^{11}C]DASB. The map represents baseline SERT distribution of a representative patient. The color code indicates binding potential. DRN, dorsal raphe nucleus; MRN, median raphe nucleus.*

Mobile phase consisted of 40% acetonitrile and 60% 0.1 mol/L ammonium acetate and was used at a flow rate of 8mL/min. The product fraction was cut and then diluted and subjected to solid phase extraction (Waters, ^{18}Cplus SepPak®) to reduce the content of residual solvents. After washing the purified product with water it was eluted with ethanol. Finally, the ethanolic product solution was formulated with saline and phosphate buffer and sterile filtrated under aseptic conditions in a laminar air flow hot cell. Typically, 2-9 GBq of [^{11}C]DASB were prepared within 35±3 min (n=66). Quality control was performed measuring radiochemical and chemical purity (using analytical HPLC), pH, isotonicity, radionuclidic purity and residual solvents (using gas chromatography). Sterility and endotoxines were analysed after the release of the product, in accordance with the regulations for radiopharmaceutical preparations as laid down by the European Pharmacopoiea. The injected radioactivity (mean = 353 MBq, SD = 91) was of high

radiochemical purity (>95%, mean 98.2%, SD=1.1) and of high specific activity (mean = 34.9 GBq/µmol, SD = 15).

References

Baker, K.G., Halliday, G.M., Halasz, P., Hornung, J.P., Geffen, L.B., Cotton, R.G., Tork, I., 1991a. Cytoarchitecture of serotonin-synthesizing neurons in the pontine tegmentum of the human brain. Synapse 7, 301-320.

Baker, K.G., Halliday, G.M., Hornung, J.P., Geffen, L.B., Cotton, R.G.H., Tork, I., 1991b. Distribution, Morphology and Number of Monoamine-Synthesizing and Substance P-Containing Neurons in the Human Dorsal Raphe Nucleus. Neuroscience 42, 757-775.

Baker, K.G., Halliday, G.M., Tork, I., 1990. Cytoarchitecture of the human dorsal raphe nucleus. J Comp Neurol 301, 147-161.

Dahlstrom, A., Fuxe, K., 1964. Evidence for Existence of Monoamine-Containing Neurons in Central Nervous System .I. Demonstration of Monoamines in Cell Bodies of Brain Stem Neurons. Acta Physiol Scand Suppl. 232, 1-55.

Haeusler, D., Mien, L.K., Nics, L., Ungersboeck, J., Philippe, C., Lanzenberger, R.R., Kletter, K., Dudczak, R., Mitterhauser, M., Wadsak, W., 2009. Simple and rapid preparation of [(11)C]DASB with high quality and reliability for routine applications. Appl Radiat Isot. 67(9), 1654-1660.

Kranz, G.S., Hahn, A., Savli, M., Lanzenberger, R., 2012. Challenges in the differentiation of midbrain raphe nuclei in neuroimaging research. Proc Natl Acad Sci U S A. 109(29), E2000.

IV. GENERAL DISCUSSION

We aimed to tackle several basic neuroscientific issues regarding the SERT and its distribution in the living human brain through three publications arising from this thesis. Using PET and [^{11}C]DASB, we were able to expand our knowledge on the SERT through elucidation of patterns relating its distribution to cerebral dominance and gender identity, SSRIs and SERT occupancy, as well as to prediction of antidepressant treatment response.

Rather than supply simple answers, our results provide a differentiated picture on the complex role of SERT distribution in the living human brain. For example, no simple differences in plain SERT BP_{ND} were found between healthy females, males or male-to-female transsexuals in the first publication. However, SERT binding was highly asymmetric in several cortical and subcortical regions. Although the three subject samples showed similar asymmetries in most regions, SERT asymmetry in the midcingulate cortex was associated with gender identity, as this region showed strong asymmetry in males, but not in females and male-to-female transsexuals. Regarding the second publication, correlations between pretreatment SERT availability and occupancy by SSRIs were restricted to the subgenual anterior cingulate cortex and not observed in other cortical or subcortical regions. However, correlations between drug plasma levels and occupancy after prolonged SSRI intake were found for most subcortical but not cortical regions. Furthermore, a significant increase in SERT occupancy after prolonged SSRI intake compared to acute intake was similarly found only in subcortical and not cortical regions. Finally, no straight forward relationship between baseline SERT binding and treatment outcome was observed in the third publication. However, normalizing SERT binding in projection areas to that of the median raphe resulted in strong correlations between several disorder-related terminal regions and treatment outcome.

Thus, our results provide novel impulses within clinical neuroscience that may stimulate new research projects and guide ways of understanding the complex relations of SERT distribution and gender identity, drug efficacy and depression. Still, as molecular imaging with PET *in vivo* relies heavily on several assumptions, our studies include limitations that may bear on the

interpretation of our results. The primary outcome measure in all three publications was the BP_{ND}, which assumes that nondisplaceable radioligand uptake is uniform across brain regions and independent of treatment effects or subject groups (Innis et al, 2007). However, these assumptions may be questionable in some pathological conditions (Huang et al, 2010) and it is therefore unknown whether they hold true for a comparison between depressed and healthy subjects. We used cerebellar gray matter as a reference region, which was shown to be the region of choice for [^{11}C]DASB *in vivo* (Parsey et al, 2006b). Although a reference region should be devoid of targets, post mortem studies indicated specific SERT binding in the cerebellum, with highest values in cerebellar vermis, followed by cerebellar gray and white matter (Kish et al, 2005; Parsey et al, 2006b). Accordingly, SSRI induced SERT occupancy may be underestimated when using BP_{ND} and cerebellar gray matter as reference region. This was confirmed in a recent study by Hinz et al. who investigated the effects of intravenous citalopram infusion on SERT occupancy by calculating both BP_{ND} and PP_P (Hinz et al, 2008, for nomenclature, see Innis et al, 2007 or section 1.3.3.). Furthermore, Hinz et al. observed that SSRI infusion led to a change in the steepness of cerebellar time activity curves (TACs), an effect that was also found in our data (Savli 2013, personal communication). A change in TAC shape reflects SSRI induced changes in the pharmacodynamics within the cerebellum. However, how these changes impact on the BP_{ND} remains unknown.

The assumption of consistency of SERT affinity for both the radioligand and the antidepressant drug must also be critically discussed. The inability to differentiate target density from target affinity is inherent to the definition of the binding potential. Thus, if an *in vivo* PET study detects differences in the binding potential between, for example, depressed subjects and healthy controls, either target density or target affinity may differ. Although the binding potential is always interpreted to reflect target density, we must keep in mind that this is done by *assuming* that the affinity is constant across subjects and brain regions. However, this may not always be the case. In their recent review, Steiner et al. gathers evidence that 5-HT clearance is not only affected by trafficking-dependent, but also by trafficking-independent SERT modulation (Steiner et al, 2008). The latter of these processes includes conformational changes of the SERT which

may not only alter transport capacity but also result in a change in 5-HT affinity (Steiner et al, 2008). Similarly, we cannot rule out that drug or radioligand SERT affinity are subject to change.

Finally, in addition to these basic issues pertaining to PET methodology *in vivo*, other factors may have confounded our results. For example, Praschak-Rieder et al. (2008) observed seasonal variations in SERT binding with higher values during fall and winter and lower values during spring and summer. Differences between highest and lowest values within one year ranged between 20-40%, depending on the brain region. Furthermore, SERT binding showed negative correlations with day length and average duration of daily sunshine. Although subsequent SPECT studies could not, or only partly, confirm seasonal variations in SERT binding (Cheng et al, 2011; Koskela et al, 2008; Ruhe et al, 2009) a recent PET study using [^{11}C]DASB found an association between daylight in minutes at the scanning day and SERT binding in the basal ganglia (Kalbitzer et al, 2010). Additionally, a recent study by our group detected positive correlations between global radiation and postsynaptic 5-HT$_{1A}$ receptor binding, which further supports the assumption of seasonal variations in serotonin function (Spindelegger et al, 2012). However, seasonal variation in SERT binding was not controlled for in the studies arising from this thesis. Still, it is less likely that these variations biased our results in a specific direction, as all subjects were scanned randomly relative to season. This indicates that this potential confounder only inflated the error variance.

V. CONCLUSION AND FUTURE PROSPECTS

This doctoral thesis was centered on studying the human SERT distribution in relation to cerebral asymmetry and gender identity, drug occupancy and antidepressant treatment response. The thesis is thus tied to modern molecular imaging research aimed at investigating an important component of the serotonergic system *in vivo* using PET and [^{11}C]DASB. The three publications arising from this thesis not only enrich our basic neuroscientific knowledge on SERT function and distribution but may also have clinical relevance. This significance especially applies to the second and third publication. Revealing the relations of regional SERT pretreatment binding to SERT occupancy in the second paper increases our understanding of antidepressant drug action and may help in the guidance of drug development tailored to individual symptoms. The last paper provides first evidence of a molecular predictor of antidepressant treatment response by analysis of pretreatment SERT binding on a system level. Should this association prove to become a valid biological marker for antidepressant treatment response, it will be a significant qualitative leap ahead for reduced individual suffering and improved compliance.

A selection of next steps which would allow for the replication and expansion of our results includes similar investigations in larger and independent samples as well as testing of other SSRIs. Lastly the establishment of the predictive value of pretreatment SERT binding on SSRI response in other psychiatric disorders would assert this relationship's relevance as a biological marker. Clinically applicable molecular based standard parameters have yet to be established within the field of psychiatry. Information gleaned in the context of this thesis may support this endeavor.

VI. REFERENCES

Alex KD, Pehek EA (2007) Pharmacologic mechanisms of serotonergic regulation of dopamine neurotransmission. *Pharmacol Ther* **113:** 296-320

Andersen J, Olsen L, Hansen KB, Taboureau O, Jorgensen FS, Jorgensen AM, Bang-Andersen B, Egebjerg J, Stromgaard K, Kristensen AS (2010) Mutational mapping and modeling of the binding site for (S)-citalopram in the human serotonin transporter. *J Biol Chem* **285:** 2051-2063

Andersen SL, Teicher MH (1999) Serotonin laterality in amygdala predicts performance in the elevated plus maze in rats. *Neuroreport* **10:** 3497-3500

Azmitia EC, Segal M (1978) An autoradiographic analysis of the differential ascending projections of the dorsal and median raphe nuclei in the rat. *J Comp Neurol* **179:** 641-667

Backstrom I, Bergstrom M, Marcusson J (1989) High affinity [3H]paroxetine binding to serotonin uptake sites in human brain tissue. *Brain Res* **486:** 261-268

Bailer UF, Frank GK, Henry SE, Price JC, Meltzer CC, Becker C, Ziolko SK, Mathis CA, Wagner A, Barbarich-Marsteller NC, Putnam K, Kaye WH (2007) Serotonin transporter binding after recovery from eating disorders. *Psychopharmacology (Berl)* **195:** 315-324

Bar KJ, Greiner W, Letsch A, Kobele R, Sauer H (2003) Influence of gender and hemispheric lateralization on heat pain perception in major depression. *J Psychiatr Res* **37:** 345-353

Bengel D, Murphy DL, Andrews AM, Wichems CH, Feltner D, Heils A, Mossner R, Westphal H, Lesch KP (1998) Altered brain serotonin homeostasis and locomotor insensitivity to 3, 4-methylenedioxymethamphetamine ("Ecstasy") in serotonin transporter-deficient mice. *Mol Pharmacol* **53:** 649-655

Benmansour S, Owens WA, Cecchi M, Morilak DA, Frazer A (2002) Serotonin clearance in vivo is altered to a greater extent by antidepressant-induced downregulation of the serotonin transporter than by acute blockade of this transporter. *J Neurosci* **22:** 6766-6772

Best J, Nijhout HF, Reed M (2011) Bursts and the efficacy of selective serotonin reuptake inhibitors. *Pharmacopsychiatry* **44 Suppl 1:** S76-83

Bethea CL, Lu NZ, Gundlah C, Streicher JM (2002) Diverse actions of ovarian steroids in the serotonin neural system. *Front Neuroendocrinol* **23:** 41-100

Brenner B, Harney JT, Ahmed BA, Jeffus BC, Unal R, Mehta JL, Kilic F (2007) Plasma serotonin levels and the platelet serotonin transporter. *J Neurochem* **102:** 206-215

Briley MS, Langer SZ, Raisman R, Sechter D, Zarifian E (1980) Tritiated imipramine binding sites are decreased in platelets of untreated depressed patients. *Science* **209:** 303-305

Buchert R, Schulze O, Wilke F, Berding G, Thomasius R, Petersen K, Brenner W, Clausen M (2006) Is correction for age necessary in SPECT or PET of the central serotonin transporter in young, healthy adults? *J Nucl Med* **47:** 38-42

Catafau AM, Perez V, Plaza P, Pascual JC, Bullich S, Suarez M, Penengo MM, Corripio I, Puigdemont D, Danus M, Perich J, Alvarez E (2006) Serotonin transporter occupancy induced by paroxetine in patients with major depression disorder: a 123I-ADAM SPECT study. *Psychopharmacology (Berl)* **189:** 145-153

Cavanagh J, Patterson J, Pimlott S, Dewar D, Eersels J, Dempsey MF, Wyper D (2006) Serotonin transporter residual availability during long-term antidepressant therapy does not differentiate responder and nonresponder unipolar patients. *Biol Psychiatry* **59:** 301-308

Celik L, Sinning S, Severinsen K, Hansen CG, Moller MS, Bols M, Wiborg O, Schiott B (2008) Binding of serotonin to the human serotonin transporter. Molecular modeling and experimental validation. *J Am Chem Soc* **130:** 3853-3865

Chen F, Larsen MB, Neubauer HA, Sanchez C, Plenge P, Wiborg O (2005a) Characterization of an allosteric citalopram-binding site at the serotonin transporter. *J Neurochem* **92:** 21-28

Chen F, Larsen MB, Sanchez C, Wiborg O (2005b) The S-enantiomer of R,S-citalopram, increases inhibitor binding to the human serotonin transporter by an allosteric mechanism. Comparison with other serotonin transporter inhibitors. *Eur Neuropsychopharmacol* **15:** 193-198

Cheng YS, Chen KC, Yang YK, Chen PS, Yeh TL, Lee IH, Chang YH, Liao MH (2011) No seasonal variation in human midbrain serotonin transporter availability in Taiwan. *Psychiatry Res* **194:** 396-399

Cherry SR, Sorenson JA, Phelps ME (eds) (2003) *Physics in Nuclear Medicine*. Philadelphia PA: Elsevier Science (USA)

Chi L, Reith ME (2003) Substrate-induced trafficking of the dopamine transporter in heterologously expressing cells and in rat striatal synaptosomal preparations. *J Pharmacol Exp Ther* **307:** 729-736

Coppen A, Prange AJ, Jr., Whybrow PC, Noguera R (1972) Abnormalities of indoleamines in affective disorders. *Arch Gen Psychiatry* **26:** 474-478

Cortes R, Soriano E, Pazos A, Probst A, Palacios JM (1988) Autoradiography of antidepressant binding sites in the human brain: localization using [3H]imipramine and [3H]paroxetine. *Neuroscience* **27:** 473-496

D'Amato RJ, Largent BL, Snowman AM, Snyder SH (1987) Selective labeling of serotonin uptake sites in rat brain by [3H]citalopram contrasted to labeling of multiple sites by [3H]imipramine. *J Pharmacol Exp Ther* **242:** 364-371

Dahlstrom A, Fuxe K (1964) Evidence for Existence of Monoamine-Containing Neurons in Central Nervous System .I. Demonstration of Monoamines in Cell Bodies of Brain Stem Neurons. *Acta Physiologica Scandinavica* **62:** 5-&

Daws LC, Callaghan PD, Moron JA, Kahlig KM, Shippenberg TS, Javitch JA, Galli A (2002) Cocaine increases dopamine uptake and cell surface expression of dopamine transporters. *Biochem Biophys Res Commun* **290:** 1545-1550

Diamond MC (1991) Hormonal effects on the development or cerebral lateralization. *Psychoneuroendocrinology* **16:** 121-129

Draca S (2010) Gender-specific functional cerebral asymmetries and unilateral cerebral lesion sequelae. *Rev Neurosci* **21:** 421-425

El Mansari M, Guiard BP, Chernoloz O, Ghanbari R, Katz N, Blier P (2010) Relevance of norepinephrine-dopamine interactions in the treatment of major depressive disorder. *CNS Neurosci Ther* **16:** e1-17

Fan P (1994) Effects of antidepressants on the inward current mediated by 5-HT3 receptors in rat nodose ganglion neurones. *Br J Pharmacol* **112:** 741-744

Flament MF, Bissada H, Spettigue W (2012) Evidence-based pharmacotherapy of eating disorders. *Int J Neuropsychopharmacol* **15:** 189-207

Gelenberg AJ, Chesen CL (2000) How fast are antidepressants? *J Clin Psychiatry* **61:** 712-721

Ginovart N, Wilson AA, Meyer JH, Hussey D, Houle S (2001) Positron emission tomography quantification of [(11)C]-DASB binding to the human serotonin transporter: modeling strategies. *J Cereb Blood Flow Metab* **21:** 1342-1353

Ginovart N, Wilson AA, Meyer JH, Hussey D, Houle S (2003) [11C]-DASB, a tool for in vivo measurement of SSRI-induced occupancy of the serotonin transporter: PET characterization and evaluation in cats. *Synapse* **47:** 123-133

Gould GG, Pardon MC, Morilak DA, Frazer A (2003) Regulatory effects of reboxetine treatment alone, or following paroxetine treatment, on brain noradrenergic and serotonergic systems. *Neuropsychopharmacology* **28:** 1633-1641

Herold N, Uebelhack K, Franke L, Amthauer H, Luedemann L, Bruhn H, Felix R, Uebelhack R, Plotkin M (2006) Imaging of serotonin transporters and its blockade by citalopram in patients with major depression using a novel SPECT ligand [123I]-ADAM. *J Neural Transm* **113:** 659-670

Hesse S, Stengler K, Regenthal R, Patt M, Becker GA, Franke A, Knupfer H, Meyer PM, Luthardt J, Jahn I, Lobsien D, Heinke W, Brust P, Hegerl U, Sabri O (2011) The serotonin transporter availability in untreated early-onset and late-onset patients with obsessive-compulsive disorder. *Int J Neuropsychopharmacol* **14:** 606-617

Hinz R, Selvaraj S, Murthy NV, Bhagwagar Z, Taylor M, Cowen PJ, Grasby PM (2008) Effects of citalopram infusion on the serotonin transporter binding of [11C]DASB in healthy controls. *J Cereb Blood Flow Metab* **28:** 1478-1490

Horschitz S, Hummerich R, Schloss P (2001) Down-regulation of the rat serotonin transporter upon exposure to a selective serotonin reuptake inhibitor. *Neuroreport* **12:** 2181-2184

Houle S, Ginovart N, Hussey D, Meyer JH, Wilson AA (2000) Imaging the serotonin transporter with positron emission tomography: initial human studies with [11C]DAPP and [11C]DASB. *Eur J Nucl Med* **27:** 1719-1722

Huang Y, Zheng MQ, Gerdes JM (2010) Development of effective PET and SPECT imaging agents for the serotonin transporter: has a twenty-year journey reached its destination? *Curr Top Med Chem* **10:** 1499-1526

Ichimiya T, Suhara T, Sudo Y, Okubo Y, Nakayama K, Nankai M, Inoue M, Yasuno F, Takano A, Maeda J, Shibuya H (2002) Serotonin transporter binding in patients with mood disorders: a PET study with [11C](+)McN5652. *Biol Psychiatry* **51:** 715-722

Ichise M, Liow JS, Lu JQ, Takano A, Model K, Toyama H, Suhara T, Suzuki K, Innis RB, Carson RE (2003) Linearized reference tissue parametric imaging methods: application to [11C]DASB positron emission tomography studies of the serotonin transporter in human brain. *J Cereb Blood Flow Metab* **23:** 1096-1112

Ichise M, Meyer JH, Yonekura Y (2001) An introduction to PET and SPECT neuroreceptor quantification models. *J Nucl Med* **42:** 755-763

Innis RB, Cunningham VJ, Delforge J, Fujita M, Gjedde A, Gunn RN, Holden J, Houle S, Huang SC, Ichise M, Iida H, Ito H, Kimura Y, Koeppe RA, Knudsen GM, Knuuti J, Lammertsma AA, Laruelle M, Logan J, Maguire RP, Mintun MA, Morris ED, Parsey R, Price JC, Slifstein M, Sossi V, Suhara T, Votaw JR, Wong DF, Carson RE (2007) Consensus nomenclature for in vivo imaging of reversibly binding radioligands. *J Cereb Blood Flow Metab* **27:** 1533-1539

Jardetzky O (1966) Simple allosteric model for membrane pumps. *Nature* **211:** 969-970

Jayanthi LD, Samuvel DJ, Blakely RD, Ramamoorthy S (2005) Evidence for biphasic effects of protein kinase C on serotonin transporter function, endocytosis, and phosphorylation. *Mol Pharmacol* **67:** 2077-2087

Jorgensen AM, Tagmose L, Topiol S, Sabio M, Gundertofte K, Bogeso KP, Peters GH (2007) Homology modeling of the serotonin transporter: insights into the primary escitalopram-binding site. *ChemMedChem* **2:** 815-826

Jovanovic H, Karlsson P, Cerin A, Halldin C, Nordstrom AL (2009) 5-HT(1A) receptor and 5-HTT binding during the menstrual cycle in healthy women examined with [(11)C] WAY100635 and [(11)C] MADAM PET. *Psychiatry Res* **172:** 31-37

Jovanovic H, Lundberg J, Karlsson P, Cerin A, Saijo T, Varrone A, Halldin C, Nordstrom AL (2008) Sex differences in the serotonin 1A receptor and serotonin transporter binding in the human brain measured by PET. *Neuroimage* **39:** 1408-1419

Kahlig KM, Javitch JA, Galli A (2004) Amphetamine regulation of dopamine transport. Combined measurements of transporter currents and transporter imaging support the endocytosis of an active carrier. *J Biol Chem* **279:** 8966-8975

Kakiuchi T, Tsukada H, Fukumoto D, Nishiyama S (2001) Effects of aging on serotonin transporter availability and its response to fluvoxamine in the living brain: PET study with [(11)C](+)McN5652 and [(11)C](-)McN5652 in conscious monkeys. *Synapse* **40:** 170-179

Kalbitzer J, Erritzoe D, Holst KK, Nielsen FA, Marner L, Lehel S, Arentzen T, Jernigan TL, Knudsen GM (2010) Seasonal changes in brain serotonin transporter binding in short serotonin transporter linked polymorphic region-allele carriers but not in long-allele homozygotes. *Biol Psychiatry* **67:** 1033-1039

Kent JM, Coplan JD, Lombardo I, Hwang DR, Huang Y, Mawlawi O, Van Heertum RL, Slifstein M, Abi-Dargham A, Gorman JM, Laruelle M (2002) Occupancy of brain serotonin transporters during treatment with paroxetine in patients with social phobia: a positron emission tomography study with 11C McN 5652. *Psychopharmacology (Berl)* **164:** 341-348

Kish SJ, Furukawa Y, Chang LJ, Tong J, Ginovart N, Wilson A, Houle S, Meyer JH (2005) Regional distribution of serotonin transporter protein in postmortem human brain: is the cerebellum a SERT-free brain region? *Nucl Med Biol* **32:** 123-128

Kittler K, Lau T, Schloss P (2010) Antagonists and substrates differentially regulate serotonin transporter cell surface expression in serotonergic neurons. *Eur J Pharmacol* **629:** 63-67

Klein N, Sacher J, Geiss-Granadia T, Attarbaschi T, Mossaheb N, Lanzenberger R, Potzi C, Holik A, Spindelegger C, Asenbaum S, Dudczak R, Tauscher J, Kasper S (2006) In vivo imaging of serotonin transporter occupancy by means of SPECT and [123I]ADAM in healthy subjects administered different doses of escitalopram or citalopram. *Psychopharmacology (Berl)* **188:** 263-272

Klein N, Sacher J, Geiss-Granadia T, Mossaheb N, Attarbaschi T, Lanzenberger R, Spindelegger C, Holik A, Asenbaum S, Dudczak R, Tauscher J, Kasper S (2007) Higher serotonin transporter occupancy after multiple dose administration of escitalopram compared to citalopram: an [123I]ADAM SPECT study. *Psychopharmacology (Berl)* **191:** 333-339

Koen N, Stein DJ (2011) Pharmacotherapy of anxiety disorders: a critical review. *Dialogues Clin Neurosci* **13:** 423-437

Kong EK, Peng L, Chen Y, Yu AC, Hertz L (2002) Up-regulation of 5-HT2B receptor density and receptor-mediated glycogenolysis in mouse astrocytes by long-term fluoxetine administration. *Neurochem Res* **27:** 113-120

Koskela A, Kauppinen T, Keski-Rahkonen A, Sihvola E, Kaprio J, Rissanen A, Ahonen A (2008) Brain serotonin transporter binding of [123I]ADAM: within-subject variation between summer and winter data. *Chronobiol Int* **25:** 657-665

Kranz GS, Kasper S, Lanzenberger R (2010) Reward and the serotonergic system. *Neuroscience* **166:** 1023-1035

Krishnamurthy H, Piscitelli CL, Gouaux E (2009) Unlocking the molecular secrets of sodium-coupled transporters. *Nature* **459:** 347-355

Kristensen AS, Andersen J, Jorgensen TN, Sorensen L, Eriksen J, Loland CJ, Stromgaard K, Gether U (2011) SLC6 neurotransmitter transporters: structure, function, and regulation. *Pharmacol Rev* **63:** 585-640

Kugaya A, Sanacora G, Staley JK, Malison RT, Bozkurt A, Khan S, Anand A, Van Dyck CH, Baldwin RM, Seibyl JP, Charney D, Innis RB (2004) Brain serotonin transporter availability predicts treatment response to selective serotonin reuptake inhibitors. *Biol Psychiatry* **56:** 497-502

Kuikka JT, Tammela L, Bergstrom KA, Karhunen L, Uusitupa M, Tiihonen J (2001a) Effects of ageing on serotonin transporters in healthy females. *Eur J Nucl Med* **28:** 911-913

Kuikka JT, Tammela L, Karhunen L, Rissanen A, Bergstrom KA, Naukkarinen H, Vanninen E, Karhu J, Lappalainen R, Repo-Tiihonen E, Tiihonen J, Uusitupa M (2001b) Reduced serotonin transporter binding in binge eating women. *Psychopharmacology (Berl)* **155:** 310-314

Kuikka JT, Tiihonen J, Bergstrom KA, Karhu J, Hartikainen P, Viinamaki H, Lansimies E, Lehtonen J, Hakola P (1995) Imaging of serotonin and dopamine transporters in the living human brain. *Eur J Nucl Med* **22:** 346-350

Laruelle M, Baldwin RM, Malison RT, Zea-Ponce Y, Zoghbi SS, al-Tikriti MS, Sybirska EH, Zimmermann RC, Wisniewski G, Neumeyer JL, et al. (1993) SPECT imaging of dopamine and serotonin transporters with [123I]beta-CIT: pharmacological characterization of brain uptake in nonhuman primates. *Synapse* **13:** 295-309

Lau T, Horschitz S, Berger S, Bartsch D, Schloss P (2008) Antidepressant-induced internalization of the serotonin transporter in serotonergic neurons. *FASEB J* **22:** 1702-1714

Le Poul E, Laaris N, Doucet E, Laporte AM, Hamon M, Lanfumey L (1995) Early desensitization of somato-dendritic 5-HT1A autoreceptors in rats treated with fluoxetine or paroxetine. *Naunyn Schmiedebergs Arch Pharmacol* **352:** 141-148

Le Poul E, Laaris N, Hamon M, Lanfumey L (1997) Fluoxetine-induced desensitization of somatodendritic 5-HT1A autoreceptors is independent of glucocorticoid(s). *Synapse* **27:** 303-312

Licht CL, Marcussen AB, Wegener G, Overstreet DH, Aznar S, Knudsen GM (2009) The brain 5-HT4 receptor binding is down-regulated in the Flinders Sensitive Line depression model and in response to paroxetine administration. *J Neurochem* **109:** 1363-1374

Lundgren JD, Newberg AB, Allison KC, Wintering NA, Ploessl K, Stunkard AJ (2008) 123I-ADAM SPECT imaging of serotonin transporter binding in patients with night eating syndrome: a preliminary report. *Psychiatry Res* **162:** 214-220

Malberg JE, Eisch AJ, Nestler EJ, Duman RS (2000) Chronic antidepressant treatment increases neurogenesis in adult rat hippocampus. *J Neurosci* **20:** 9104-9110

Malison RT, Price LH, Berman R, van Dyck CH, Pelton GH, Carpenter L, Sanacora G, Owens MJ, Nemeroff CB, Rajeevan N, Baldwin RM, Seibyl JP, Innis RB, Charney DS (1998) Reduced brain serotonin transporter availability in major depression as measured by [123I]-2 beta-

carbomethoxy-3 beta-(4-iodophenyl)tropane and single photon emission computed tomography. *Biol Psychiatry* **44:** 1090-1098

Manev H, Uz T, Smalheiser NR, Manev R (2001) Antidepressants alter cell proliferation in the adult brain in vivo and in neural cultures in vitro. *Eur J Pharmacol* **411:** 67-70

Maron E, Toru I, Hirvonen J, Tuominen L, Lumme V, Vasar V, Shlik J, Nutt DJ, Helin S, Nagren K, Tiihonen J, Hietala J (2011) Gender differences in brain serotonin transporter availability in panic disorder. *J Psychopharmacol* **25:** 952-959

Massou JM, Trichard C, Attar-Levy D, Feline A, Corruble E, Beaufils B, Martinot JL (1997) Frontal 5-HT2A receptors studied in depressive patients during chronic treatment by selective serotonin reuptake inhibitors. *Psychopharmacology (Berl)* **133:** 99-101

Mateo Y, Ruiz-Ortega JA, Pineda J, Ugedo L, Meana JJ (2000) Inhibition of 5-hydroxytryptamine reuptake by the antidepressant citalopram in the locus coeruleus modulates the rat brain noradrenergic transmission in vivo. *Neuropharmacology* **39:** 2036-2043

McQueen JK, Wilson H, Fink G (1997) Estradiol-17 beta increases serotonin transporter (SERT) mRNA levels and the density of SERT-binding sites in female rat brain. *Brain Res Mol Brain Res* **45:** 13-23

McQueen JK, Wilson H, Sumner BE, Fink G (1999) Serotonin transporter (SERT) mRNA and binding site densities in male rat brain affected by sex steroids. *Brain Res Mol Brain Res* **63:** 241-247

Menten L, Michaelis MI (1913) Die Kinetik der Invertinwirkung. *Biochemische Zeitschrift* **49:** 333-369

Meyer JH (2007) Imaging the serotonin transporter during major depressive disorder and antidepressant treatment. *J Psychiatry Neurosci* **32:** 86-102

Meyer JH, Houle S, Sagrati S, Carella A, Hussey DF, Ginovart N, Goulding V, Kennedy J, Wilson AA (2004a) Brain serotonin transporter binding potential measured with carbon 11-labeled DASB positron emission tomography: effects of major depressive episodes and severity of dysfunctional attitudes. *Arch Gen Psychiatry* **61:** 1271-1279

Meyer JH, Wilson AA, Ginovart N, Goulding V, Hussey D, Hood K, Houle S (2001) Occupancy of serotonin transporters by paroxetine and citalopram during treatment of depression: a [(11)C]DASB PET imaging study. *Am J Psychiatry* **158:** 1843-1849

Meyer JH, Wilson AA, Sagrati S, Hussey D, Carella A, Potter WZ, Ginovart N, Spencer EP, Cheok A, Houle S (2004b) Serotonin transporter occupancy of five selective serotonin reuptake inhibitors at different doses: an [11C]DASB positron emission tomography study. *Am J Psychiatry* **161:** 826-835

Miller JM, Hesselgrave N, Ogden RT, Sullivan GM, Oquendo MA, Mann JJ, Parsey RV (2013) Positron Emission Tomography Quantification of Serotonin Transporter in Suicide Attempters with Major Depressive Disorder. *Biol Psychiatry*

Miller JM, Oquendo MA, Ogden RT, Mann JJ, Parsey RV (2008) Serotonin transporter binding as a possible predictor of one-year remission in major depressive disorder. *Journal of Psychiatric Research* **42:** 1137-1144

Mintun MA, Raichle ME, Kilbourn MR, Wooten GF, Welch MJ (1984) A quantitative model for the in vivo assessment of drug binding sites with positron emission tomography. *Ann Neurol* **15:** 217-227

Mirza NR, Nielsen EO, Troelsen KB (2007) Serotonin transporter density and anxiolytic-like effects of antidepressants in mice. *Prog Neuropsychopharmacol Biol Psychiatry* **31:** 858-866

Mortensen OV, Kristensen AS, Wiborg O (2001) Species-scanning mutagenesis of the serotonin transporter reveals residues essential in selective, high-affinity recognition of antidepressants. *J Neurochem* **79:** 237-247

Muller CP, Jacobs BL (eds) (2010) *Handbook of the Behavioral Neurobiology of Serotonin*. London: Elsevier B V.

Mullins UL, Gianutsos G, Eison AS (1999) Effects of antidepressants on 5-HT7 receptor regulation in the rat hypothalamus. *Neuropsychopharmacology* **21:** 352-367

Newman ME, Shalom G, Ran A, Gur E, Van de Kar LD (2004) Chronic fluoxetine-induced desensitization of 5-HT1A and 5-HT1B autoreceptors: regional differences and effects of WAY-100635. *Eur J Pharmacol* **486:** 25-30

Nutt D, Demyttenaere K, Janka Z, Aarre T, Bourin M, Canonico PL, Carrasco JL, Stahl S (2007) The other face of depression, reduced positive affect: the role of catecholamines in causation and cure. *J Psychopharmacol* **21:** 461-471

Ostad Haji E, Tadic A, Wagner S, Dragicevic A, Muller MJ, Boland K, Rao ML, Fric M, Laux G, Hiemke C (2011) Association between citalopram serum levels and clinical improvement of patients with major depression. *J Clin Psychopharmacol* **31:** 281-286

Parsey RV, Hastings RS, Oquendo MA, Huang YY, Simpson N, Arcement J, Huang Y, Ogden RT, Van Heertum RL, Arango V, Mann JJ (2006a) Lower serotonin transporter binding potential in the human brain during major depressive episodes. *Am J Psychiatry* **163:** 52-58

Parsey RV, Kent JM, Oquendo MA, Richards MC, Pratap M, Cooper TB, Arango V, Mann JJ (2006b) Acute occupancy of brain serotonin transporter by sertraline as measured by [11C]DASB and positron emission tomography. *Biol Psychiatry* **59:** 821-828

Paul SM, Rehavi M, Skolnick P, Ballenger JC, Goodwin FK (1981) Depressed patients have decreased binding of tritiated imipramine to platelet serotonin "transporter". *Arch Gen Psychiatry* **38:** 1315-1317

Pearlstein T (2012) Psychotropic medications and other non-hormonal treatments for premenstrual disorders. *Menopause Int* **18:** 60-64

Perry EK, Marshall EF, Blessed G, Tomlinson BE, Perry RH (1983) Decreased imipramine binding in the brains of patients with depressive illness. *Br J Psychiatry* **142:** 188-192

Pichika R, Buchsbaum MS, Bailer U, Hoh C, Decastro A, Buchsbaum BR, Kaye W (2012) Serotonin transporter binding after recovery from bulimia nervosa. *Int J Eat Disord* **45:** 345-352

Pineyro G, Blier P (1999) Autoregulation of serotonin neurons: role in antidepressant drug action. *Pharmacol Rev* **51:** 533-591

Pirker W, Asenbaum S, Hauk M, Kandlhofer S, Tauscher J, Willeit M, Neumeister A, Praschak-Rieder N, Angelberger P, Brucke T (2000) Imaging serotonin and dopamine transporters with 123I-beta-CIT SPECT: binding kinetics and effects of normal aging. *J Nucl Med* **41:** 36-44

Praschak-Rieder N, Willeit M, Wilson AA, Houle S, Meyer JH (2008) Seasonal variation in human brain serotonin transporter binding. *Arch Gen Psychiatry* **65:** 1072-1078

Ramamoorthy S, Bauman AL, Moore KR, Han H, Yang-Feng T, Chang AS, Ganapathy V, Blakely RD (1993) Antidepressant- and cocaine-sensitive human serotonin transporter: molecular cloning, expression, and chromosomal localization. *Proc Natl Acad Sci U S A* **90:** 2542-2546

Ramamoorthy S, Blakely RD (1999) Phosphorylation and sequestration of serotonin transporters differentially modulated by psychostimulants. *Science* **285:** 763-766

Ramamoorthy S, Giovanetti E, Qian Y, Blakely RD (1998) Phosphorylation and regulation of antidepressant-sensitive serotonin transporters. *J Biol Chem* **273:** 2458-2466

Ramamoorthy S, Samuvel DJ, Buck ER, Rudnick G, Jayanthi LD (2007) Phosphorylation of threonine residue 276 is required for acute regulation of serotonin transporter by cyclic GMP. *J Biol Chem* **282:** 11639-11647

Ravna AW (2006) Three-dimensional models of neurotransmitter transporters and their interactions with cocaine and S-citalopram. *World J Biol Psychiatry* **7:** 99-109

Reimold M, Batra A, Knobel A, Smolka MN, Zimmer A, Mann K, Solbach C, Reischl G, Schwarzler F, Grunder G, Machulla HJ, Bares R, Heinz A (2008) Anxiety is associated with reduced central serotonin transporter availability in unmedicated patients with unipolar major depression: a [11C]DASB PET study. *Mol Psychiatry* **13:** 606-613, 557

Rosen GD, Finklestein S, Stoll AL, Yutzey DA, Denenberg VH (1984) Neurochemical asymmetries in the albino rat's cortex, striatum, and nucleus accumbens. *Life Sci* **34:** 1143-1148

Ruhe HG, Booij J, Reitsma JB, Schene AH (2009) Serotonin transporter binding with [123I]beta-CIT SPECT in major depressive disorder versus controls: effect of season and gender. *Eur J Nucl Med Mol Imaging* **36:** 841-849

Saulin A, Savli M, Lanzenberger R (2012) Serotonin and molecular neuroimaging in humans using PET. *Amino Acids* **42:** 2039-2057

Savaki H, Malgouris C, Benavides J, Laplace C, Uzan A, Gueremy C, Le Fur G (1985) Quantitative autoradiography of [3H]indalpine binding sites in the rat brain: II. Regional distribution. *J Neurochem* **45:** 521-526

Savli M, Bauer A, Mitterhauser M, Ding YS, Hahn A, Kroll T, Neumeister A, Haeusler D, Ungersboeck J, Henry S, Isfahani SA, Rattay F, Wadsak W, Kasper S, Lanzenberger R (2012) Normative database of the serotonergic system in healthy subjects using multi-tracer PET. *Neuroimage* **63:** 447-459

Selvaraj S, Murthy NV, Bhagwagar Z, Bose SK, Hinz R, Grasby PM, Cowen PJ (2011) Diminished brain 5-HT transporter binding in major depression: a positron emission tomography study with [11C]DASB. *Psychopharmacology (Berl)* **213:** 555-562

Shi L, Quick M, Zhao Y, Weinstein H, Javitch JA (2008) The mechanism of a neurotransmitter:sodium symporter--inward release of Na+ and substrate is triggered by substrate in a second binding site. *Mol Cell* **30:** 667-677

Simpson HB, Lombardo I, Slifstein M, Huang HY, Hwang DR, Abi-Dargham A, Liebowitz MR, Laruelle M (2003) Serotonin transporters in obsessive-compulsive disorder: a positron emission tomography study with [(11)C]McN 5652. *Biol Psychiatry* **54:** 1414-1421

Sinning S, Musgaard M, Jensen M, Severinsen K, Celik L, Koldso H, Meyer T, Bols M, Jensen HH, Schiott B, Wiborg O (2010) Binding and orientation of tricyclic antidepressants within the central substrate site of the human serotonin transporter. *J Biol Chem* **285:** 8363-8374

Slifstein M, Laruelle M (2001) Models and methods for derivation of in vivo neuroreceptor parameters with PET and SPECT reversible radiotracers. *Nucl Med Biol* **28:** 595-608

Spindelegger C, Stein P, Wadsak W, Fink M, Mitterhauser M, Moser U, Savli M, Mien LK, Akimova E, Hahn A, Willeit M, Kletter K, Kasper S, Lanzenberger R (2012) Light-dependent alteration of serotonin-1A receptor binding in cortical and subcortical limbic regions in the human brain. *World J Biol Psychiatry* **13:** 413-422

Staley JK, Krishnan-Sarin S, Zoghbi S, Tamagnan G, Fujita M, Seibyl JP, Maciejewski PK, O'Malley S, Innis RB (2001) Sex differences in [123I]beta-CIT SPECT measures of dopamine and serotonin transporter availability in healthy smokers and nonsmokers. *Synapse* **41:** 275-284

Staley JK, Sanacora G, Tamagnan G, Maciejewski PK, Malison RT, Berman RM, Vythilingam M, Kugaya A, Baldwin RM, Seibyl JP, Charney D, Innis RB (2006) Sex differences in diencephalon serotonin transporter availability in major depression. *Biol Psychiatry* **59:** 40-47

Stanley M, Virgilio J, Gershon S (1982) Tritiated imipramine binding sites are decreased in the frontal cortex of suicides. *Science* **216:** 1337-1339

Steiner JA, Carneiro AM, Blakely RD (2008) Going with the flow: trafficking-dependent and -independent regulation of serotonin transport. *Traffic* **9:** 1393-1402

Stockmeier CA (2003) Involvement of serotonin in depression: evidence from postmortem and imaging studies of serotonin receptors and the serotonin transporter. *J Psychiatr Res* **37:** 357-373

Swaab DF, Garcia-Falgueras A (2009) Sexual differentiation of the human brain in relation to gender identity and sexual orientation. *Funct Neurol* **24:** 17-28

Szabo Z, Kao PF, Scheffel U, Suehiro M, Mathews WB, Ravert HT, Musachio JL, Marenco S, Kim SE, Ricaurte GA, et al. (1995) Positron emission tomography imaging of serotonin transporters in the human brain using [11C](+)McN5652. *Synapse* **20:** 37-43

Takano A, Arakawa R, Hayashi M, Takahashi H, Ito H, Suhara T (2007) Relationship between neuroticism personality trait and serotonin transporter binding. *Biol Psychiatry* **62:** 588-592

Takano A, Suhara T, Ichimiya T, Yasuno F, Suzuki K (2006) Time course of in vivo 5-HTT transporter occupancy by fluvoxamine. *J Clin Psychopharmacol* **26:** 188-191

Tauscher J, Pirker W, Willeit M, de Zwaan M, Bailer U, Neumeister A, Asenbaum S, Lennkh C, Praschak-Rieder N, Brucke T, Kasper S (2001) [123I] beta-CIT and single photon emission computed tomography reveal reduced brain serotonin transporter availability in bulimia nervosa. *Biol Psychiatry* **49:** 326-332

Tellez R, Rocha L, Castillo C, Meneses A (2010) Autoradiographic study of serotonin transporter during memory formation. *Behav Brain Res* **212:** 12-26

Valdes JJ, Mactutus CF, Cory RN, Cameron WR (1981) Lateralization of norepinephrine, serotonin and choline uptake into hippocampal synaptosomes of sinistral rats. *Physiol Behav* **27:** 381-383

van Dyck CH, Malison RT, Seibyl JP, Laruelle M, Klumpp H, Zoghbi SS, Baldwin RM, Innis RB (2000) Age-related decline in central serotonin transporter availability with [(123)I]beta-CIT SPECT. *Neurobiol Aging* **21:** 497-501

Varnas K, Halldin C, Hall H (2004) Autoradiographic distribution of serotonin transporters and receptor subtypes in human brain. *Hum Brain Mapp* **22:** 246-260

Vidal R, Valdizan EM, Mostany R, Pazos A, Castro E (2009) Long-term treatment with fluoxetine induces desensitization of 5-HT4 receptor-dependent signalling and functionality in rat brain. *J Neurochem* **110:** 1120-1127

Wadsak W, Mitterhauser M (2010) Basics and principles of radiopharmaceuticals for PET/CT. *Eur J Radiol* **73:** 461-469

Walsh A, McDowall J, Grimshaw GM (2010) Hemispheric specialization for emotional word processing is a function of SSRI responsiveness. *Brain Cogn* **74:** 332-340

Whitworth TL, Herndon LC, Quick MW (2002) Psychostimulants differentially regulate serotonin transporter expression in thalamocortical neurons. *J Neurosci* **22:** RC192

Willins DL, Alsayegh L, Berry SA, Backstrom JR, Sanders-Bush E, Friedman L, Khan N, Roth BL (1998) Serotonergic antagonist effects on trafficking of serotonin 5-HT2A receptors in vitro and in vivo. *Ann N Y Acad Sci* **861:** 121-127

Wong DT, Bymaster FP, Engleman EA (1995) Prozac (fluoxetine, Lilly 110140), the first selective serotonin uptake inhibitor and an antidepressant drug: twenty years since its first publication. *Life Sci* **57:** 411-441

Yamamoto M, Suhara T, Okubo Y, Ichimiya T, Sudo Y, Inoue M, Takano A, Yasuno F, Yoshikawa K, Tanada S (2002) Age-related decline of serotonin transporters in living human brain of healthy males. *Life Sci* **71:** 751-757

Yamashita A, Singh SK, Kawate T, Jin Y, Gouaux E (2005) Crystal structure of a bacterial homologue of Na+/Cl--dependent neurotransmitter transporters. *Nature* **437:** 215-223

Zhou Z, Zhen J, Karpowich NK, Goetz RM, Law CJ, Reith ME, Wang DN (2007) LeuT-desipramine structure reveals how antidepressants block neurotransmitter reuptake. *Science* **317:** 1390-1393

Zhou Z, Zhen J, Karpowich NK, Law CJ, Reith ME, Wang DN (2009) Antidepressant specificity of serotonin transporter suggested by three LeuT-SSRI structures. *Nat Struct Mol Biol* **16:** 652-657

Zhu CB, Hewlett WA, Feoktistov I, Biaggioni I, Blakely RD (2004) Adenosine receptor, protein kinase G, and p38 mitogen-activated protein kinase-dependent up-regulation of serotonin transporters involves both transporter trafficking and activation. *Mol Pharmacol* **65:** 1462-1474

APPENDIX – CV

Georg S. Kranz, Mag. rer.nat.
Functional, Molecular & Translational Neuroimaging Lab
Department of Psychiatry and Psychotherapy
Medical University of Vienna, Austria
www.meduniwien.ac.at/neuroimaging
Phone: +43 1 40400 3825
Mobile: +43 650 5969401
Email: georg.kranz@meduniwien.ac.at

Personal Data:

Date of birth:	14.04.1981
Place of birth:	Nürnberg, Germany
Nationality:	Austria
Academic degree:	Magister der Naturwissenschaften
Martial status:	single

Current Position:

11/2008 – present	Researcher at the Functional, Molecular and Translational Neuroimaging Lab (http://www.meduniwien.ac.at/neuroimaging/, Head: Assoc.-Prof. Dr. Rupert Lanzenberger, MD PD) at the Department of Psychiatry and Psychotherapy (Head: Prof. Dr. h.c. mult. Siegfried Kasper, MD), MUW.
10/2006 – present:	Scientific assistant at the Viktor Frankl Institute (VFI) Vienna and the International Academy of Philosophy in the Principality of Liechtenstein. Assistance at the private archives of Viktor E. Frankl

Education:

11/2008 – present	PhD Program of applied Medical Sciences: Clinical Neuroscience, Medical University of Vienna
11/2008	Mag. rer. nat. (with distinction) Degree in Psychology
2002 – 2008	Faculty of Psychology, University of Vienna with the focus on: Biological Psychology (Prof. H. Bauer) und General Psychology (Prof. G. Benetka)
2001	“Matura” (with distinction), university entrance certificate

Special Training & Courses:

2010 8th Summer School of Neuroscience; Focus theme: Schizophrenia, Sicily, Italy

2011 HBM advanced fMRI, Peking, China

2012 SPM Course Hamburg, Germany

2002-2008 several SPSS courses, Vienna, Austria

Additional Skills:

Languages: Fluent in English

Elementary French and Spanish

Mother tongue: German

Computer: Matlab, MRIcro, PMOD, SPM, SPSS, GIMP

Karate trainer (1st Dan)

Grants & Fellowships: 10 projects, € 1.389.799.-

Co-investigator: 6 projects, € 919.992.-

1. **Influence of light exposure on cerebral Monoamine oxidase A in Seasonal Affective Disorder and Healthy Controls measured by PET**. Funding: FWF Austrian Science Fund P 24359, 2012-2014. PI: Assoc.-Prof. PD Dr. Dietmar Winkler, MD, MUW Austria.
2. **The Norepinephrine Transporter in Attention Deficit Hyperactivity Disorder investigated with PET**. Funding: FWF Austrian Science Fund P 22981, 2011-2014. PI: Assoc.-Prof. PD Dr. Rupert Lanzenberger, MD, MUW Austria.
3. **Brain Network Dysfunction as a Model for Schizophrenia: Connectivity Alterations using Ketamine and pharmacological Magnetic Resonance Imaging**. Funding: Austrian National Bank, Jubiläumsfonds Project # 14193, 2011 - 2012. PI: Assoc.-Prof. PD Dr. Dietmar Winkler, MD, MUW Austria.
4. **Effects of sex steroid hormones on human brain function, structure and connectivity: A longitudinal study using 7 Tesla Ultrahigh-field Magnetic Resonance Imaging.** Funding: FWF Austrian Science Fund P 23021, 2010 – 2014. PI: Assoc.-Prof. PD Dr. Rupert Lanzenberger, MD, MUW Austria.
5. **The Serotonin Transporter in Attention Deficit Hyperactivity Disorder Investigated with Positron Emission Tomography**. Funding: Austrian National Bank, Jubiläumsfonds Project # 13675, 2010 – 2013. PI: Assoc.-Prof. PD Mag. Dr. Markus Mitterhauser, Department of Nuclear Medicine, MUW, Austria.

6. **The influence of sex steroid hormones on serotonin transporter binding in the human brain investigated by PET.** Funding: Austrian National Bank, Jubiläumsfonds Project # 13214, 2009 – 2013. PI: Assoc.-Prof. PD Dr. Rupert Lanzenberger, MD, MUW Austria.

Collaborator: 4 projects, € 469.807.-

7. **Multimodal Neuroimaging in Clinical Neurosciences – Assessment of neurobiological markers for psychiatric disorders.** Funding: Austrian National Bank, Jubiläumsfonds Project # 14577, 2012-2015. PI: O.Univ.-Prof. Dr.h.c. mult. Dr.med. Siegfried Kasper, MD, MUW Austria.
8. **Multimodal Neuroimaging in Clinical Neurosciences – Assessment of neurobiological markers for psychiatric disorders.** Funding: Research Cluster between Medical University & University of Vienna, 2011–2014. PI: Assoc. Prof. Dr. Rupert Lanzenberger & Prof. Dr. Claus Lamm.
9. **Effects of electroconvulsive therapy on serotonin-1A receptor binding in major depression investigated by positron emission tomography (PET).** Funding: USA National Alliance for Research on Schizophrenia and Depression (NARSAD). PI: Assoc.-Prof. PD Dr. Rupert Lanzenberger, MD, MUW Austria.
10. **The influence of hormone replacement therapy on serotonin 1A receptor distribution and mood in postmenopausal women -- A longitudinal study using Positron Emission Tomography (PET) and the radioligand [*carbonyl*-11 C]WAY-100635.** Funding: Austrian National Bank, Jubiläumsfonds Project # 12809, 2008 – 2011. PI: O.Univ.Prof.Dr.h.c.mult. Dr.med. Siegfried Kasper, MUW Austria.

Honours & Awards:

- ECNP Travel Award 2012 (€ 500)
- Scholarships for the participation at the ECNP Workshop on Neuropsychopharmacology for Young Scientists in Europe, Nice, 2011 and 2012
- EPHAR Fellowship for the participation at the 8th Summer School of Neuroscience 2010. (€ 1.000)
- Travel Grants OeFG for HBM Conference 2010, 2012, 2013 (€ 290, 2x€ 700)

Invited Lectures & Talks:

03/2013 **Gendereffekte der Serotonintransporter-asymmetrie**
Winterseminar “BIOLOGISCHE PSYCHIATRIE” Oberlech

03/2012 **Serotonin transporter ratio between raphe nuclei and projection areas predicts SSRI treatment response in major depression.** ECNP Workshop, 15-18 March 2012, Nice, France

03/2012 **Kann das Zusammenspiel von Serotonintransportern in Ursprungs- und Projektionsgebieten die antidepressive Wirkung von SSRIs vorhersagen?** Winterseminar "BIOLOGISCHE PSYCHIATRIE" Oberlech

09/2011 **Antidepressants and reward processing in humans.** Response to Philip J. Cowen. Targeted Expert Meeting: Affective Disorders and Antidepressants, 24th ECNP Congress, Paris

03/2011 **Pharmakologische fMRT bei Hormontherapie**
Winterseminar "BIOLOGISCHE PSYCHIATRIE" Oberlech

11/2010 **Funktionelle und Molekulare Bildgebung bei Transsexualität**
Wissenschaftliches Seminar, Department of Psychiatry and Psychotherapy, MUW

11/2010 **Funktionelle und Molekulare Bildgebung bei Transsexualität**
Fortbildungsveranstaltung, Department of Obstetrics and Gynecology, MUW

External Referee / Invited Reviewer:

- Journal of Neuroscience *[2011, IF: 7.115] since 2011*
- PLoS ONE *[2011, IF: 4.092] since 2012*
- Psychoneuroendocrinology *[2011, IF: 5.809] since 2012*
- Journal of the Neurological Sciences *[2011, IF: 2.353] since 2011*
- Journal für Neurologie Neurochirurgie und Psychiatrie *since 2010*
- Springer Verlag Books *since 2012*

Memberships in Professional Organizations:

2011 – now ECNP (European College of Neuropsychopharmacology)
http://www.ecnp.eu/

2010 – now OHBM (Organization for Human Brain Mapping)
http://www.humanbrainmapping.org/

Memberships in Editorial Boards:

2012 – now Dataset Papers in Medicine

http://www.datasets.com/journals/medicine/

Publications: accumulated IF: 83, *h*-index: 6 (ISI 2011)

First author: 57 citations

1. **Kranz G.S.**, Hahn A., Baldinger P., Haeusler D., Philippe C., Kaufmann U., Wadsak W., Savli M., Hoeflich A., Kraus C., Vanicek T., Mitterhauser M., Kasper S., Lanzenberger R. (2012). Cerebral Serotonin Transporter Asymmetry in Females, Males and Male-to-Female Transsexuals measured by PET in vivo. *Brain Structure and Function*, in press. [2011, IF: 5.628]
2. **Kranz G.S.,** Hahn, A., Savli, M., & Lanzenberger R. (2012). Challenges in the differentiation of midbrain raphe nuclei in neuroimaging research. *Proceedings of the National Academy of Sciences of the United States of America (PNAS), 109(29),* doi:10.1073/pnas.1206247109. [2011, IF: 9.681]
3. **Kranz G.S.**, Kasper S., & Lanzenberger R. (2010). Reward and the Serotonergic System. *Neuroscience* 166 (4), 1023-1035. [2011, IF: 3.380]
4. **Kranz G.S.** (2008). Prosocial behaviour and the influence of being observed. An ERP study. [German] *Diploma Thesis*. University of Vienna.

Co-author:

1. Kranz G, Shamim EA, Lin PT, **Kranz GS**, Hallett M (2012). Long-term depression-like plasticity of the blink reflex for the treatment of blepharospasm. *Movement Disorders*, in press. *[2011, IF: 4.505]*
2. Lanzenberger R, **Kranz G.S.**, Häusler D, Akimova E, Savli M, Hahn A, Wadsak W, Spindelegger C, Philippe C, Fink M, Mitterhauser M, Kasper S. (2012). Prediction of SSRI treatment response in major depression based on serotonin transporter interplay between median raphe nucleus and projection areas. *NeuroImage* 63(2):874-881. *[2011, IF: 5.895]*
3. Kraus C, Hahn A, Savli M, **Kranz G.S.**, Baldinger P, Höflich A, Spindelegger C, Ungersböck J, Häusler D, Mitterhauser M, Windischberger C, Wadsak W, Kasper S, Lanzenberger R. (2012). Serotonin-1A receptor binding is positively associated gray matter volume – A

multimodal neuroimaging study combining PET and structural MRI. *NeuroImage* 63(3):1091-1098 *[2011, IF: 5.895]*

4. Hahn A, Wadsak W, Windischberger C, Baldinger P, Höflich A, Losak J, Nics L, Philippe C, **Kranz GS**, Kraus C, Mitterhauser M, Karanikas G, Kasper S, Lanzenberger R. (2012). Differential modulation of self-referential processing in the default mode network via serotonin-1A receptors. *Proceedings of the National Academy of Sciences (PNAS), 109(7):2619-24. [2011, IF 9.681]*

5. Baldinger P, **Kranz G. S.**, Höflich A, Savli M, Stein P, Lanzenberger R, Kasper S. (2012). Hormonersatztherapie und deren Wirkung auf Psyche und Gehirn. *Nervenarzt. DOI 10.1007/s00115-011-3456-7, [2011, IF: 0.681]*

6. Sladky, R., Baldinger, P., **Kranz, G.S.**, Tröstl, J., Höflich, A., Lanzenberger, R., Moser, E., Windischberger, C. (2011). High-resolution functional MRI of the human amygdala at 7 Tesla. *European Journal of Radiology (in print). [2011, IF: 2.606]*

7. Lanzenberger, R., Mitterhauser, M., **Kranz, G.S.**, Spindelegger, Ch., Wadsak, W., Stein, P., Moser, U., Savli, M., Kletter, K. & Kasper, S. (2011). Progesterone level predicts serotonin-1A receptor binding in the male human brain. *Neuroendocrinology,* 94(1):84-8. *[2011, IF: 2.376]*

8. Kranz, G., Shamim, E.A., Lin, P.T., **Kranz, G.S.**, & Hallett, M. (2010). Deep transcranial magnetic brain stimulation modulates blepharospasm: A randomized sham-controlled study. *Neurology*, 75(16): 1465-71. *[2011, IF: 8.312]*

9. Lanzenberger, R., Wadsak, W., Spindelegger, C., Mitterhauser, M., Akimova, E., Mien, LK., Fink, M., Moser, U., Savli, M., **Kranz G.S**., Hahn, A., Kletter, K. & Kasper, S. (2010). Cortisol plasma levels in Social Anxiety Disorder patients correlate with serotonin-1A receptor binding in limbic brain regions. *International Journal of Neuropsychopharmacology*. 13(9):1129-43. *[2011, IF:4.578]*

10. Paul, A., Kranz, G., Schindl, A., **Kranz, G.S**., Auff, E., & Sycha, T. (2010). Diode laser removal does not interfere with Botulinum toxin A treatment against axillary hyperhidrosis. *Lasers in Surgery & Medicine,* 42(3), 211-4. *[2011, IF: 2.748]*

11. Lanzenberger, R., Hackhofer, S., **Kranz G.S.**, & Kasper, S. (2010). Wie viel Gehirn braucht der Affekt? Bildgebende Verfahren und affektive Symptome bei Schizophrenie. *Psychiatrie & Psychotherapie 2009; Sonderheft Grazer Psychosentage 2007*, 6(3), 133-138. *[2011, IF: 0]*

12. Kranz, G., Shamim, E., Lin, P., **Kranz, G.S.**, Voller, B., & Hallett M. (2009). Blepharospasm and the modulation of cortical excitability in primary and secondary motor areas. *Neurology,* 73 (23), 2031-6. *[2011, IF: 8.312]*

13. Batthyany, A., **Kranz, G.S.**, & Erber, A. (2009). Moderating factors in precognitive habituation: The roles of situational vigilance, emotional reactivity and affect regulation. *Journal of the Society for Psychical Research, 73*, 65-82. *[2011, IF: 0]*

14. Kranz, G., Sycha, T., Voller, B., **Kranz, G.S**., Schnider, P. & Auff, E. (2008). Neutralizing antibodies in dystonic patiens who still respond well to botullinum toxin type A. *Neurology*, 70 (2), 133-6. *[2011, IF: 8.312]*

15. Frankl, V.E. (2008). *Die Psychotherapie in der Praxis und ausgewählte Texte über angewandte Psychotherapie.* Edited by: A. Batthyany, E. Fizzotti & K-H. Biller; Special Editor: **Kranz, G.S.**, Wien: Böhlau.

Conference PROCEEDINGS and published ABSTRACTS

15 first-authorships, 23 co-authorships